Outer Continental Shelf
Model Application and Evaluation
Volume III

Chukchi Sea

Devil's Paw Prospect

November 2011

Model Application and Evaluation

ConocoPhillips Chukchi Sea
WRF Modeling Application

Prepared by:

Dennis McNally
Dr. James G. Wilkinson

Alpine Geophysics, LLC
7341 Poppy Way
Arvada, Colorado 80007

27 November 2011

Table of Contents

1 INTRODUCTION 1-1

1.1 WRF OVERVIEW 1-1
1.2 JUSTIFICATION FOR USE OF WRF MODEL 1-2

2 METHODOLOGY 2-1

2.1 MODEL SELECTION AND APPLICATION 2-1
2.2 EVALUATION APPROACH 2-5
2.2.1 Components of the WRF Evaluation 2-5
2.2.2 Data Supporting Meteorological Model Evaluation 2-6
2.2.3 Evaluation Tools 2-7

3 WRF PERFORMANCE EVALUATION RESULTS 3-1

3.1 QUANTITATIVE MODEL EVALUATION RESULTS 3-1
3.1.1 Temperature Bias and Error 3-1
3.1.2 Mixing Ratio Bias and Error 3-3
3.1.3 Wind Direction Bias, Wind Direction Error, and Wind Speed RMSE 3-4
3.2 QUALITATIVE MONTHLY PRECIPITATION ANALYSIS 3-7
3.3 RADIOSONDE EVALUATION 3-7
3.4 SUMMARY OF MODEL PERFORMANCE EVALUATION 3-8

Table of Figures

Figure 2-1. 36 km (Outer), 12 km and 4km (Inner) WRF Domain. 2-12
Figure 2-2. 4 km WRF Meteorological Modeling Domain. Units on Bottom and Left Axes are Grid Cells. Units on Top and Right Axes are Kilometers 2-13
Figure 2-3. MADIS Stations in the 4km WRF Domain. 2-14
Figure 3-1. Temperature Bias and Error Soccer Plots by Month for All Stations in the 4km Domain for (a) 2007, (b) 2008, and (c) 2009. 3-15
Figure 3-2. Temperature Bias and Error Soccer Plot by Month for North Coast Stations in the 4km Domain for (a) 2007, (b) 2008, and (c) 2009. 3-16
Figure 3-3. Temperature (C) Spatial Plot for 4km Grid at 0Z (3:00 pm LST) 15 July 2009. Diamonds Represent Observations. 3-17
Figure 3-4. Temperature (C) Spatial Plot for 4km Grid at 4Z (7:00 pm LST) 15 July 2009. Diamonds Represent Observations. 3-17
Figure 3-5. Temperature (C) Spatial Plot for 4km Grid at 8Z (11:00 pm LST) 15 July 2009. Diamonds Represent Observations. 3-18
Figure 3-6. Temperature (C) Spatial Plot for 4km Grid at 12Z (3:00 am LST) 15 July 2009. Diamonds Represent Observations. 3-18
Figure 3-7. Temperature (C) Spatial Plot for 4km Grid at 16Z (7:00 am LST) 15 July 2009. Diamonds Represent Observations. 3-19
Figure 3-8. Temperature (C) Spatial Plot for 4km Grid at 20Z (11:00 am LST) 15 July 2009. Diamonds Represent Observations. 3-19
Figure 3-9. Hourly Temperature (C) Spatial Time Series for Wainwright on the 4km Grid for July through November 2009. The Spatial Envelope, which is Shown by the Black Line (minimum temperature) and Red Line (maximum temperature) and Generally Brackets the Blue Asterisks (observed temperature), Represents a Nominal 14km (3.5, 4km grid cells) Search Radius about the Wainwright Monitor. 3-20
Figure 3-10. Hourly Temperature (C) Spatial Time Series for the ARM Barrow Tall Tower on the 4km Grid for July through September through September 2009. The Graphics on the Left are a Comparison of the 20m observation with the 18 m (Level 2) Model Estimate. The Graphics on the Right are a Comparison of the 40m observation with the 32m (Level 2) Model Estimate. The Spatial Envelope, which is Shown by the Black Line (minimum mixing ratio) and Red Line (maximum mixing ratio) and Generally Brackets the Blue Asterisks (observed mixing ratio), Represents a Nominal 14km (3.5, 4km grid cells) Search Radius about the Monitor. 3-21
Figure 3-11. Hourly Temperature (C) Spatial Time Series for the ARM Barrow Tall Tower on the 4km Grid for October and November 2009. The Graphics on the Left are a Comparison of the 20m observation with the 18 m (Level 2) Model Estimate. The Graphics on the Right are a Comparison of the 40m observation with the 32m (Level 2) Model Estimate. The Spatial Envelope, which is Shown by the Black Line (minimum mixing ratio) and Red Line (maximum mixing ratio) and Generally Brackets the Blue Asterisks (observed mixing ratio), Represents a Nominal 14km (3.5, 4km grid cells) Search Radius about the Monitor. 3-22
Figure 3-12. Hourly Spatial Mean Temperature (C) Time Series for North Coast Stations in the 4km Grid for July through November 2009. The Black Asterisks Represent the Hourly Mean of the Observed Temperatures from the North Coast Stations in the 4km Grid. The Red Line Represents the Hourly Mean of the Predicted Temperatures at the North Coast Stations in the 4km Grid. 3-23
Figure 3-13. Hourly Spatial Mean Temperature (C) Time Series for All Stations in the 4km Grid for July through November 2009. The Black Asterisks Represent the Hourly Mean of the Observed Temperatures from All Stations in the 4km Grid. The Red Line Represents the Hourly Mean of the Predicted Temperatures at All Stations in the 4km Grid. 3-24

Figure 3-14. Mixing Ratio Bias and Error Soccer Plot by Month for All Stations in the 4km Domain for (a) 2007, (b) 2008, and (c) 2009. 3-25
Figure 3-15. Mixing Ratio Bias and Error Soccer Plot by Month for North Coast Stations in the 4km Domain for (a) 2007, (b) 2008, and (c) 2009. 3-26
Figure 3-16. Mixing Ratio (g/kg) Spatial Plot for 4km Grid at 0Z (3:00 pm LST) 15 July 2009. Diamonds Represent Observations. 3-27
Figure 3-17. Mixing Ratio (g/kg) Spatial Plot for 4km Grid at 4Z (7:00 pm LST) 15 July 2009. Diamonds Represent Observations. 3-27
Figure 3-18. Mixing Ratio (g/kg) Spatial Plot for 4km Grid at 8Z (11:00 pm LST) 15 July 2009. Diamonds Represent Observations. 3-28
Figure 3-19. Mixing Ratio (g/kg) Spatial Plot for 4km Grid at 12Z (3:00 am LST) 15 July 2009. Diamonds Represent Observations. 3-28
Figure 3-20. Mixing Ratio (g/kg) Spatial Plot for 4km Grid at 16Z (7:00 am LST) 15 July 2009. Diamonds Represent Observations. 3-29
Figure 3-21. Mixing Ratio (g/kg) Spatial Plot for 4km Grid at 20Z (11:00 am LST) 15 July 2009. Diamonds Represent Observations. 3-29
Figure 3-22. Hourly Mixing Ratio (g/kg) Spatial Time Series for Wainwright on the 4km Grid for July through November 2009. The Spatial Envelope, which is Shown by the Black Line (minimum mixing ratio) and Red Line (maximum mixing ratio) and Generally Brackets the Blue Asterisks (observed mixing ratio), Represents a Nominal 14km (3.5, 4km grid cells) Search Radius about the Wainwright Monitor. 3-30
Figure 3-23. Hourly Mixing Ratio (g/kg) Spatial Time Series for the ARM Barrow Tall Tower on the 4km Grid for July through September through September 2009. The Graphics on the Left are a Comparison of the 20m observation with the 18 m (Level 2) Model Estimate. The Graphics on the Right are a Comparison of the 40m observation with the 32m (Level 2) Model Estimate. The Spatial Envelope, which is Shown by the Black Line (minimum mixing ratio) and Red Line (maximum mixing ratio) and Generally Brackets the Blue Asterisks (observed mixing ratio), Represents a Nominal 14km (3.5, 4km grid cells) Search Radius about the Monitor. 3-31
Figure 3-24. Hourly Mixing Ratio (g/kg) Spatial Time Series for the ARM Barrow Tall Tower on the 4km Grid for October and November 2009. The Graphics on the Left are a Comparison of the 20m observation with the 18 m (Level 2) Model Estimate. The Graphics on the Right are a Comparison of the 40m observation with the 32m (Level 2) Model Estimate. The Spatial Envelope, which is Shown by the Black Line (minimum mixing ratio) and Red Line (maximum mixing ratio) and Generally Brackets the Blue Asterisks (observed mixing ratio), Represents a Nominal 14km (3.5, 4km grid cells) Search Radius about the Monitor. 3-32
Figure 3-25. Hourly Spatial Mean Mixing Ratio (g/kg) Time Series for North Coast Stations in the 4km Grid for July through November 2009. The Black Asterisks Represent the Hourly Mean of the Observed Mixing Ratio from the North Coast Stations in the 4km Grid. The Red Line Represents the Hourly Mean of the Predicted Mixing Ratio at the North Coast Stations in the 4km Grid. 3-33
Figure 3-26. Hourly Spatial Mean Mixing Ratio (g/kg) Time Series for All Stations in the 4km Grid for July through November 2009. The Black Asterisks Represent the Hourly Mean of the Observed Mixing Ratio from All Stations in the 4km Grid. The Red Line Represents the Hourly Mean of the Predicted Mixing Ratio at All Stations in the 4km Grid. 3-34
Figure 3-27. Wind Speed RMSE (m/s) Bias versus Wind Direction Error (deg) Soccer Plot by Month for All Stations in the 4km Domain for (a) 2007, (b) 2008, and (c) 2009. 3-35
Figure 3-28. Wind Speed RMSE (m/s) Bias versus Wind Direction Error (deg) Soccer Plot by Month for North Coast Stations in the 4km Domain for (a) 2007, (b) 2008, and (c) 2009. 3-36
Figure 3-29. Hourly Spatial Mean Wind Direction (deg) Time Series for North Coast Stations in the 4km Grid for July through November 2009. The Black Asterisks Represent the Hourly Mean of the Observed Wind Direction from the North Coast Stations in the 4km Grid. The Red Line Represents the Hourly Mean of the Predicted Wind Direction at the North Coast Stations in the 4km Grid. 3-37

Figure 3-30. Hourly Spatial Mean Wind Direction (deg) Time Series for All Stations in the 4km Grid for July through November 2009. The Black Asterisks Represent the Hourly Mean of the Observed Wind Direction from All Stations in the 4km Grid. The Red Line Represents the Hourly Mean of the Predicted Wind Direction at All Stations in the 4km Grid. 3-38
Figure 3-31. Wind Speed Bias (m/s) versus Wind Direction Error (deg) Soccer Plot by Month for All Stations in the 4km Domain for (a) 2007, (b) 2008, and (c) 2009. 3-39
Figure 3-32. Wind Speed Bias (m/s) versus Wind Direction Error (deg) Soccer Plot by Month for North Coast Stations in the 4km Domain for (a) 2007, (b) 2008, and (c) 2009. 3-40
Figure 3-33. Hourly Spatial Vector Mean Wind Speed (m/s) Time Series for North Coast Stations in the 4km Grid for July through November 2009. The Black Asterisks Represent the Hourly Mean of the Observed Vector Wind Speed from North Coast Stations in the 4km Grid. The Red Line Represents the Hourly Mean of the Predicted Vector Wind Speed at North Coast Stations in the 4km Grid. 3-41
Figure 3-34. Hourly Spatial Vector Mean Wind Speed (m/s) Time Series for All Stations in the 4km Grid for July through November 2009. The Black Asterisks Represent the Hourly Mean of the Observed Vector Wind Speed from All Stations in the 4km Grid. The Red Line Represents the Hourly Mean of the Predicted Vector Wind Speed at All Stations in the 4km Grid. 3-42
Figure 3-35. Vector Wind Speed (m/s) Spatial Plot for 4km Grid at 0Z (3:00 pm LST) 15 July 2009. Red arrows Represent Observations. 3-43
Figure 3-36. Vector Wind Speed (m/s) Spatial Plot for 4km Grid at 4Z (7:00 pm LST) 15 July 2009. Red arrows Represent Observations. 3-43
Figure 3-37. Vector Wind Speed (m/s) Spatial Plot for 4km Grid at 8Z (11:00 pm LST) 15 July 2009. Red Arrows Represent Observations. 3-44
Figure 3-38. Vector Wind Speed (m/s) Spatial Plot for 4km Grid at 12Z (3:00 am LST) 15 July 2009. Red Arrows Represent Observations. 3-44
Figure 3-39. Vector Wind Speed (m/s) Spatial Plot for 4km Grid at 16Z (7:00 am LST) 15 July 2009. Red Arrows Represent Observations. 3-45
Figure 3-40. Vector Wind Speed (m/s) Spatial Plot for 4km Grid at 20Z (11:00 am LST) 15 July 2009. Red Arrows Represent Observations. 3-45
Figure 3-41. Monthly Total Precipitation (mm) Spatial Plot for 4km Grid for July 2007. Diamonds Represent Observations. 3-46
Figure 3-42. Monthly Total Precipitation (mm) Spatial Plot for 4km Grid for August 2007. Diamonds Represent Observations. 3-46
Figure 3-43. Monthly Total Precipitation (mm) Spatial Plot for 4km Grid for September 2007. Diamonds Represent Observations. 3-47
Figure 3-44. Monthly Total Precipitation (mm) Spatial Plot for 4km Grid for October 2007. Diamonds Represent Observations. 3-47
Figure 3-45. Monthly Total Precipitation (mm) Spatial Plot for 4km Grid for November 2007. Diamonds Represent Observations. 3-48
Figure 3-46. Monthly Total Precipitation (mm) Spatial Plot for 4km Grid for July 2008. Diamonds Represent Observations. 3-49
Figure 3-47. Monthly Total Precipitation (mm) Spatial Plot for 4km Grid for August 2008. Diamonds Represent Observations. 3-49
Figure 3-48. Monthly Total Precipitation (mm) Spatial Plot for 4km Grid for September 2008. Diamonds Represent Observations. 3-50
Figure 3-49. Monthly Total Precipitation (mm) Spatial Plot for 4km Grid for October 2008. Diamonds Represent Observations. 3-50
Figure 3-50. Monthly Total Precipitation (mm) Spatial Plot for 4km Grid for November 2008. Diamonds Represent Observations. 3-51
Figure 3-51. Monthly Total Precipitation (mm) Spatial Plot for 4km Grid for July 2009. Diamonds Represent Observations. 3-52
Figure 3-52. Monthly Total Precipitation (mm) Spatial Plot for 4km Grid for August 2009. Diamonds Represent Observations. 3-52

Figure 3-53. Monthly Total Precipitation (mm) Spatial Plot for 4km Grid for September 2009. Diamonds Represent Observations. 3-53
Figure 3-54. Monthly Total Precipitation (mm) Spatial Plot for 4km Grid for October 2009. Diamonds Represent Observations. 3-53
Figure 3-55. Monthly Total Precipitation (mm) Spatial Plot for 4km Grid for November 2009. Diamonds Represent Observations. 3-54
Figure 3-56. Skew-T-log-P Diagram for Barrow at 12Z (3:00 am LST) on 15 July 2009. Red Lines Denote WRF Estimates. Black Lines Denote Observations. 3-55
Figure 3-57. Skew-T-log-P Diagram for Barrow at 12Z (3:00 am LST) on 15 July 2009. Red Lines Denote WRF Estimates. Black Lines Denote Observations. 3-56
Figure 3-58. Skew-T-log-P Diagram for Barrow at 0Z (3:00 pm LST) on 16 July 2009. Red Lines Denote WRF Estimates. Black Lines Denote Observations. 3-57
Figure 3-59. Skew-T-log-P Diagram for Barrow at 12Z (3:00 am LST) on 15 August 2009. Red Lines Denote WRF Estimates. Black Lines Denote Observations. 3-58
Figure 3-60. Skew-T-log-P Diagram for Barrow at 0Z (3:00 pm LST) on 16 August 2009. Red Lines Denote WRF Estimates. Black Lines Denote Observations. 3-59
Figure 3-61. Skew-T-log-P Diagram for Barrow at 12Z (3:00 am LST) on 15 September 2009. Red Lines Denote WRF Estimates. Black Lines Denote Observations. 3-60
Figure 3-62. Skew-T-log-P Diagram for Barrow at 0Z (3:00 pm LST) on 16 September 2009. Red Lines Denote WRF Estimates. Black Lines Denote Observations. 3-61
Figure 3-63. Skew-T-log-P Diagram for Barrow at 12Z (3:00 am LST) on 15 October 2009. Red Lines Denote WRF Estimates. Black Lines Denote Observations. 3-62
Figure 3-64. Skew-T-log-P Diagram for Barrow at 0Z (3:00 pm LST) on 16 October 2009. Red Lines Denote WRF Estimates. Black Lines Denote Observations. 3-63
Figure 3-65. Skew-T-log-P Diagram for Barrow at 12Z (3:00 am LST) on 15 November 2009. Red Lines Denote WRF Estimates. Black Lines Denote Observations. 3-64
Figure 3-66. Skew-T-log-P Diagram for Barrow at 0Z (3:00 pm LST) on 16 November 2009. Red Lines Denote WRF Estimates. Black Lines Denote Observations. 3-65

Table of Tables

Table 2-1. WRF Vertical Domain Specification. 2-8
Table 2-2. Observation Sites In the 4km WRF Domain. 2-9
Table 2-3. WRF Version 3.3.1 Physics Options. 2-10
Table 2-4. Episodic and Long-term Benchmarks for Meteorological Model Performance. 2-11
Table 3-1. List of Stations and Their Associated Subdomains. 3-10
Table 3-2. Temperature Bias (K) for WRF by Month and Analysis Region in the 4 km Domain. 3-11
Table 3-3. Temperature Error (K) for WRF by Month and Analysis Region in the 4 km Domain. 3-11
Table 3-4. Mixing Ratio Bias (g/kg) for WRF by Month and Analysis Region in the 4 km Domain. 3-12
Table 3-5. Mixing Ratio Error (g/kg) for WRF by Month and Analysis Region in the 4 km Domain. 3-12
Table 3-6. Wind Direction Bias (deg.) for WRF by Month and Analysis Region in the 4 km Domain. 3-13
Table 3-7. Wind Direction Error (deg.) for WRF by Month and Analysis Region in the 4 km Domain. 3-13
Table 3-8. Wind Speed RMSE (m/s) for WRF by Month and Analysis Region in the 4 km Domain. 3-14

1 INTRODUCTION

The tool used for this meteorological modeling study is the Weather Research and Forecasting (WRF) model[1,2], more specifically, the Advanced Research WRF dynamic core (WRF-ARW, henceforth simply called WRF). WRF is a next-generation mesoscale numerical weather prediction system designed to serve both operational forecasting and atmospheric research needs[3,4,5]. WRF contains separate modules to compute different physical processes such as surface energy budgets and soil interactions, turbulence, cloud microphysics, and atmospheric radiation. Within WRF, the user has many options for selecting the different schemes for each type of physical process. The WRF Preprocessing System (WPS) was used for this project to generate the initial and boundary conditions used by WRF, based on topographic datasets, land use information, and larger-scale atmospheric and oceanic models.

This report describes the application and performance evaluation of WRF for an atmospheric simulation over Alaska and the Chukchi Sea for the months of July through November for the years 2007, 2008 and 2009. The WRF results will be used to provide the first-step fields for a CALMET[6] application.

1.1 WRF Overview

WRF features multiple dynamic cores and a software architecture allowing for computational parallelism and system extensibility. WRF is suitable for a broad spectrum of applications across scales ranging from meters to thousands of kilometers. The effort to develop WRF has been a collaborative partnership, principally among the National Center for Atmospheric Research (NCAR), the National Oceanic and Atmospheric Administration (NOAA), the National Centers for Environmental Prediction (NCEP) and the Forecast Systems Laboratory (FSL), the Air Force Weather Agency (AFWA), the Naval Research Laboratory, the University of Oklahoma, and the Federal Aviation Administration (FAA). WRF allows researchers the ability to conduct simulations reflecting either real data or idealized configurations. WRF provides an operational forecasting model that is flexible and computationally efficient, while offering the advances in

---

1 Skamarock, W.C., J.B. Klemp, J. Dudhia, D.O. Gill, M. Barker, M.G. Duda, X.-Y. Huang, W. Wang, and J.G. Powers, 2008: A description of the Advanced Research WRF version 3. NCAR Technical Note NCAR/TN475+STR.

2 http://www.wrf-model.org/index.php

3 Skamarock, W. C. 2004. Evaluating Mesoscale NWP Models Using Kinetic Energy Spectra. *Mon. Wea. Rev.*, Volume 132, pp. 3019-3032. December. (http://www.mmm.ucar.edu/individual/skamarock/spectra_mwr_2004.pdf)

4 Skamarock, W. C., J. B. Klemp, J. Dudhia, D. O. Gill, D. M. Barker, W. Wang and J. G. Powers. 2005. A Description of the Advanced Research WRF Version 2. National Center for Atmospheric Research (NCAR), Boulder, CO. June. (http://www.mmm.ucar.edu/wrf/users/docs/arw_v2.pdf)

5 Skamarock, W. C. 2006. Positive-Definite and Monotonic Limiters for Unrestricted-Time-Step Transport Schemes. *Mon. Wea. Rev.*, Volume 134, pp. 2241-2242. June. (http://www.mmm.ucar.edu/individual/skamarock/advect3d_mwr.pdf).

6 Earth Tech, Inc. 2000. A User's Guide for the Calmet Meteorological Model (Version 5). Earth Tech, Inc. Concord, MA 01742.

physics, numerics, and data assimilation contributed by the research community. Information on running the WRF system can be found in the WRF User's Guide[7].

1.2 Justification for Use of WRF model

The WRF meteorological model was developed as a replacement to MM5; therefore, MM5 is no longer supported. While the MM5 model was the primary mesoscale modeling tool to support air quality modeling for the past decade, WRF is now routinely used in air quality model applications and has been obtaining model performance that is as good as or better than MM5. WRF has not only been applied in warm region climes, but it has also seen recent, extensive adaptation to Arctic regions for both seasonal and multi-year simulations.[8,9,10,11,12] EPA has also adopted the WRF meteorological model for their regulatory air quality model applications. For these reasons, the WRF meteorological model was selected for the Chukchi Sea modeling.

---

7 User's Guide for the Advanced Research WRF (ARW) Modeling System version 3.3. http://www.mmm.ucar.edu/wrf/users/docs/user_guide_V3/contents.html

8 Cassano, J. J., M. E. Higgins, and M. W. Seefeldt, 2011. "Performance of the Weather Research and Forecasting (WRF) Model for Month-long pan-Arctic Simulations." *Mon. Wea. Rev*., in press, doi:10.1175/MWR-D-10-05065.1.

9 Porter, D.F., J.J. Cassano, and M.C. Serreze, 2011. "The sensitivity of the Arctic atmosphere to sea ice changes in the WRF model." *J. Geophys. Res.*

10 Porter, D.F., J.J. Cassano, and M.C. Serreze, 2011. "Analysis of the Arctic heat budget in WRF: A comparison with reanalyses and satellite observations." *J. Geophys. Res*., doi:10.1029/2011JD016622, in press.

11 A. B. Wilson, D. H. Bromwich, and K. M. Hines, 2011. "Evaluation of Polar WRF forecasts on the Arctic System Reanalysis domain: Surface and upper air analysis." *J. Geophys. Res*., 116, D11112, doi:10.1029/2010JD015013.

12 D. H. Bromwich, K. M. Hines, and L.-S. Bai, 2009." "Development and testing of Polar Weather Research and Forecasting model: 2. Arctic Ocean." *J. Geophys. Res*., 114, D08122, doi:10.1029/2008JD010300.

2 METHODOLOGY

The methodology to apply WRF for the current meteorological modeling study was straightforward. WRF simulations were developed for the months July through November for the years 2007, 2008, and 2009, and the model results (e.g., wind speeds, wind directions, temperatures) were compared with available surface and aloft meteorological observations.

2.1 Model Selection and Application

Meteorological inputs for the Chukchi Sea modeling were generated using the Weather Research and Forecasting (WRF) Preprocessing System (WPS). The Advanced Research WRF (ARW) core of the WRF modeling system was used to run the meteorological simulations. The WRF model configuration was based on recent modeling conducted by the University of Alaska Fairbanks (UAF) for the Bureau of Ocean Energy Management, Regulation and Enforcement (BOEMRE) Chukchi/Beaufort Seas Mesoscale Meteorology Study[13].

A brief summary of the WRF input data preparation procedures used for this modeling exercise is provided in the following text.

Model Selection: WRF Version 3.3.1 (September 21, 2011 release) was used. The justification for using the WRF meteorological model was previously provided. The WPS preprocessor programs include GEOGRID, UNGRIB, and METGRID were used to develop model inputs.

Horizontal Domain Definition: The computational domain on which WRF was applied was sufficiently sized to accommodate the anticipated air quality modeling. The WRF 36/12/4 km domains were defined with at least a 5 grid cell buffer in all directions from the air quality modeling domain to minimize any potential numeric noise along domain boundaries. The WRF horizontal domains are presented in Figure 2-1 and Figure 2-2. The grid projection was Polar Stereographic with a pole of projection of 70 degrees North, 155 degrees West.

In regards to Figure 2-2, this is the standard "spatial plot" that is used throughout this report. There are four axes on all spatial plots: (1) the bottom horizontal axis is WRF's east-west grid cell; (2) the left vertical axis is WRF's north-south grid cell; (3) the top horizontal axis is the map projection (i.e., polar stereographic) east-west coordinate in kilometers; and (4) the right vertical axis is the map projection north-south coordinate in kilometers. In order to streamline the presentation of the spatial graphics, the axes on subsequent spatial plots are removed.

Vertical Domain Definition: The WRF modeling was based on 37 vertical layers with an approximately 12 meter deep surface layer. The vertical domain is presented in both sigma and height coordinates in Table 2-1.

13 BOEMRE. http://mms-meso.gi.alaska.edu/

Topographic Inputs: Standard WRF land-use/land-cover data were used. The 36km, 12km and 4km domains used the 10min, 2min, and 30 second resolution data, respectively.

Vegetation Type and Land Use Inputs: Vegetation type and land use information was developed using the most recently released WRF databases provided with the MM5 distribution. Standard WRF surface characteristics corresponding to each land use category were employed.

Atmospheric Data Inputs: The National Centers for Environmental Prediction (NCEP) Global Forecast System (GFS)[14] ½ degree dataset was used for model initialization and analysis nudging. The GFS dataset was selected based on its current use in the Fairbanks modeling, the large (i.e., global) spatial coverage that allows sufficient coarse grid coverage so that WRF-predicted synoptic patterns can develop for the higher resolution grids, and the sufficiently high horizontal resolution to capture synoptic systems. The data were obtained from the Research Data Archive (RDA), which is maintained by the Computational and Information Laboratory (CISL) at the National Center for Atmospheric Research (NCAR). NCAR is sponsored by the National Science Foundation (NSF). The original data are available from the RDA[15] in dataset number ds335.0.

Sea Ice Initialization: Sea ice was obtained from the GFS initialization files, and WRF was run using the Sea Surface Temperature (SST) update option to ingest new SST and sea ice fields every six hours during the model simulation. In the GFS model, the sea-ice is obtained from an analysis algorithm using the 5-minute latitude-longitude grid from the 85GHz channel on the Special Sensor Microwave Imager (SSM/I) satellite based instrument[16].

Time Integration: Third-order Runge-Kutta integration was used with a fixed time step of 90 seconds for 36km domain, 30 seconds for 12km domain, and 10 seconds for the 4km domain.

Diffusion Options: Horizontal Smagorinsky first-order closure with sixth-order numerical diffusion and suppressed up-gradient diffusion was used.

Lateral Boundary Conditions: Lateral boundary conditions were specified from the initialization dataset on the 36km domain with continuous updates nested from the 36km domain to the 12km domain and continuous updates nested from the 12km domain to the 4km domain.

Top and Bottom Boundary Conditions: The top boundary condition was selected as an implicit Rayleigh dampening for the vertical velocity. Consistent with the model application for non-idealized cases, the bottom boundary condition was selected as physical, not free-slip.

---

14 National Weather Service Environmental Modeling Center. http://www.emc.ncep.noaa.gov/GFS/
15 CISL Research Data Archive. http://dss.ucar.edu
16 Sea Ice in the NCEP Climate Forecast System. http://www.nws.noaa.gov/ost/climate/STIP/seaice.htm

Water Temperature Inputs: The water temperature data were taken from the NCEP RTG global one-twelfth degree analysis[17].

FDDA Data Assimilation: The WRF model was run with a combination of analysis and observation nudging. Analysis nudging was used on the 36km and 12km domain. For winds and temperature, analysis nudging coefficients of $5x10^{-4}$ and $3.0x10^{-4}$ were used on the 36 km and 12 km grids, respectively. For mixing ratio, an analysis nudging coefficient of $1.0x10^{-5}$ was used for both the 36km and 12km grids. The nudging used both surface and aloft nudging with nudging for temperature and mixing ratio excluded in the boundary layer. Observation nudging was performed on the 4km grid using the Meteorological Assimilation Data Ingest System (MADIS)[18] observation archive. The MADIS archive in Alaska includes the National Climatic Data Center (NCDC)[19] observations in addition to the Mesowest[20] and the National Data Buoy Center (NDBC) Coastal-Marine Automated Network C-MAN[21] stations. The MADIS stations are presented in Table 2-2 and Figure 2-3. The observational nudging coefficients for winds, temperatures and mixing ratios were $1.0x10^{-4}$, $1.0x10^{-4,}$ and $1.0x10^{-5}$, respectively and the radius of influence was set to 50km.

Physics Options: The WRF model contains many different physics options. The WRF model configuration was based on recent modeling conducted by the University of Alaska, Fairbanks (UAF) for the Bureau of Ocean Energy Management, Regulation and Enforcement (BOEMRE), Chukchi/Beaufort Seas Mesoscale Meteorology Study[22]. The physics options employed in this analysis are summarized in Table 2-3 and discussed below:

> Microphysics: The Morrison double moment microphysics scheme was used. The Morrison scheme was specifically developed for high-latitude cold temperature microphysics and includes the prediction of two moments (mixing ratio and number concentration) for rain, snow, graupel and cloud ice, in addition to single moment prediction of cloud water.
>
> Longwave Radiation: The updated Radiative Transfer Model (RRTMG)[23] was used. The RRTMG is an accurate scheme using look-up tables for efficiency. The scheme accounts for multiple bands, trace gases, and microphysics species and includes a method of

17 Real-time, global, sea surface temperature (RTG-SST) analysis. http://polar.ncep.noaa.gov/sst/oper/Welcome.html
18 Meteorological Assimilation Data Ingest System. http://madis.noaa.gov/
19 National Climatic Data Center. http://lwf.ncdc.noaa.gov/oa/ncdc.html
20 MesoWest. http://mesowest.utah.edu/index.html
21 National Data Buoy Center. http://www.ndbc.noaa.gov/cman.php
22 BOEMRE. http://mms-meso.gi.alaska.edu
23 Iacono, M.J., J.S. Delamere, E.J. Mlawer, M.W. Shephard, S.A. Clough, and W.D. Collins, 2008. "Radiative forcing by long-lived greenhouse gases: Calculations with the AER radiative transfer models." *J. Geophys. Res.*, 113, D13103, doi:10.1029/2008JD009944.

random cloud overlap. Zhang[24] compared multiple radiation schemes and found the RRTM (the predecessor to RRTMG) scheme to have a smaller bias than the other options examined.

Shortwave Radiation: The RRTMG shortwave radiation scheme was used. Gaudet and Stauffer[25] found that the RRTMG package led to significantly reduced warm biases and better RMSE statistics compared with other options they examined for an Alaska WRF application.

Land Surface Model: The Noah Land Surface Model (LSM) was used. The Noah LSM scheme is a 4-layer soil temperature and moisture model with canopy moisture and snow cover prediction. The scheme provides sensible and latent heat fluxes to the boundary-layer scheme and predicts soil ice and fractional sow cover effects. Zhang[24] compared the Noah LSM against the Pleim-Xiu LSM and found that Noah LSM had a smaller wind speed bias than Pleim-Xiu LSM. The RUC LSM was not selected as modeling conducted for winter conditions in the Upper Green River Basin in Wyoming[26] found that the RUC scheme exhibited a significant surface warm bias which weakened vertical temperature gradients, which in-turn impact boundary layer stability.

Planetary Boundary Layer (PBL) Scheme: The Yonsei University (YSU) scheme was used. Zhang[27] did extensive testing on model responses to different PBL schemes. His work showed that the while the model was not overly sensitive to the choice of PBL scheme, the YSU scheme performed better for surface temperature, particularly at night, than the other schemes. However, his work showed that the ACM2 scheme performed somewhat better for radiation and only slightly better for wind speed. Because of these factors, and upon advice of UAF, the YSU scheme was selected for use in this modeling effort[28].

Cumulus Parameterization: No cumulus parameterization was used on the 4km grid as a 4km grid can explicitly develop convective precipitation. On the 12km and 36km grids the Kain-Fritsch scheme was employed. The Kain-Fritsch scheme utilizes a simple cloud

---

24 Zhang, J., 2010. "Chukchi and Beaufort Seas Meteorology Study: Model Effort with the Weather Research and Forecasting Model," Presentation at U.S. EPA Outer Continental Shelf Meteorological Data and Air Quality Models Meeting, Anchorage, AK. 18 May, 2010.

25 Gaudet, B. and D. R. Stauffer, 2010. "Stable Boundary Layers Representation in Meteorological Models in Extremely Cold Wintertime Conditions." Prepared for the USEPA, prepared by The Pennsylvania State University, University Park, PA.

26 Hahn, R, B. Brashers, C. Emery, and D. McNally, 2011. "Winter 2008 WRF Modeling of the Upper Green River Basin." Prepared for the Wyoming Department of Environmental Quality, prepared by ENVIRON International Corporation, Novato, CA.

27 Zhang, J.. and J. Krieger: "Optimization of WRF Model for the Chukchi/Beaufort Seas Meteorology and Surface Wind Field Modeling." Presentation at Chukchi/Beaufort SeasMesoscale Meteorology Modeling Study Midterm Project Meeting Fairbanks, AK 18-19 November 2010. ftp://research.iarc.uaf.edu/incoming/xdz/Model-Sensitivity.pdf

28 Zhang, Jing: Personal Communication to Jason Reed, AECOM 14 October, 2011.

model with moist updrafts and downdrafts, including the effects of detrainment and entrainment, and relatively simple microphysics. Kain-Fritsch is widely used, including for multi-annual simulations by USEPA Office of Research and Development (ORD) and by UAF for the BOEMRE Chukchi/Beaufort Seas modeling.

Application Methodology: The WRF model was executed in 5-day blocks initialized at 12Z every 5 days with a 90 second time step. Model results were output every 60 minutes and output files were split at 24 hour intervals. Twelve (12) hours of spin-up was included in each 5-day block before the data were used in the subsequent evaluation. The model was run from 16 June to 3 December, for of the years 2007, 2008 and 2009. WRF was configured to run in distributed memory parallel mode and was executed using 8 MPICH2 processes per segment on a Linux cluster using Intel Xeon processors. A sample WPS namelist is presented in Appendix A. A sample WRF namelist is presented in Appendix B.

2.2 Evaluation Approach

Meteorological inputs required by the CALMET model include hourly estimates of the three-dimensional distribution of winds, temperatures and humidity. Accordingly, the objective of the WRF performance evaluation was to assess the adequacy of these meteorological fields for the Chukchi Sea modeling episodes.

2.2.1 Components of the WRF Evaluation

The WRF modeling system is now well-established with a development and refinement history of almost a decade. The model has seen extensive use worldwide by many agencies, consultants, university scientists and research groups. Thus, the current version of the model, as well as its predecessor versions, has been extensively "peer-reviewed" and considerable algorithm development and module testing has been performed with all of the important process components. Given that the WRF model code and algorithms have already undergone significant peer review, performance testing of the WRF model in this study was focused on an operational versus a scientific evaluation for the specific Chukchi Sea modeling periods.

Typical of other meteorological model application studies for air quality modeling purposes, the WRF model performance was compared both against established metrics and against other modeling studies. Emery and co-workers (2001)[29] derived and proposed a set of daily performance “benchmarks” for typical meteorological model performance. These standards were based upon the evaluation of about thirty mesoscale meteorological model simulations of *multi-day episodes* in support of air quality modeling. During this time (the mid to late 1990’s) the mesoscale meteorological models were typically applied to provide meteorological fields

29 Emery, C., E. Tai, and G. Yarwood, 2001. “Enhanced Meteorological Modeling and Performance Evaluation for Two Texas Ozone Episodes.” Prepared for the Texas Natural Resource Conservation Commission, prepared by ENVIRON International Corporation, Novato, CA. 31-August. http://www.tceq.texas.gov/assets/public/implementation/air/am/contracts/reports/mm/EnhancedMetModelingAndPerformanceEvaluation.pdf

for ozone air quality models. These multi-day episodes were typically chosen because of the high ozone levels which often occur during fairly stagnant summertime conditions.

Because of a lack of other information, these benchmarks have been adopted for use in *annual* and *seasonal* meteorological modeling studies. Since the synoptic conditions are so varied during a year, and are often times so different than the synoptic conditions typical of high urban ozone concentrations, the use of such benchmarks is problematic. They must be viewed as being applied as *guideline* and not *bright-line* numbers. That is, the purpose of these benchmarks is not to give a passing or failing grade to any one particular meteorological model application, but rather to put its results into the proper context of other models and meteorological data sets.

Recognizing that the episodic benchmarks may not be appropriate for longer term simulations, McNally (2009)[30] analyzed multiple annual runs and suggested an alternative set of benchmarks for temperature, namely a guideline of +/- 1.0 K for bias and 3.0 K for gross error, and recognized that a single set of criteria may not be appropriate given the competing complexities of meteorological modeling in different areas.

The benchmark for each variable to judge whether predictions from a meteorological model are on par with previous meteorological modeling studies is presented in Table 2-4.

2.2.2 Data Supporting Meteorological Model Evaluation

Hourly surface and upper-air meteorological observations were obtained from the MADIS and other sources to support the evaluation of WRF surface temperature, water vapor, and wind fields. In Alaska, the MADIS system includes surface and upper-air meteorological data from numerous networks including NCDC observations in addition to the Mesowest and the NDBC C-MAN stations.

In addition to the MADIS data, the Department of Energy (DOE) Atmospheric Radiation Measurement (ARM)[31] data were used. At the ARM Barrow site, the model was evaluated against the Surface Meteorological Instrumentation (MET) (wind, temperature, humidity), the Multi-level Meteorological Instrument (TWR) (temperature and humidity), and the Balloon-Borne Sounding System (SONDE). At the ARM Atqasuk site, the MET data were used for the model performance evaluation.

For a portion of 2009 (August-October), Shell Oil operated a buoy in the Chukchi Sea. These data were used to evaluate the WRF for wind speed and temperature.

A list of stations and the corresponding observation network that were used in the performance evaluation are listed in Table 2-2.

---

30 McNally, D. E., 2009. "12km MM5 Performance Goals." Presentation to the Ad-hov Meteorology Group. 25-June. http://www.epa.gov/scram001/adhoc/mcnally2009.pdf

31 Atmospheric Radiation Measurement Program. http://www.arm.gov/about

2.2.3 Evaluation Tools

The primary tools used for evaluating the WRF surface meteorological fields were the METSTAT program[32] and the Alpine Geophysics MAPS[33] package. Both of these tools calculate a suite of model performance statistics using surface wind speed, wind direction, temperature and water vapor mixing ratio for user specified subdomains. Model performance evaluation metrics used in evaluating the WRF model include temperature and water mixing ratio bias and error, wind direction bias and error, and wind speed RMSE. The MAPS package computes nearly the full suite of statistical metrics from Tesche, 2002[34], although few of the metrics have been widely enough used to be useful in comparing this simulation to other WRF/MM5 simulations.

Aloft comparisons used the WRF_UAPLOT package. WRF_UAPLOT generates skew-T-log-P graphics with traces for both the modeled and observed temperature, dew point temperature and winds. These sounding plots can be used to compare PBL depth estimates for the model as well as stability and aloft winds.

32 CAMx Processors Downloads. METSTAT. http://www.camx.com/files/metstat.27oct09.tar.gz
33 McNally, D. E., and T. W. Tesche, 1994. "MAPS2.3 User's Guide", Alpine Geophysics, LLC, Golden, CO.
34 Tesche, T. W., D. E. McNally, and C. Tremback., 2002. “Operational Evaluation of the MM5 Meteorological Model over the Continental United States: Protocol for Annual and Episodic Evaluation.” Prepared for the EPA OAQPS. Prepared by Alpine Geophysics, LLC, Ft. Wright, KY.
http://www.epa.gov/scram001/reports/tesche_2002_evaluation_protocol.pdf

Table 2-1. WRF Vertical Domain Specification.

Level	eta	Pressure (mb)	Height (m)	Mid Height (m)
1	1	1000	0.0	6.0
2	0.9985	998.575	12.0	18.0
3	0.997	997.15	24.1	32.1
4	0.995	995.25	40.1	48.2
5	0.993	993.35	56.2	64.3
6	0.991	991.45	72.4	84.5
7	0.988	988.6	96.6	108.7
8	0.985	985.75	120.9	141.2
9	0.98	981	161.5	202.4
10	0.97	971.5	243.2	284.4
11	0.96	962	325.6	367.1
12	0.95	952.5	408.6	450.4
13	0.94	943	492.3	534.4
14	0.93	933.5	576.6	662.1
15	0.91	914.5	747.5	834.4
16	0.89	895.5	921.2	1009.6
17	0.87	876.5	1098.0	1233.5
18	0.84	848	1369.1	1555.6
19	0.8	810	1742.2	1936.0
20	0.76	772	2129.7	2331.4
21	0.72	734	2533.1	2743.4
22	0.68	696	2953.7	3173.5
23	0.64	658	3393.4	3623.7
24	0.6	620	3854.1	4158.7
25	0.55	572.5	4463.3	4789.1
26	0.5	525	5114.9	5465.5
27	0.45	477.5	5816.1	6196.2
28	0.4	430	6576.3	6992.1
29	0.35	382.5	7407.9	7867.8
30	0.3	335	8327.8	8843.9
31	0.25	287.5	9360.1	9950.7
32	0.2	240	10541.2	11235.5
33	0.15	192.5	11929.7	12780.0
34	0.1	145	13630.3	14492.7
35	0.06	107	15355.1	16280.0
36	0.027	75.65	17204.9	18232.5
37	0	50	19260.0	9630.0

Table 2-2. Observation Sites In the 4km WRF Domain.

Station ID	Station Name	City	Network
Surface Stations			
BROA2	CRN Site Near Barrow		AK_COOP
DCKA2	Dahl Creek Near Kobuk		AK_COOP
HDOA2	Hoodoo Hill		RAWS
HOGA2	Hogatyza River		RAWS
IKAA2	Ikalukrok Creek		Snotel
IKPA2	Ikpikpuk River		AK_COOP
KAVA2	Kavet Creek		RAWS
KELA2	Kelly		RAWS
KOYA2	Koyukuk NWR		RAWS
KTZA2	Noatak		RAWS
MDEA2	Meade River at Atqasak		AK_COOP
NRUA2	Norutak Lake		RAWS
PABL	Buckland Airport	Buckland, AK	Other-MTR
PABR	Wiley Post-Will Rogers Memorial Airport	Barrow, AK	Other-MTR
PADE	Deering Airport	Deering, AK	Other-MTR
PADG	Red Dog Airport	Red Dog, AK	Other-MTR
PAFM	Ambler Airport	Ambler, AK	Other-MTR
PAIK	Bob Baker Memorial Airport	Kiana, AK	Other-MTR
PAIM	Indian Mountain LRRS Airport	Utopia Creek, AK	Other-MTR
PAIW	Wales Airport	Wales, AK	Other-MTR
PALU	Cape Lisburne LRRS Airport	Cape Lisburne, AK	Other-MTR
PAOT	Ralph Wien Mrmorial Airport	Kotzebue, AK	Other-MTR
PAPO	Point Home Airport	Point Hope, AK	Other-MTR
PASH	Shishmaref Airport	Shishmaref, AK	Other-MTR
PASK	Selawik Airport	Selawik, AK	Other-MTR
PATC	Tin City LRRS Airport	Tin City, AK	Other-MTR
PATQ	Atqasuk Edward Burnell Sr. Memorial Airport	Atqasuk, AK	Other-MTR
PAVL	Kivalina Airport	Kivalina, AK	Other-MTR
PAWI	Wainwright Airport	Wainwright, AK	Other-MTR
PAWN	Noatak Airport	Noatak, AK	Other-MTR
PPIZ	Point Lay LRRS Airport	Point Lay, AK	Other-MTR
RDDA2	Red Dog Dock	Red Dog, AK	CMAN
SRKA2	Kiana		RAWS
SWKA2	Selawik		RAWS
WULA2	Wulik River Near Kivalina		AK_DCP
Upper Air			
BRW	Barrow	Barrow, AK	Raob
OTZ	Kotzebue	Kotzebue, AK	Raob
Special Studies			
ARM-Barrow	Dept. of Energy ARM Barrow (MET, TWR and SONDE)	Barrow, AK	ARM
ARM-Atqasuk	Dept. of Energy ARM Atqasuk (MET)	Atqasuk, AK	ARM
Shell Buoy		Offshore	

Table 2-3. WRF Version 3.3.1 Physics Options.

WRF Treatment	Option Selected	Notes
Microphysics	Morrison Double Moment Microphysics[35]	This scheme was developed specifically for high-latitude cold temperature microphysics, and includes the prediction of two moments (mixing ratio and number concentration) for rain, snow, graupel, and cloud ice, in addition to single moment prediction of cloud water.
Longwave Radiation	RRTMG	Rapid Radiative Transfer Model for GCMs includes random cloud overlap and improved efficiency over RRTM.
Shortwave Radiation	RRTMG	Same as above, but for shortwave radiation.
LSM	NOAH	Two-layer scheme with vegetation and sub-grid tiling.
PBL scheme	YSU	Asymmetric Convective Model with non-local upward mixing and local downward mixing.
Cumulus parameterization	Kain –Fritsch on 36km and 12km domains. None on 4km domain	Previous testing with WRF has indicated a strong tendency to overestimate precipitation if cumulus parameterizations are employed.
Analysis nudging	Nudging applied to winds, temperature and moisture in the 36km and 12km domains	Temperature and moisture nudged above PBL only
Observation Nudging	Nudging applied only in the 4km domain	
Initialization Dataset	½ degree Global Forecast System (GFS)	

35 Morrison, H., J.A. Curry, and V.I. Khvorostyanov, 2005. "A new double-moment microphysics parameterization for application in cloud and climate models. Part I: Description." *J. Atmos. Sci.*, **62**, 1665-1677.

Table 2-4. Episodic and Long-term Benchmarks for Meteorological Model Performance.

Model Performance Statistic	Episodic Benchmark[1]	Long-term Benchmark[2]
Temperature bias	$-0.5\ K \leq x \leq 0.5\ K$	$-1.0\ K \leq x \leq 1.0\ K$
Temperature error	$x \leq 2.0\ K$	$x \leq 3.0\ K$
Mixing ratio bias	$-1.0\ g/kg \leq x \leq 1.0\ g/kg$	
Mixing ratio error	$x \leq 2.0\ g/kg$	
Wind direction bias	$-10.0^{o} \leq x \leq 10.0^{o}$	
Wind direction error	$x \leq 30^{o}$	
Wind speed root mean square error (RMSE)	$x \leq 2.0\ m/s$	

[1] Episodic benchmark applies to multi-day meteorological modeling episodes of duration less than 60 days that do not cross climatological seasons.
[2] Long-term benchmark applies to episodes of greater than 60 days or episodes that cross climatological seasons. If the long-term benchmark is not presented, use the episodic benchmark in order to assess performance.

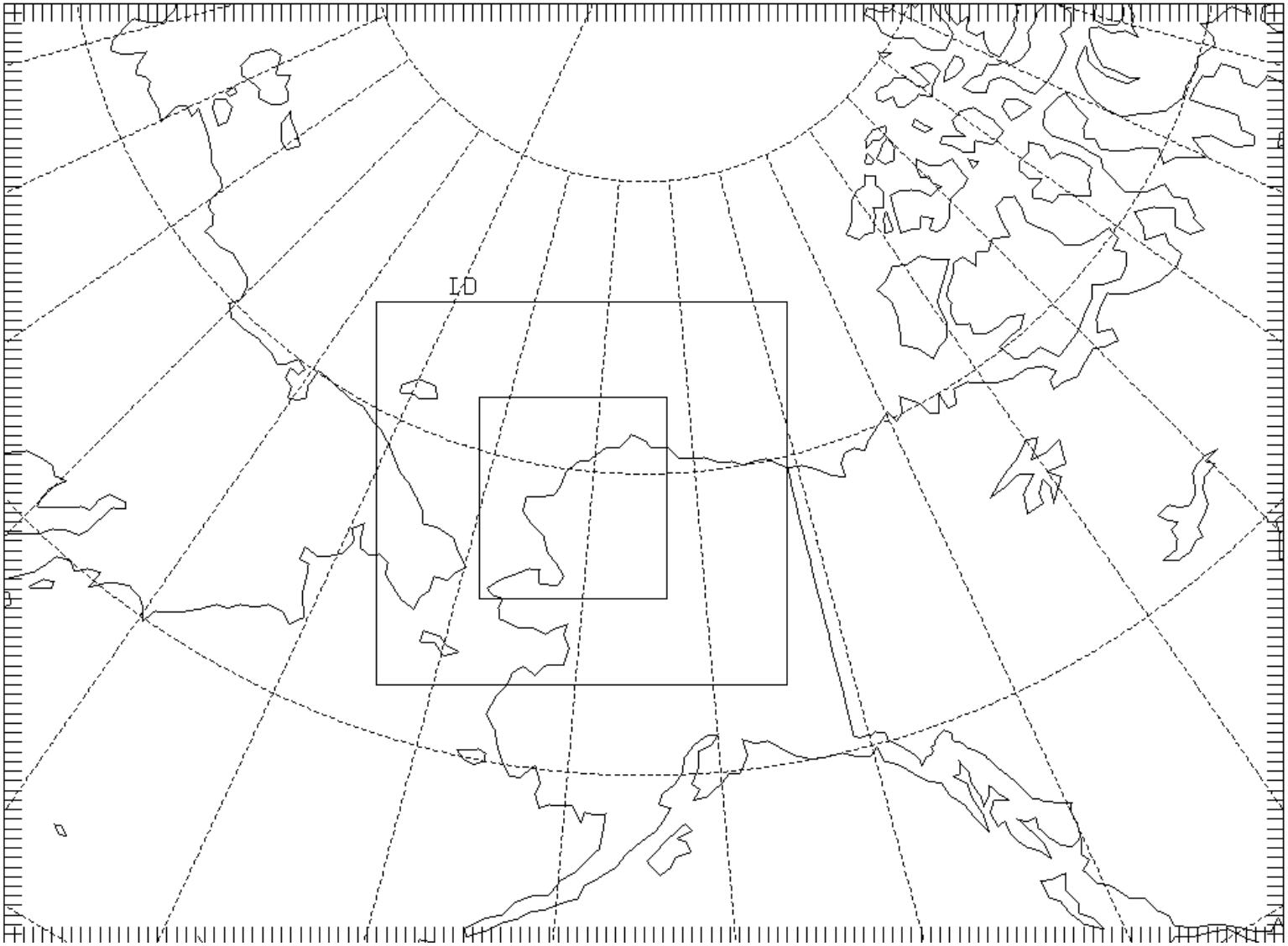

Figure 2-1. 36 km (Outer), 12 km and 4km (Inner) WRF Domain.

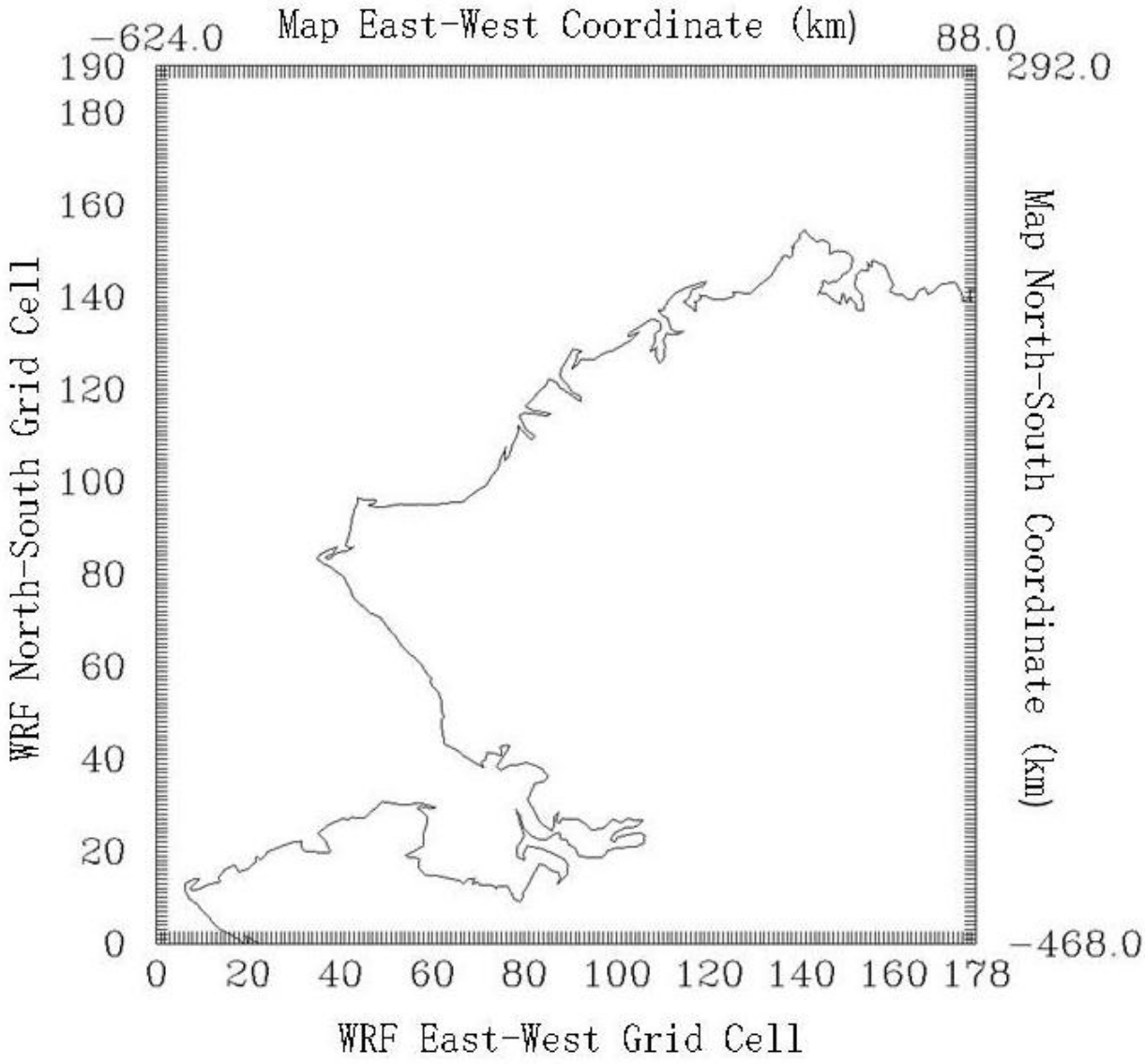

Figure 2-2. 4 km WRF Meteorological Modeling Domain. Units on Bottom and Left Axes are Grid Cells. Units on Top and Right Axes are Kilometers

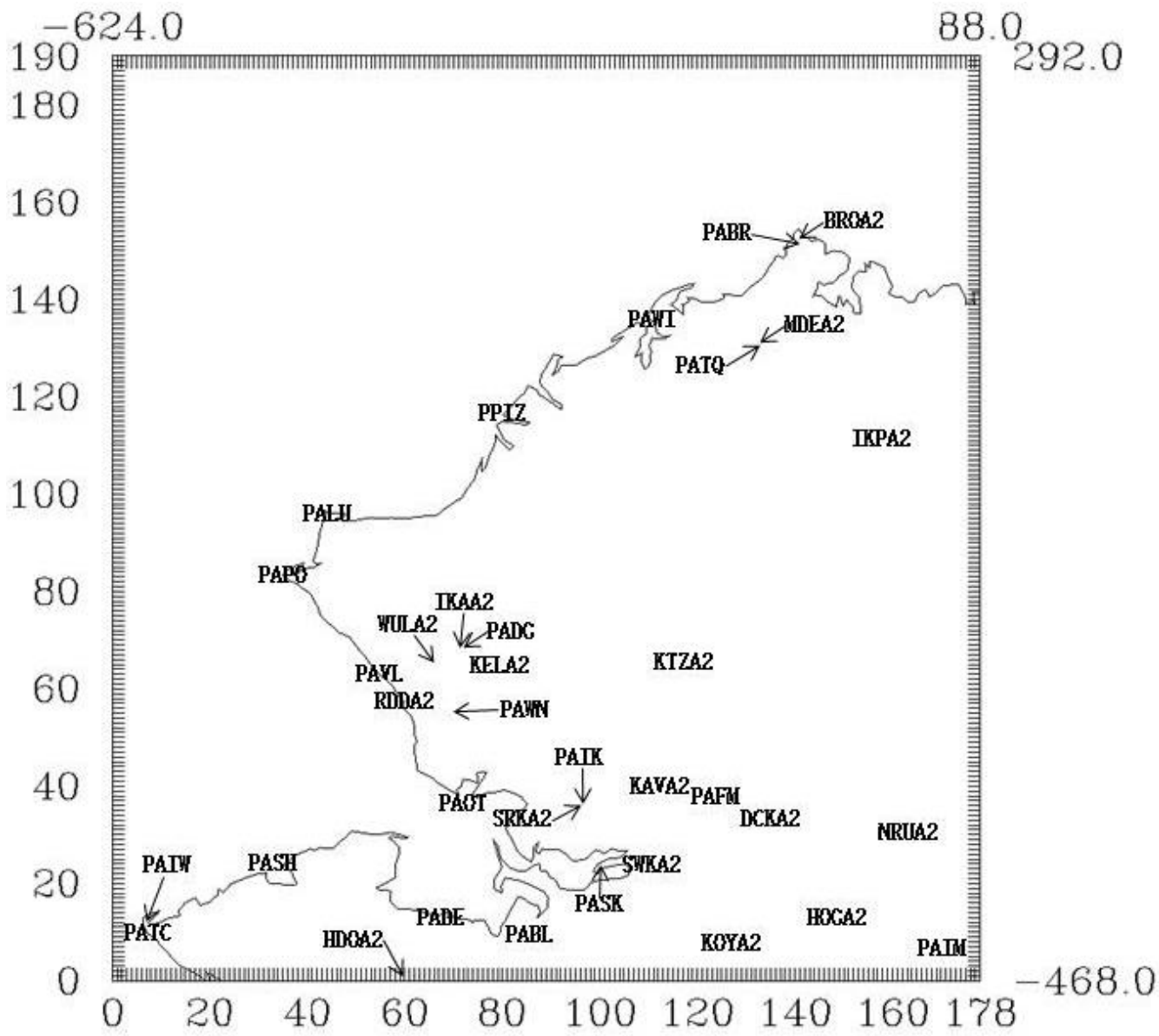

Figure 2-3. MADIS Stations in the 4km WRF Domain.

3 WRF PERFORMANCE EVALUATION RESULTS

Statistical operational model performance evaluation results are presented in this section. A multi-season, multi-year model evaluation is very difficult to summarize in a single document. The WRF results presented represent a synopsis of the analyses performed.

In summary, the WRF model simulations for 2007, 2008, and 2009 in aggregate exhibit very good model performance over the 4km modeling domain. Indeed, these are some of the best WRF model simulations that the study team has ever evaluated. Mean temperature bias and error statistics routinely fall within the long-term benchmarks and generally fall within the episodic benchmarks. Mean mixing ratio bias and error statistics all fall within the episodic benchmarks. Mean wind direction bias and error statistics routinely fall within the episodic benchmarks. Finally, the wind speed RMSE statistic routinely falls within the episodic benchmark.

3.1 Quantitative Model Evaluation Results

Model performance was conducted for all stations within the 4km modeling domain as well as for selected subdomains within the 4km modeling domain. The stations that are included in each subdomain are specified in Table 3-1.

3.1.1 Temperature Bias and Error

Temperature bias statistics for the 4km modeling domain are presented in Table 3-2. As can be seen in Table 3-2, the mean temperature bias over each modeling period for each analysis subdomain (column MEAN in Table 3-2) easily falls within the long-term benchmark statistic of $\pm$ 1.0 K (Table 2-4) with the exception of the SCOAST subdomain in 2009 (1.14 K). Similarly, mean temperature bias for each month over the entire domain (i.e., rows identified as ALL in the REGION column of Table 3-2) also meets the long-term benchmark with the exceptions of October in 2008 (1.13 K) and 2009 (1.15 K). Temperature bias for individual subdomains by month for each modeling period shows a mix of performance with a maximum temperature bias occurring in the SCOAST subdomain in November, 2009 (3.20 K). In general, WRF tends to overpredict temperatures during September and October and underpredict temperatures during July, August, and November.

Gross absolute temperature error statistics for the 4km modeling domain are presented in Table 3-3. As can be seen in Table 3-3, the mean temperature error over each modeling period for each analysis subdomain (column MEAN in Table 3-3) easily falls within the long-term benchmark statistic of 3.0 K (Table 2-4). Similarly, mean temperature error for each month over the entire domain (i.e., rows identified as ALL in the REGION column of Table 3-3) also meets the long-term benchmark with the exceptions of October, 2008 (4.40 K) and November, 2009 (3.78 K). Temperature error for individual subdomains by month for each modeling period shows a mix of performance with a maximum temperature error occurring in the SCOAST subdomain in October of 2009 (5.59 K). In general, WRF tends to better predict

temperatures during the warmer months of July, August, and September than it does during the colder months of October and November.

The domain average temperature bias and error are displayed graphically in Figure 3-1. This "soccer plot" depicts the monthly average bias verses the monthly average error over the entire 4km modeling domain. It is desirable to have all monthly values lay inside the long-term benchmark figure (a "goal"). Examination of Figure 3-1 shows that with the exceptions of October, 2008 (Figure 3-1b) and October and November, 2009 (Figure 3-1c), WRF meets the "goal."

Figure 3-2 depicts typical WRF temperature performance over an individual subdomain – North Coast. In this case, WRF does not meet the long-term benchmark "goal" for 2007 (Figure 3-2a), 2008 (Figure 3-2b), and 2009 (Figure 3-2c) with the exceptions of September in 2007, 2008 and 2009. These misses are due to the spread in the temperature bias more so than the spread in the temperature error. In the subdomains where WRF misses the "goal," the cause is about evenly divided between (1) spread in bias, (2) spread in error, and (3) both spread in bias and spread in error as the governing factor resulting in the miss.

An example of typical hourly spatial distributions of temperatures is presented in Figure 3-3 through Figure 3-8. Each figure represents the spatial distribution of temperature for a particular hour starting at 0Z (3:00 pm LST) on 15-July-2009 (Figure 3-3) progressing by four hours for each figure and finishing at 20Z (11:00 am) on 15-July-2009 (Figure 3-8). Colored diamonds in each figure show the location and magnitude of the observed temperature for those hours. It is interesting to note the extremely steep temperature gradient at the coast. With these steep gradients, it is little wonder that the bias and error statistics for the North Coast domain are outside of the guidelines. With these steep temperature gradients a small wind direction shift can dramatically influence the temperature at the coastal sites.

Figure 3-9 presents the hourly time series of observed and predicted temperatures at Wainwright for each month of the 2009 simulation. In Figure 3-9, the observed hourly temperatures are shown as blue asterisks with the minimum (black line) and maximum (red line) predicted temperatures extracted from a seven-by-seven, 4km grid cell subset centered on the monitor (approximately a 14km search radius), which is standard practice in model performance evaluations. As can be observed, WRF simulates the diurnal pattern at Wainwright well with the minimum and maximum temperature predictions generally bracketing the observed temperatures. In many situations the temperature gradient across the 28km area can be as large as 10 degrees C.

This study area was fortunate to have access to continuous tower data which was used to enhance the model performance evaluation. The ARM program operates a tower near Barrow that collects wind, temperature, and moisture at 2, 10, 20 and 40 meters above ground level. Figure 3-10 and Figure 3-11 present the ARM tower monthly temperature time series, analogous to the surface data presented in Figure 3-9. In Figure 3-10 and Figure 3-11, the left time series compare the 20m tower data as blue asterisks and the WRF level 2 temperatures

(~18m), whereas the series on the right compare the 40m tower data with the WRF level 3 temperatures (~32m). The model generally brackets the observations at both levels for June through September. In November the model tends to underestimate the temperature at 20m. Unfortunately the 40m instrument was not operational in November.

Figure 3-12 depicts an indicative example of the spatial mean hourly temperature for each month across the North Coast subdomain monitoring stations (i.e., NCOAST in Table 3-1) for 2009. Black asterisks present the mean hourly observed temperature, and the red line presents the mean hourly predicted temperature. Here again, we can observe that WRF does well at predicting the diurnal pattern of temperatures across the modeling period as well as capturing the general synoptic and seasonal temperature changes across the months in 2009. Similarly, WRF performs well for all stations within the 4km modeling domain in regards to the spatial mean hourly temperature (Figure 3-13).

3.1.2 Mixing Ratio Bias and Error

Mixing ratio bias statistics for the 4km modeling domain are presented in Table 3-4. As can be seen in Table 3-4, the mean mixing ratio bias over each modeling period for all analysis subdomains (column MEAN in Table 3-4) easily meets the episodic benchmark statistic of $\pm$ 1.0 g/kg (Table 2-4). The three year average for the full domain has an overall bias of -0.01 g/kg. Similarly, mean mixing ratio biases for each month over the entire domain (i.e., rows identified as ALL in the REGION column of Table 3-4) also meet the episodic benchmark. Mixing ratio biases for individual subdomains by month for each modeling year only fail to meet the episodic benchmark for the month of July, 2009 in the subdomains COAST (-1.01 g/kg), NCOAST (-1.39 g/kg), and NBROOKS (-1.30 g/kg). All three of these subdomains are dominated by coastal sites. In general, WRF tends to overpredict mixing ratio during September and October, underpredict mixing ratio during July, August, and has little bias during November.

Gross absolute mixing ratio error statistics for the 4km modeling domain are presented in Table 3-5. As can be seen in Table 3-5, the mean mixing ratio error over each modeling period for each analysis subdomain (column MEAN in Table 3-5) easily meets the episodic benchmark statistic of 2.0 g/kg (Table 2-4). Similarly, mean mixing ratio error for each month over the entire domain (i.e., rows identified as ALL in the REGION column of Table 3-5) also easily meets the episodic benchmark. The gross absolute error for all sites for the three mulit-month periods is 0.52 g/kg. Further, mixing ratio error for individual subdomains by month for each modeling period meet or exceed the episodic benchmark. In general, WRF does well at predicting mixing ratio across all groups of months.

Soccer plots of the domain average mixing ratio bias and error are presented in Figure 3-14. Examination of Figure 3-14 shows that WRF easily scores “goals” in all months for 2007 (Figure 3-14a), 2008 (Figure 3-14b), and 2009 (Figure 3-14c).

Figure 3-15 depicts typical WRF mixing ratio performance over the North Coast subdomain. In this case, WRF meets the long-term benchmark “goal” for 2007 (Figure 3-15a), 2008 (Figure

3-15b), and 2009 (Figure 3-15c) with the exception of July, 2009 where the miss is due to a larger bias spread. By examination of Table 3-4 and Table 3-5, WRF meets the episodic benchmark for the remaining subdomains with the exceptions of COAST and NBROOKS in July, 2009 again due more so to the spread in bias than the spread in error.

An example of typical hourly spatial distributions of mixing ratio is presented in Figure 3-16 through Figure 3-21. Each figure represents the spatial distribution of mixing ratio for a particular hour starting at 0Z (3:00 pm LST) on 15-July-2009 (Figure 3-16) progressing by four hours for each figure and finishing at 20Z (11:00 am) on 15-July-2009 (Figure 3-21). Colored diamonds in each figure show the location and magnitude of the observed mixing ratio for those hours. Examination of Figure 3-16 through Figure 3-21 indicates that WRF is generally within $\pm$ 1.0 g/kg of the observed mixing ratio which demonstrates WRF captures well the diurnal evolution of the mixing ratio. As with the temperature, it is interesting how steep the moisture gradient is along the coast.

Figure 3-22 presents the hourly time series of observed and predicted mixing ratio at Wainwright for each month of the 2009 simulation. In Figure 3-22, the observed hourly mixing ratios are shown as blue asterisks with the minimum (black line) and maximum (red line) predicted temperatures extracted from a seven-by-seven, 4km grid cell subset centered on the monitor. As can be observed, WRF does fairly well at simulating the mixing ratio diurnal pattern at Wainwright with the minimum and maximum mixing ratio predictions generally within $\pm$ 1.0 g/kg of the observed mixing ratios.

Figure 3-23 and Figure 3-24 present the ARM tower monthly mixing ratio time series, analogous to the surface data presented in Figure 3-22. In Figure 3-23 and Figure 3-24, the left time series compare the 20m tower data as blue asterisks and the WRF level 2 mixing ratios (~18m), whereas the series on the right compare the 40m tower data with the WRF level 3 mixing ratios (~32m). The model generally follows the synoptic moisture cycles but tends to somewhat underestimate mixing ratio in much of the latter half of July. The 20m observations are suspect in the latter half of October where the data exhibits unrealistic hour to hour scatter. The 40m observations are missing for November.

Figure 3-21 depicts an indicative example of the spatial mean hourly mixing ratio for each month across the North Coast subdomain monitoring stations (i.e., NCOAST in Table 3-1) for 2009. Black asterisks present the mean hourly observed mixing ratio, and the red line presents the mean hourly predicted mixing ratio. Here again, we can observe that WRF does well at predicting the synoptic pattern of mixing ratios across the modeling period. Similarly, WRF performs well for all stations within the 4km modeling domain in regards to the spatial mean hourly mixing ratio (Figure 3-26).

3.1.3 Wind Direction Bias, Wind Direction Error, and Wind Speed RMSE

Comparisons between the current WRF modeling and winds from the NCDC MADIS surface observations were made using the wind direction bias, and wind direction error, and the wind

speed Root Mean Square Error (RMSE) statistics. The wind direction bias model performance results for the 4km domain are presented in Table 3-6. Examination of Table 3-6 indicates that the mean wind direction bias over each modeling period for all analysis subdomains (column MEAN in Table 3-6) meets the episodic benchmark statistic of $\pm$ 10.0^o (Table 2-4) with the exceptions of NBROOKS in 2007 (-10.84^o) and 2008 (-12.53^o) and NCOAST in 2007 (-10.40^o) and 2008 (-11.43^o), where the benchmark is slightly exceeded. Further, mean wind direction biases for each month over the entire domain (i.e., rows identified as ALL in the REGION column of Table 3-6) meet the episodic benchmark with the exception of July, 2008 (-12.48^o). On a subdomain basis by month, WRF generally meets the episodic benchmark with the maximum wind direction bias occurring in NBROOKS and NCOAST during September of all three modeling years.

Wind direction error for the 4km grid is presented in Table 3-7. Examination of Table 3-7 indicates that the mean wind direction error over each modeling period for all analysis subdomains (column MEAN in Table 3-7) meets the episodic benchmark statistic of 30.0^o (Table 2-4) with the exceptions of SOUTH in 2007 (33.96^o) and 2009 (32.40^o). Mean wind direction errors for each month over the entire domain (i.e., rows identified as ALL in the REGION column of Table 3-7) meet the episodic benchmark with the exception of July, 2007 (49.19^o), October, 2007 (32.37^o), and October, 2009 (46.97^o). Though WRF generally is able to adequately replicate wind direction in the subdomains by month, it appears to have its greatest performance difficulties in the SCOAST and SOUTH in 2007 and 2009.

Wind speed root mean square error (RMSE) for the 4km grid is presented in Table 3-8. Examination of Table 3-8 indicates that the mean wind direction error over each modeling period for all analysis subdomains (column MEAN in Table 3-8) meets the episodic benchmark statistic of 2.0 m/s (Table 2-4) with the exceptions of a small exceedences by ALL in 2007 (2.03 m/s) and SOUTH in 2007 (2.07 m/s). Wind speed RMSE for each month over the entire domain (i.e., rows identified as ALL in the REGION column of Table 3-8) meets the episodic benchmark with the exception of October (2.26 m/s) and November (3.59 m/s) in 2007 and August (2.40 m/s) and November (2.01 m/s) in 2009. Though WRF generally is able to adequately replicate wind speeds in the subdomains by month, it appears to have its greatest performance difficulties in October and November of 2007 and August and November of 2009.

Soccer plots of wind speed RMSE versus wind direction error for all stations in the 4km modeling domain are presented in Figure 3-27. Figure 3-27 shows that the model generally meets the episodic benchmark goal with best performance showing in 2008 (Figure 3-27b), followed by 2009 (Figure 3-27c) and 2007 (Figure 3-27a).

An example of subdomain model performance for wind speed RMSE versus wind direction error is shown for NCOAST in Figure 3-28. Examination of Figure 3-28 shows that for NCOAST, WRF performs best during 2009 (Figure 3-28c) meeting the “goal” for all months followed by roughly equal performance characteristics for 2007 (Figure 3-28a) and 2008 (Figure 3-28b) where the “goal” is missed during November.

Hourly spatial mean wind direction for all NCOAST stations is presented in Figure 3-29 where observed hourly spatial mean wind direction is shown as red asterisks and predicted hourly spatial mean wind direction is shown as a black line. As can be observed in Figure 3-29, WRF routinely reproduces observed hourly spatial mean wind directions, including the wind shifts indicative of frontal passages. This is important, for these coastal sites, as it indicates the model is altering the land-sea breeze in response to large scale forcing. Similarly, Figure 3-30 shows WRF does well at reproducing hourly spatial mean wind direction for all stations in the 4km modeling domain.

Soccer plots of wind speed bias versus wind speed RMSE for all stations in the 4km modeling domain are presented in Figure 3-31. Figure 3-31 shows that the model routinely meets the episodic benchmark goal with best performance showing in 2008 (Figure 3-31b), followed by 2009 (Figure 3-31c) and 2007 (Figure 3-31a). In all three years November is separated from the rest of the months.

An example of subdomain model performance for wind speed bias versus wind speed RMSE is shown for NCOAST in Figure 3-32. Examination of Figure 3-32 shows that for NCOAST, WRF performs best during 2008 (Figure 3-32b) meeting the "goal" for all months except November followed by 2009 (Figure 3-32a) with the "goal" missed in October and 2007 (Figure 3-32b) where the "goal" is missed during October and November. As with the full domain (Figure 3-31), November is separated from the other months for all three years. October is separated in 2007 and 2009.

Hourly spatial mean vector wind speed for all NCOAST stations is presented in Figure 3-33 where observed hourly spatial mean wind direction is shown as red asterisks and predicted hourly spatial mean wind direction is shown as a black line. As can be observed in Figure 3-33, WRF adequately reproduces observed hourly spatial mean vector wind speeds with an absolute error that rarely exceeds 2.0 m/s even under stagnating conditions. Similarly, Figure 3-34 shows WRF does well at reproducing hourly spatial mean vector wind speed for all stations in the 4km modeling domain again with absolute errors that rarely exceed 2.0 m/s. Not surprisingly, the WRF simulation has less hour to hour wind speed variation than the observations. The WRF simulation does a very good job on the timing of wind speed increases from synoptic events.

An example of typical hourly spatial distributions of wind speed and direction is presented in Figure 3-35 through Figure 3-40. Each figure represents the spatial distribution of wind speed and direction for a particular hour starting at 0Z (3:00 pm LST) on 15-July-2009 (Figure 3-35) progressing by four hours for each figure and finishing at 20Z (11:00 am) on 15-July-2009 (Figure 3-40). Red arrows in each figure show the location, magnitude, and direction of the observed wind field for those hours. Examination of Figure 3-35 Figure 3-40 indicates that WRF generally does well at replicating the magnitudes and direction of the winds with a very good capability of capturing the land-sea breeze interface. Additionally, it appears the WRF simulation is accurately capturing the quite complex flows around Point Hope.

3.2 Qualitative Monthly Precipitation Analysis

This section presents qualitative comparisons of WRF estimated monthly precipitation with the available monthly precipitation measurements. This evaluation is qualitative given that predicting individual precipitation events, both duration and magnitude, is very difficult to accomplish; therefore, the goal of this qualitative comparison is to determine if the WRF monthly precipitation predictions can capture, in an aggregate sense, observed monthly total (i.e., does WRF show precipitation when there is observed precipitation?).

Monthly total precipitation comparisons for 2007 for the 4km modeling domain are presented in Figure 3-41 through Figure 3-45. The shaded diamonds represent monthly total observed precipitation. Examination of these figures indicates that WRF routinely is able to model total monthly precipitation within about a factor of four when there is observed precipitation. The noticeable exception is Shishmaref Airport (PASH) in July (Figure 3-41) and August (Figure 3-42) where WRF underpredicts precipitation by more than a factor of ten. However, when taken in aggregate, WRF is modeling precipitation when there is observed precipitation during the 2007 simulation.

Monthly total precipitation comparisons for 2008 for the 4km modeling domain are presented in Figure 3-46 through Figure 3-50. Examination of these figures indicates that WRF routinely is able to model total monthly precipitation within about a factor of four when there is observed precipitation, though there is a noticeable overprediction of precipitation in the northern half of the 4km modeling domain during the month of October. However, when taken in aggregate, WRF is modeling precipitation when there is observed precipitation during the 2008 simulation with a small overprediction bias overall.

Monthly total precipitation comparisons for 2009 for the 4km modeling domain are presented in Figure 3-51 through Figure 3-55. Examination of these figures indicates that WRF routinely is able to model total monthly precipitation within about a factor of four when there is observed precipitation. When taken in aggregate, WRF is modeling precipitation when there is observed precipitation during the 2009 simulation with a small overprediction bias overall.

3.3 Radiosonde Evaluation

A radiosonde is an electronic instrument package that hangs beneath a helium-filled weather balloon. The instruments in a radiosonde measure temperature, air pressure, and relative humidity as a function of height as the balloon floats upward to a maximum height of about 31 kilometers. Because the instruments have a radio transmitter attached, continuous upper-air readings are sent to ground stations. Also, radiosondes are typically tracked via radar, or contain Global Positioning System (GPS) instrumentation, thus allowing for estimates of wind speed and direction with height.

Representative Skew T-log P plots are presented for the radiosonde located in Barrow for the following dates:

- 12Z (3:00 am LST) on 15-July-2009 (Figure 3-57);
- 0Z (3:00 pm LST) on 16-July-2009 (Figure 3-58);
- 12Z (3:00 am LST) on 15-August-2009 (Figure 3-59);
- 0Z (3:00 pm LST) on 16-August-2009 (Figure 3-60);
- 12Z (3:00 am) on 15-September-2009 (Figure 3-61);
- 0Z (3:00 pm LST) on 16-September-2009 (Figure 3-62);
- 12Z (3:00 am) on 15-October-2009 (Figure 3-63);
- 0Z (3:00 pm LST) on 16- October -2009 (Figure 3-64);
- 12Z (3:00 am) on 15-November-2009 (Figure 3-65); and
- 0Z (3:00 pm LST) on 16- November -2009 (Figure 3-66).

The black lines and black wind flags are the observations, and the red lines and red wind flags are the WRF model predictions. The black and red lines that are located in the left part of the plot represent the dew point temperature whereas the black and red lines on the right part of the plot represent the atmospheric temperature (note that the black lines on the left and right hand side of the plot will only lay on top of one another under extremely moist (saturation) conditions). Units on the Skew-T-log P are millibars for pressure and Celsius for temperature.

In terms of atmospheric temperature, WRF does reasonably well at reproducing the observed atmospheric temperature throughout the depth of the atmosphere for periods presented in 2009. WRF has more difficulty in replicating the dew point temperatures during this period especially above about 300 mb. In terms of wind speed and direction, WRF also does reasonably well at replicating observations. Overall, for Barrow, WRF is performing well in terms of reproducing observations from the radiosondes.

3.4 Summary of Model Performance Evaluation

Temperature bias and error statistics, mixing ratio bias and error statistics, wind direction bias and error, and wind speed RMSE statistics were estimated for the model predictions in 4km modeling domain. In addition to the aforementioned statistics, spatial distributions and temporal evolutions of temperatures, mixing ratios, and wind speeds and directions were explored both for the entire 4km modeling domain, for selected clusters of stations, and for an individual station. Further, a qualitative examination of model predicted precipitation, both total and spatial extent, and gridded wind vectors was performed. Finally, WRF model performance was explored for an individual radiosonde over the course of the simulations.

When these metrics were explored over the entire domain, we find that WRF routinely does well at replicating observed atmospheric values of temperature, mixing ratio, wind speeds and direction, and precipitation. Our examination of the same metrics by month over the entire 4km modeling domain also indicates that WRF, in general, does well at reproducing observations. When we further refine our investigation by subdomain, we also see that WRF

does reasonably well at predicting the observations, even in the challenging coastal regions. Taken in aggregate, this is probably the best performing set of WRF simulations that the study team has had the privilege of evaluating, including both annual and winter simulations in the intermountain west, multi-annual simulations in the Gulf Coast, and annual simulations along the eastern seaboard of the United States. The study team has no reservations in recommending the use of these data for subsequent air quality modeling analyses.

Table 3-1. List of Stations and Their Associated Subdomains.

Station ID	Station Name	Subdomains				
		COAST	NCOAST	SCOAST	SOUTH	NBROOKS
BROA2	CRN Site Near Barrow	√	√			√
DCKA2	Dahl Creek Near Kobuk				√	
HDOA2	Hoodoo Hill				√	
HOGA2	Hogatyza River				√	
IKAA2	Ikalukrok Creek				√	
IKPA2	Ikpikpuk River				√	
KAVA2	Kavet Creek				√	
KELA2	Kelly				√	
KOYA2	Koyukuk NWR				√	
KTZA2	Noatak				√	
MDEA2	Meade River at Atqasak					√
NRUA2	Norutak Lake				√	
PABL	Buckland Airport				√	
PABR	Wiley Post-Will Rogers Memorial Airport	√	√			√
PADE	Deering Airport	√		√	√	
PADG	Red Dog Airport				√	
PAFM	Ambler Airport				√	
PAIK	Bob Baker Memorial Airport				√	
PAIM	Indian Mountain LRRS Airport				√	
PAIW	Wales Airport	√		√	√	
PALU	Cape Lisburne LRRS Airport	√	√			√
PAOT	Ralph Wien Mrmorial Airport	√		√	√	
PAPO	Point Home Airport	√	√			√
PASH	Shishmaref Airport	√		√	√	
PASK	Selawik Airport	√		√	√	
PATC	Tin City LRRS Airport	√		√	√	
PATQ	Atqasuk Edward Burnell Sr. Memorial Airport					√
PAVL	Kivalina Airport	√		√	√	
PAWI	Wainwright Airport	√	√			√
PAWN	Noatak Airport				√	
PPIZ	Point Lay LRRS Airport	√	√			√
RDDA2	Red Dog Dock	√		√	√	
SRKA2	Kiana				√	
SWKA2	Selawik	√		√	√	
WULA2	Wulik River Near Kivalina				√	

Table 3-2. Temperature Bias (K) for WRF by Month and Analysis Region in the 4 km Domain.

Region	Jul	Aug	Sep	Oct	Nov	Mean
2007						
ALL	-0.34	-0.36	0.28	0.65	-0.32	-0.02
COAST	-1.08	-0.93	0.36	1.20	-0.54	-0.20
NBROOKS	-1.21	-1.21	0.26	1.15	-2.10	-0.62
NCOAST	-1.65	-1.58	0.10	1.20	-2.22	-0.83
SCOAST	-0.70	-0.48	0.50	1.22	0.77	0.26
SOUTH	-0.07	-0.08	0.28	0.50	0.34	0.19
2008						
ALL	-0.49	-0.38	0.00	1.13	-0.88	-0.12
COAST	-1.11	-0.59	0.15	1.81	-1.23	-0.19
NBROOKS	-1.48	-1.01	0.01	1.40	-2.31	-0.68
NCOAST	-1.74	-1.13	-0.01	1.47	-2.33	-0.75
SCOAST	-0.61	-0.18	0.26	2.05	-0.29	0.25
SOUTH	-0.11	-0.09	0.04	1.07	-0.38	0.11
2009						
ALL	-0.71	0.21	0.39	1.15	0.41	0.29
COAST	-2.14	-0.03	0.93	2.08	0.81	0.33
NBROOKS	-2.50	-0.85	0.61	1.64	-1.91	-0.60
NCOAST	-2.94	-1.08	0.66	1.89	-1.42	-0.58
SCOAST	-1.52	0.65	1.12	2.25	3.20	1.14
SOUTH	-0.18	0.49	0.32	0.98	1.60	0.64
Average						
ALL	-0.51	-0.18	0.22	0.98	-0.26	0.05
COAST	-1.44	-0.52	0.48	1.70	-0.32	-0.02
NBROOKS	-1.73	-1.02	0.29	1.40	-2.11	-0.63
NCOAST	-2.11	-1.26	0.25	1.52	-1.99	-0.72
SCOAST	-0.94	0.00	0.63	1.84	1.23	0.55
SOUTH	-0.12	0.11	0.21	0.85	0.52	0.31

Table 3-3. Temperature Error (K) for WRF by Month and Analysis Region in the 4 km Domain.

Region	Jul	Aug	Sep	Oct	Nov	Mean
2007						
ALL	2.49	1.62	0.94	2.45	2.87	2.07
COAST	3.65	1.46	0.87	2.57	2.56	2.22
NBROOKS	2.37	1.68	0.94	2.64	3.72	2.27
NCOAST	2.62	1.77	0.93	2.45	3.21	2.20
SCOAST	4.32	1.24	0.84	2.68	2.14	2.24
SOUTH	2.53	1.60	0.94	2.38	2.60	2.01
2008						
ALL	0.85	1.46	1.50	2.88	2.45	1.83
COAST	0.76	1.31	1.73	3.04	2.79	1.93
NBROOKS	0.96	1.64	1.64	2.53	1.86	1.73
NCOAST	0.96	1.59	1.83	2.55	2.04	1.79
SCOAST	0.60	1.11	1.64	3.35	3.34	2.01
SOUTH	0.83	1.42	1.50	3.01	2.69	1.89
2009						
ALL	1.51	1.30	1.55	4.40	3.78	2.51
COAST	1.44	1.41	1.94	5.53	3.77	2.82
NBROOKS	2.11	1.40	1.68	5.03	2.25	2.49
NCOAST	2.34	1.27	2.07	5.46	2.43	2.71
SCOAST	0.99	1.52	1.84	5.59	4.83	2.95
SOUTH	1.34	1.27	1.51	4.14	4.36	2.52
Average						
ALL	1.62	1.46	1.33	3.24	3.03	2.14
COAST	1.95	1.39	1.51	3.71	3.04	2.32
NBROOKS	1.81	1.57	1.42	3.40	2.61	2.16
NCOAST	1.97	1.54	1.61	3.49	2.56	2.23
SCOAST	1.97	1.29	1.44	3.87	3.44	2.40
SOUTH	1.57	1.43	1.32	3.18	3.22	2.14

Table 3-4. Mixing Ratio Bias (g/kg) for WRF by Month and Analysis Region in the 4 km Domain.

Region	Jul	Aug	Sep	Oct	Nov	Mean
2007						
ALL	-0.43	-0.28	0.16	0.26	0.00	-0.06
COAST	-0.35	-0.34	0.21	0.33	-0.01	-0.03
NBROOKS	-0.68	-0.58	0.20	0.26	-0.22	-0.20
NCOAST	-0.59	-0.67	0.19	0.31	-0.22	-0.20
SCOAST	-0.14	-0.02	0.24	0.36	0.18	0.12
SOUTH	-0.28	-0.08	0.13	0.27	0.16	0.04
2008						
ALL	-0.28	-0.13	0.11	0.30	-0.02	0.00
COAST	-0.38	-0.15	0.16	0.37	-0.05	-0.01
NBROOKS	-0.59	-0.18	0.16	0.33	-0.13	-0.08
NCOAST	-0.54	-0.17	0.19	0.35	-0.13	-0.06
SCOAST	-0.23	-0.13	0.12	0.38	0.01	0.03
SOUTH	-0.10	-0.11	0.11	0.30	0.04	0.05
2009						
ALL	-0.72	0.03	0.27	0.49	0.16	0.05
COAST	-1.01	0.13	0.43	0.63	0.23	0.08
NBROOKS	-1.30	-0.11	0.32	0.47	-0.01	-0.13
NCOAST	-1.39	-0.09	0.36	0.54	0.02	-0.11
SCOAST	-0.67	0.28	0.49	0.70	0.43	0.25
SOUTH	-0.42	0.10	0.25	0.50	0.28	0.14
Average						
ALL	-0.48	-0.13	0.18	0.35	0.05	-0.01
COAST	-0.58	-0.12	0.27	0.44	0.06	0.01
NBROOKS	-0.86	-0.29	0.23	0.35	-0.12	-0.14
NCOAST	-0.84	-0.31	0.25	0.40	-0.11	-0.12
SCOAST	-0.35	0.04	0.28	0.48	0.21	0.13
SOUTH	-0.27	-0.03	0.16	0.36	0.16	0.08

Table 3-5. Mixing Ratio Error (g/kg) for WRF by Month and Analysis Region in the 4 km Domain.

Region	Jul	Aug	Sep	Oct	Nov	Mean
2007						
ALL	0.82	0.73	0.46	0.36	0.34	0.54
COAST	0.80	0.74	0.44	0.41	0.36	0.55
NBROOKS	0.86	0.87	0.46	0.37	0.42	0.60
NCOAST	0.80	0.83	0.41	0.40	0.43	0.57
SCOAST	0.79	0.65	0.46	0.42	0.29	0.52
SOUTH	0.79	0.64	0.45	0.35	0.28	0.50
2008						
ALL	0.68	0.52	0.40	0.37	0.22	0.44
COAST	0.71	0.53	0.42	0.44	0.24	0.47
NBROOKS	0.75	0.42	0.33	0.39	0.27	0.43
NCOAST	0.73	0.43	0.36	0.40	0.28	0.44
SCOAST	0.70	0.61	0.47	0.47	0.21	0.49
SOUTH	0.64	0.59	0.44	0.38	0.20	0.45
2009						
ALL	0.98	0.56	0.50	0.56	0.36	0.59
COAST	1.17	0.56	0.55	0.66	0.45	0.68
NBROOKS	1.34	0.47	0.43	0.51	0.30	0.61
NCOAST	1.42	0.49	0.47	0.57	0.32	0.65
SCOAST	0.94	0.61	0.61	0.74	0.57	0.69
SOUTH	0.80	0.60	0.53	0.58	0.40	0.58
Average						
ALL	0.83	0.60	0.45	0.43	0.31	0.52
COAST	0.89	0.61	0.47	0.50	0.35	0.57
NBROOKS	0.98	0.59	0.41	0.42	0.33	0.55
NCOAST	0.98	0.58	0.41	0.46	0.34	0.56
SCOAST	0.81	0.62	0.51	0.54	0.36	0.57
SOUTH	0.74	0.61	0.47	0.44	0.29	0.51

Table 3-6. Wind Direction Bias (deg.) for WRF by Month and Analysis Region in the 4 km Domain.

Region	Jul	Aug	Sep	Oct	Nov	Mean
2007						
ALL	-1.49	-6.43	-6.86	-4.16	-0.93	-3.97
COAST	0.56	-11.25	-5.39	-3.10	0.31	-3.77
NBROOKS	-6.49	-11.32	-22.91	-8.85	-4.62	-10.84
NCOAST	-7.32	-11.16	-21.99	-7.85	-3.68	-10.40
SCOAST	6.11	-11.31	2.33	0.83	3.17	0.23
SOUTH	0.52	-4.75	-2.29	-2.13	0.53	-1.62
2008						
	-12.48	-7.28	-9.92	-9.49	-2.60	-8.35
COAST	-13.04	-7.85	-14.63	-4.75	-7.82	-9.62
NBROOKS	-11.60	-10.48	-23.44	-13.40	-3.72	-12.53
NCOAST	-9.68	-11.43	-25.61	-6.72	-3.72	-11.43
SCOAST	-15.86	-5.77	-8.11	-4.05	-9.43	-8.64
SOUTH	-12.80	-6.24	-6.13	-8.71	-2.27	-7.23
2009						
ALL	-7.98	0.42	-7.10	-6.74	-9.30	-6.14
COAST	-9.91	-4.11	-12.56	0.55	-10.57	-7.32
NBROOKS	3.26	-4.72	-17.81	12.21	-8.95	-3.20
NCOAST	2.18	-5.64	-18.63	12.61	-7.29	-3.35
SCOAST	-16.16	-3.19	-8.63	-6.28	-12.74	-9.40
SOUTH	-11.72	1.88	-4.24	-12.69	-9.46	-7.25
Average						
ALL	-7.32	-4.43	-7.96	-6.80	-4.28	-6.16
COAST	-7.46	-7.74	-10.86	-2.43	-6.03	-6.90
NBROOKS	-4.94	-8.84	-21.39	-3.35	-5.76	-8.86
NCOAST	-4.94	-9.41	-22.08	-0.65	-4.90	-8.40
SCOAST	-8.64	-6.76	-4.80	-3.17	-6.33	-5.94
SOUTH	-8.00	-3.04	-4.22	-7.84	-3.73	-5.37

Table 3-7. Wind Direction Error (deg.) for WRF by Month and Analysis Region in the 4 km Domain.

Region	Jul	Aug	Sep	Oct	Nov	Mean
2007						
ALL	49.19	27.05	18.40	32.37	17.78	28.96
COAST	45.42	20.91	18.60	23.94	10.67	23.91
NBROOKS	18.51	16.55	24.83	14.67	9.72	16.86
NCOAST	21.06	17.24	24.55	14.63	9.79	17.45
SCOAST	62.59	23.50	15.84	31.64	11.30	28.97
SOUTH	61.55	30.66	16.57	40.06	20.97	33.96
2008						
ALL	22.17	21.52	21.36	20.76	27.78	22.72
COAST	21.44	17.53	19.39	15.26	22.24	19.17
NBROOKS	15.49	16.77	26.52	25.47	12.06	19.26
NCOAST	14.33	19.09	29.26	21.20	13.09	19.39
SCOAST	27.42	16.63	13.53	13.15	25.83	19.31
SOUTH	24.61	23.06	19.91	19.81	32.42	23.96
2009						
ALL	29.63	15.22	23.14	46.97	27.12	28.42
COAST	25.05	11.45	22.57	33.75	23.41	23.25
NBROOKS	19.75	10.15	21.50	17.68	14.86	16.79
NCOAST	19.38	10.97	22.74	19.77	14.61	17.49
SCOAST	27.98	11.74	22.45	41.68	29.23	26.62
SOUTH	32.92	16.66	23.58	56.16	32.69	32.40
Average						
ALL	33.66	21.26	20.97	33.37	24.23	26.70
COAST	30.64	16.63	20.19	24.32	18.77	22.11
NBROOKS	17.92	14.49	24.28	19.27	12.21	17.64
NCOAST	18.26	15.77	25.52	18.53	12.50	18.11
SCOAST	39.33	17.29	17.27	28.82	22.12	24.97
SOUTH	39.69	23.46	20.02	38.68	28.69	30.11

Table 3-8. Wind Speed RMSE (m/s) for WRF by Month and Analysis Region in the 4 km Domain.

Region	Jul	Aug	Sep	Oct	Nov	Mean
2007						
ALL	1.29	1.30	1.69	2.26	3.59	2.03
COAST	1.35	1.10	1.32	1.97	3.02	1.75
NBROOKS	1.47	1.12	1.50	2.01	3.37	1.89
NCOAST	1.45	0.99	1.39	2.08	3.35	1.85
SCOAST	1.28	1.17	1.29	1.88	2.76	1.68
SOUTH	1.21	1.36	1.74	2.37	3.67	2.07
2008						
ALL	1.69	1.39	1.70	1.65	1.60	1.61
COAST	1.04	1.25	1.37	1.67	1.70	1.41
NBROOKS	2.14	1.32	1.05	1.41	1.73	1.53
NCOAST	1.16	1.09	0.86	1.40	1.37	1.18
SCOAST	0.93	1.33	1.59	1.75	1.82	1.48
SOUTH	1.49	1.42	1.84	1.69	1.56	1.60
2009						
ALL	1.75	2.40	1.67	1.56	2.01	1.88
COAST	1.72	2.49	1.56	1.56	2.05	1.88
NBROOKS	1.60	2.13	1.52	1.48	1.85	1.72
NCOAST	1.66	2.18	1.48	1.34	1.83	1.70
SCOAST	1.75	2.66	1.61	1.67	2.18	1.97
SOUTH	1.79	2.47	1.71	1.59	2.08	1.93
Average						
ALL	1.58	1.70	1.69	1.82	2.40	1.84
COAST	1.37	1.61	1.42	1.73	2.26	1.68
NBROOKS	1.74	1.52	1.36	1.63	2.32	1.71
NCOAST	1.42	1.42	1.24	1.61	2.18	1.58
SCOAST	1.32	1.72	1.50	1.77	2.25	1.71
SOUTH	1.50	1.75	1.76	1.88	2.44	1.87

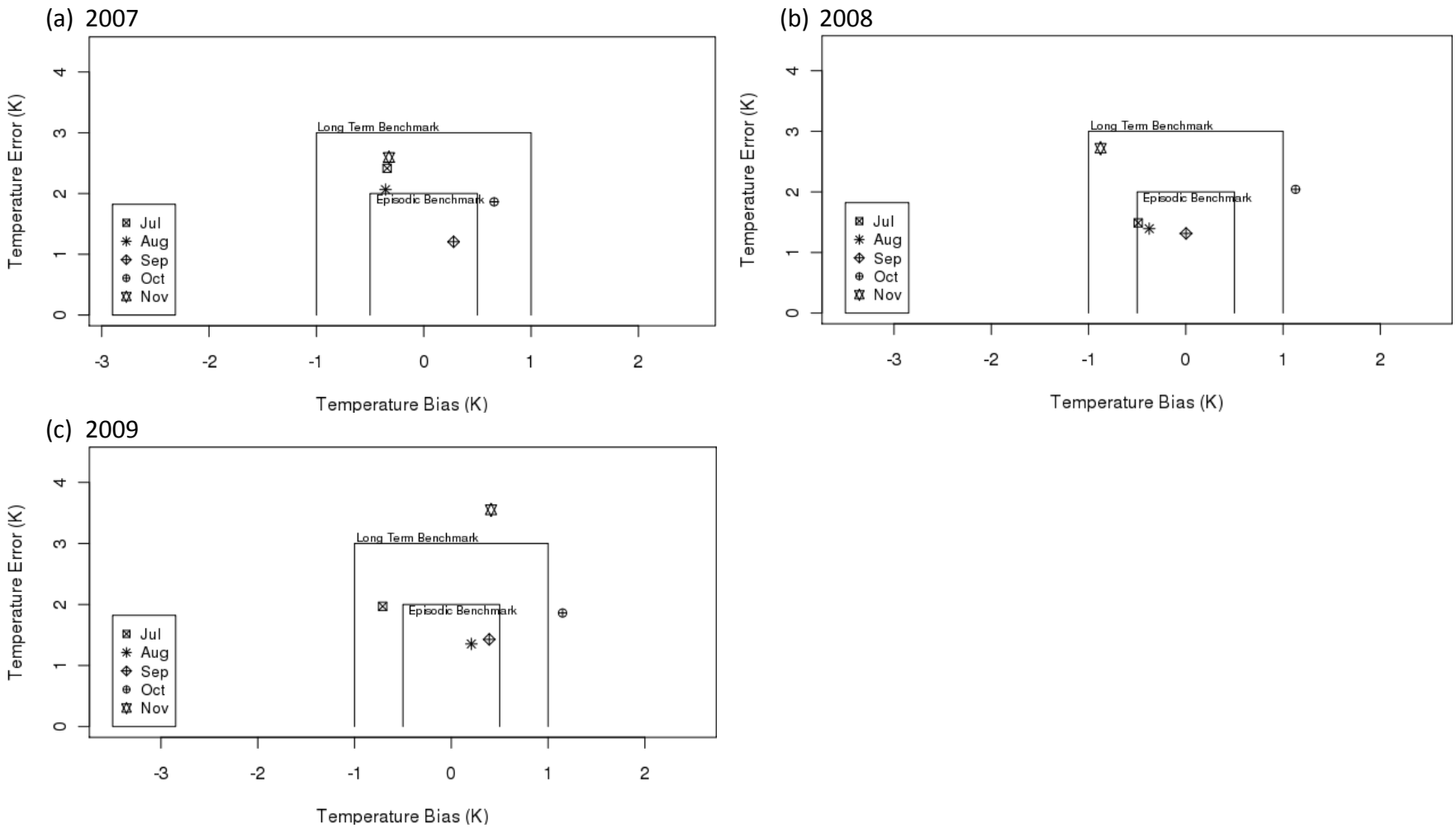

Figure 3-1. Temperature Bias and Error Soccer Plots by Month for All Stations in the 4km Domain for (a) 2007, (b) 2008, and (c) 2009.

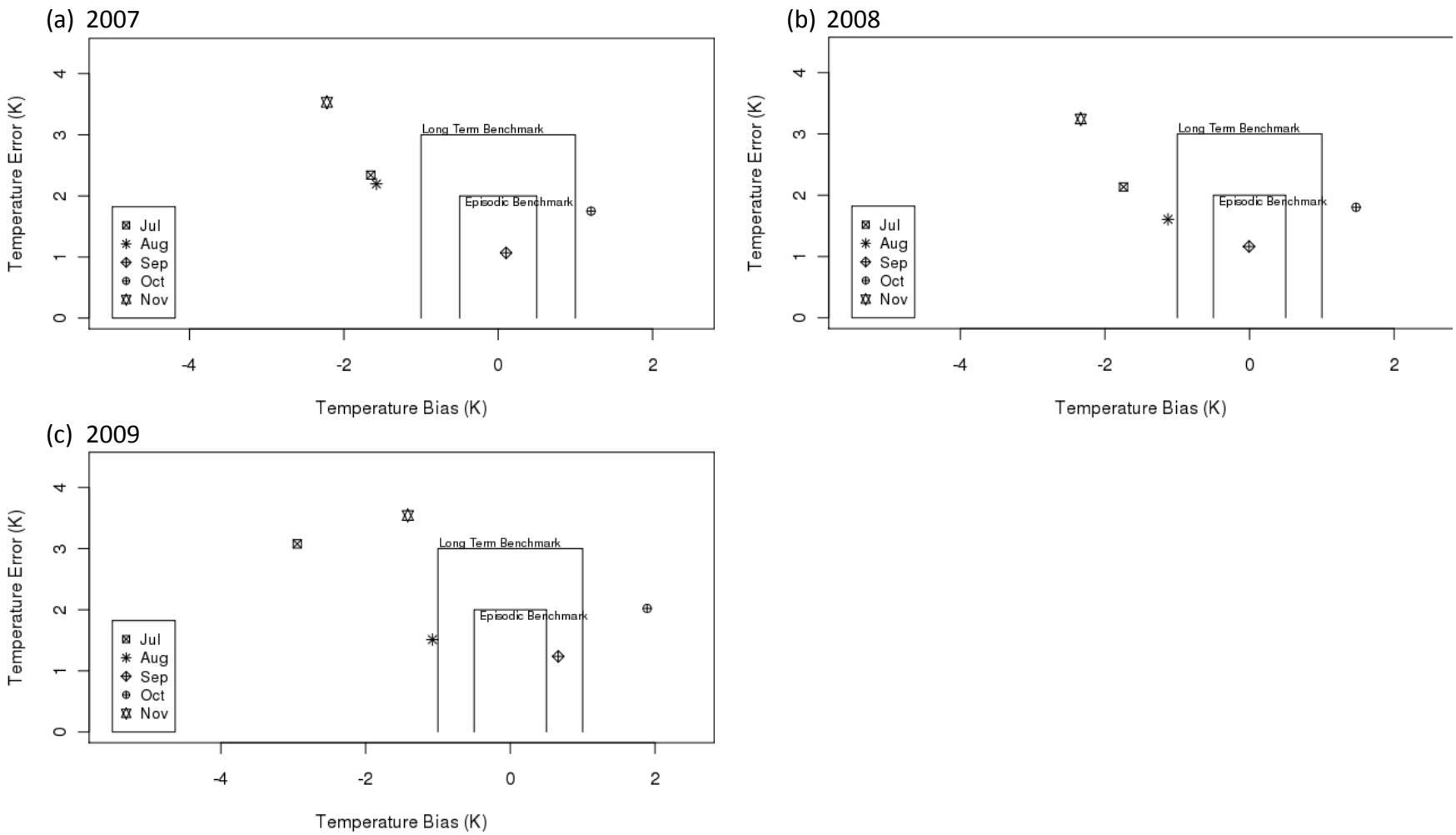

Figure 3-2. Temperature Bias and Error Soccer Plot by Month for North Coast Stations in the 4km Domain for (a) 2007, (b) 2008, and (c) 2009.

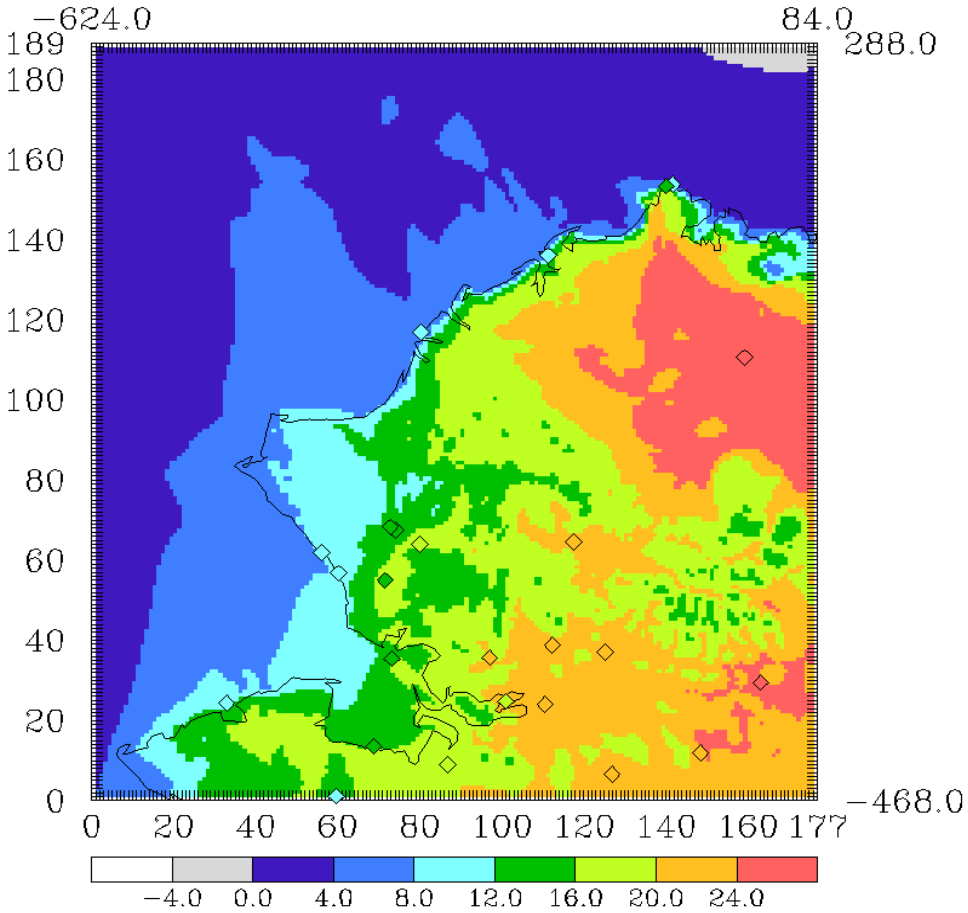

Figure 3-3. Temperature (C) Spatial Plot for 4km Grid at 0Z (3:00 pm LST) 15 July 2009. Diamonds Represent Observations.

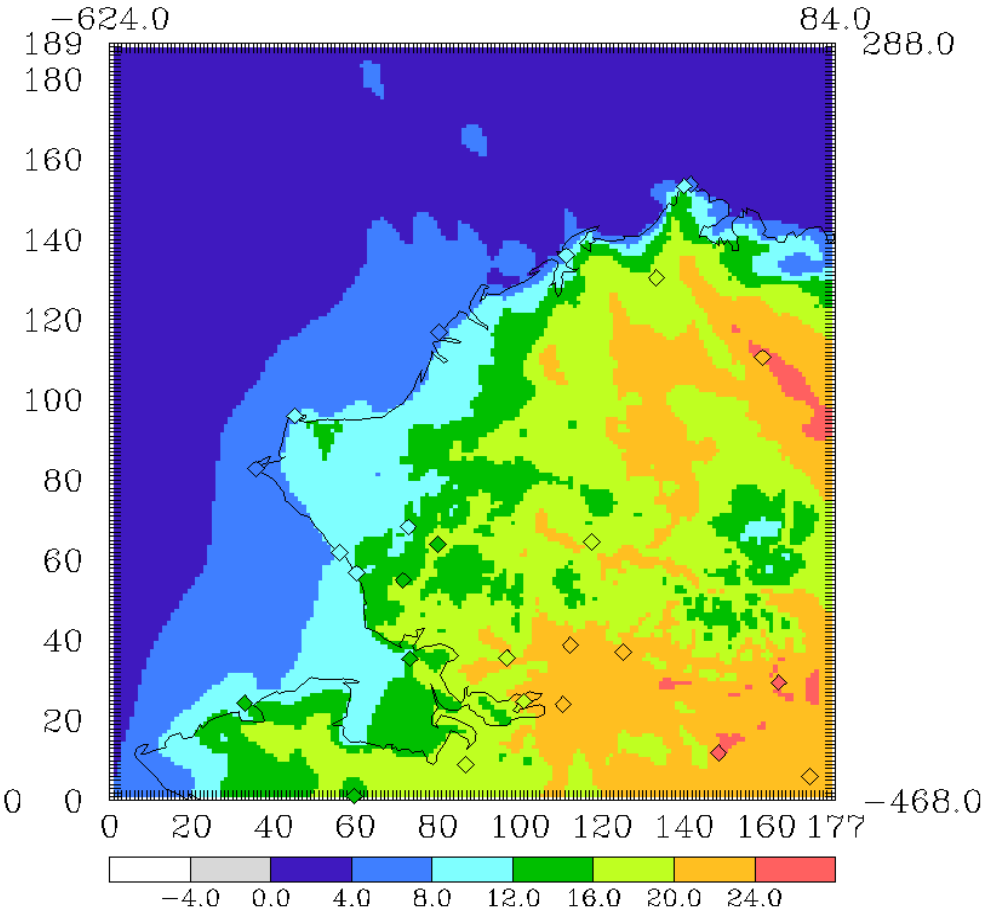

Figure 3-4. Temperature (C) Spatial Plot for 4km Grid at 4Z (7:00 pm LST) 15 July 2009. Diamonds Represent Observations.

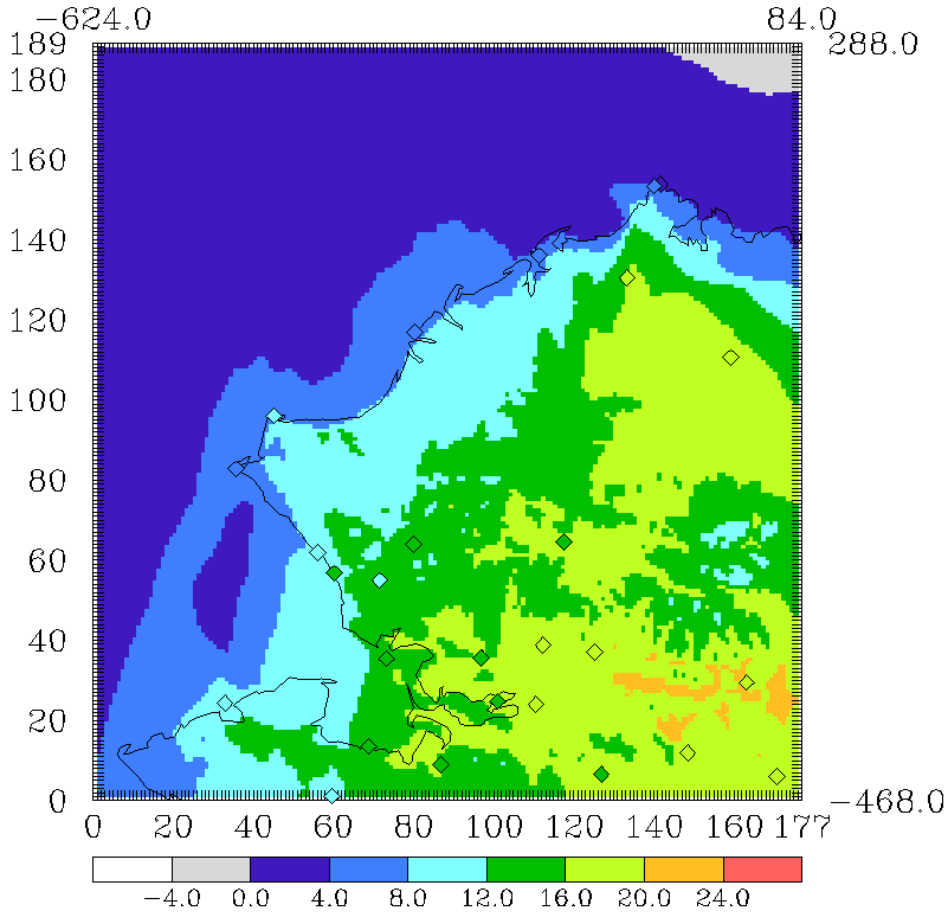

Figure 3-5. Temperature (C) Spatial Plot for 4km Grid at 8Z (11:00 pm LST) 15 July 2009. Diamonds Represent Observations.

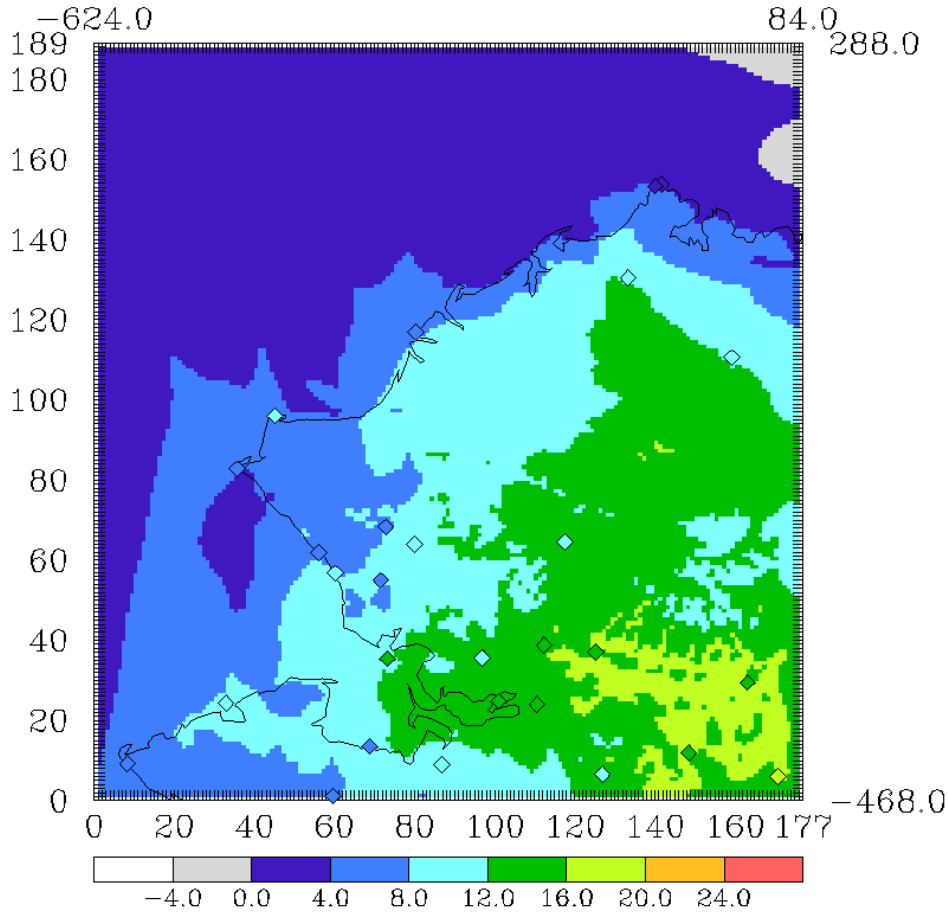

Figure 3-6. Temperature (C) Spatial Plot for 4km Grid at 12Z (3:00 am LST) 15 July 2009. Diamonds Represent Observations.

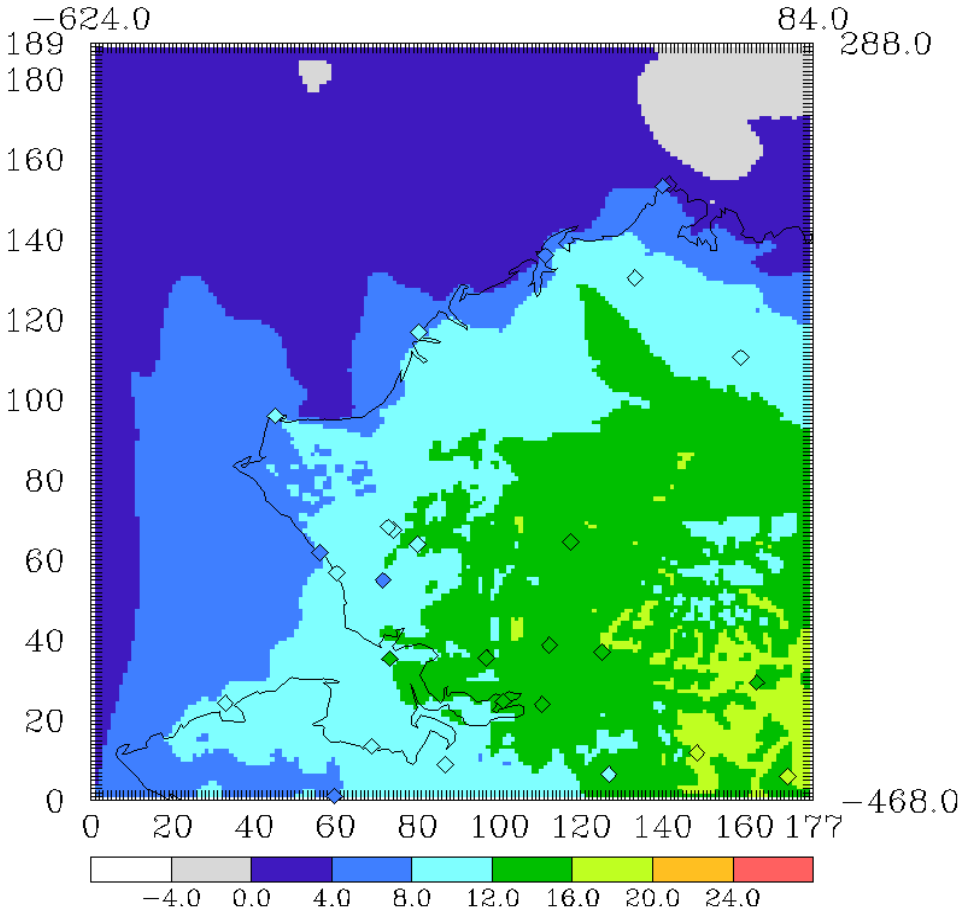

Figure 3-7. Temperature (C) Spatial Plot for 4km Grid at 16Z (7:00 am LST) 15 July 2009. Diamonds Represent Observations.

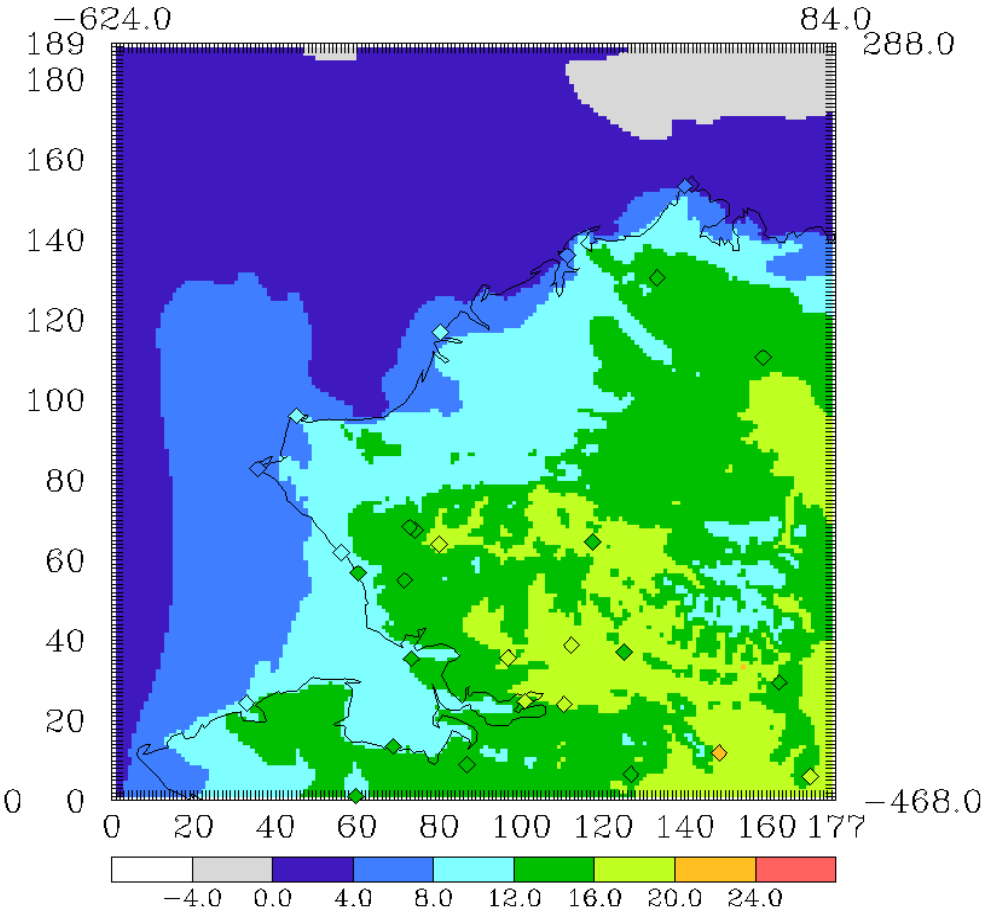

Figure 3-8. Temperature (C) Spatial Plot for 4km Grid at 20Z (11:00 am LST) 15 July 2009. Diamonds Represent Observations.

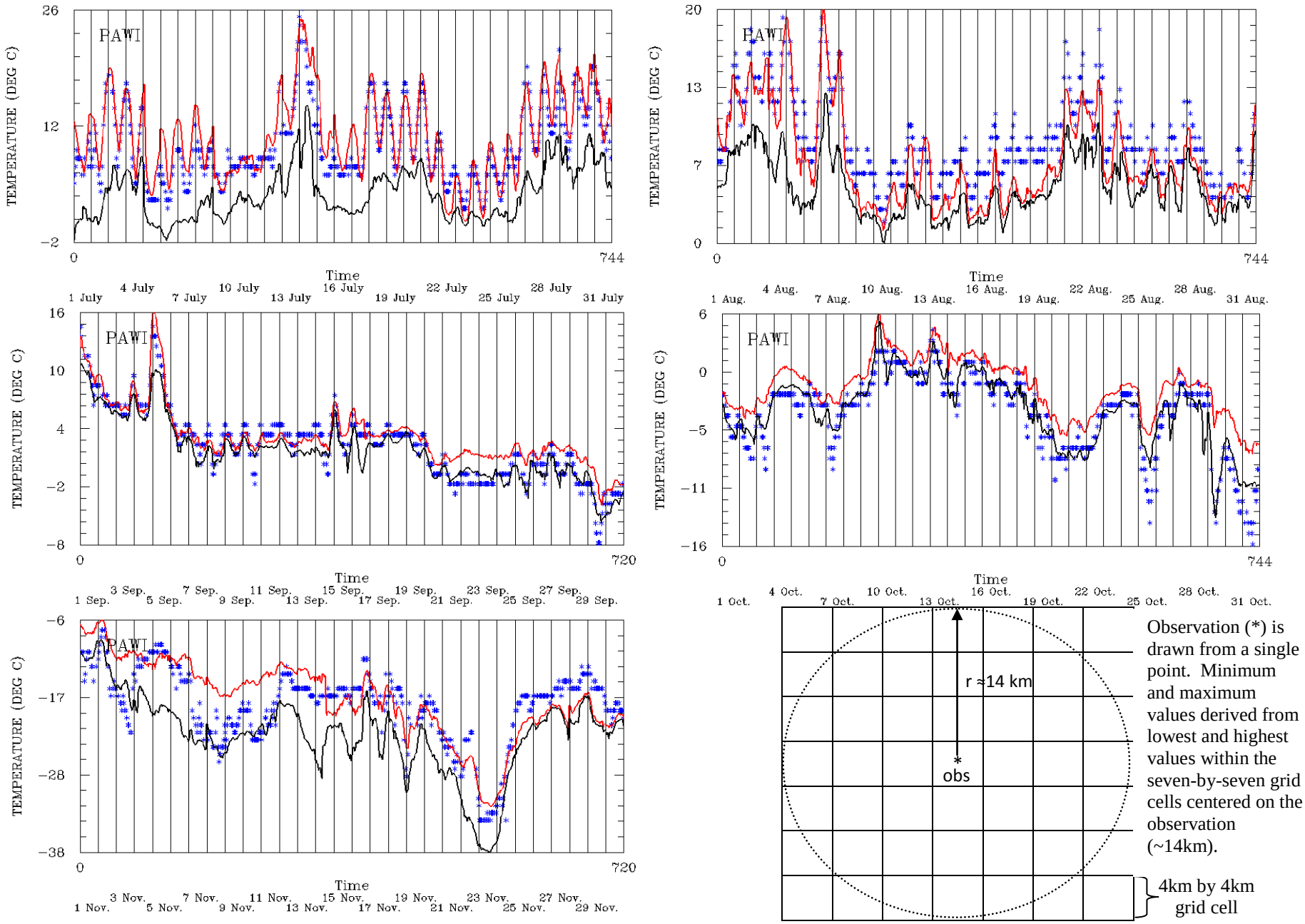

Figure 3-9. Hourly Temperature (C) Spatial Time Series for Wainwright on the 4km Grid for July through November 2009. The Spatial Envelope, which is Shown by the Black Line (minimum temperature) and Red Line (maximum temperature) and Generally Brackets the Blue Asterisks (observed temperature), Represents a Nominal 14km (3.5, 4km grid cells) Search Radius about the Wainwright Monitor.

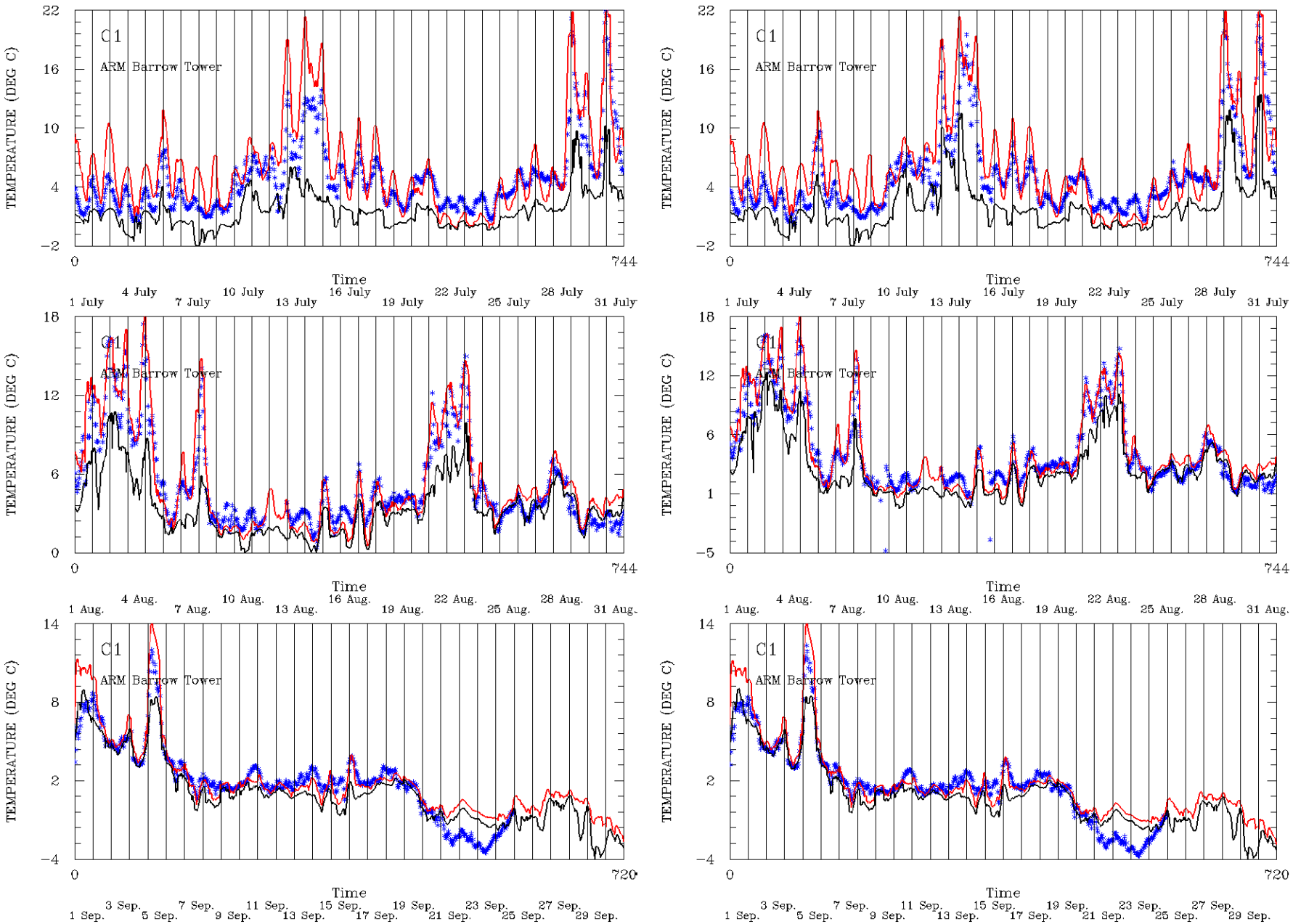

Figure 3-10. Hourly Temperature (C) Spatial Time Series for the ARM Barrow Tall Tower on the 4km Grid for July through September through September 2009. The Graphics on the Left are a Comparison of the 20m observation with the 18 m (Level 2) Model Estimate. The Graphics on the Right are a Comparison of the 40m observation with the 32m (Level 2) Model Estimate. The Spatial Envelope, which is Shown by the Black Line (minimum mixing ratio) and Red Line (maximum mixing ratio) and Generally Brackets the Blue Asterisks (observed mixing ratio), Represents a Nominal 14km (3.5, 4km grid cells) Search Radius about the Monitor.

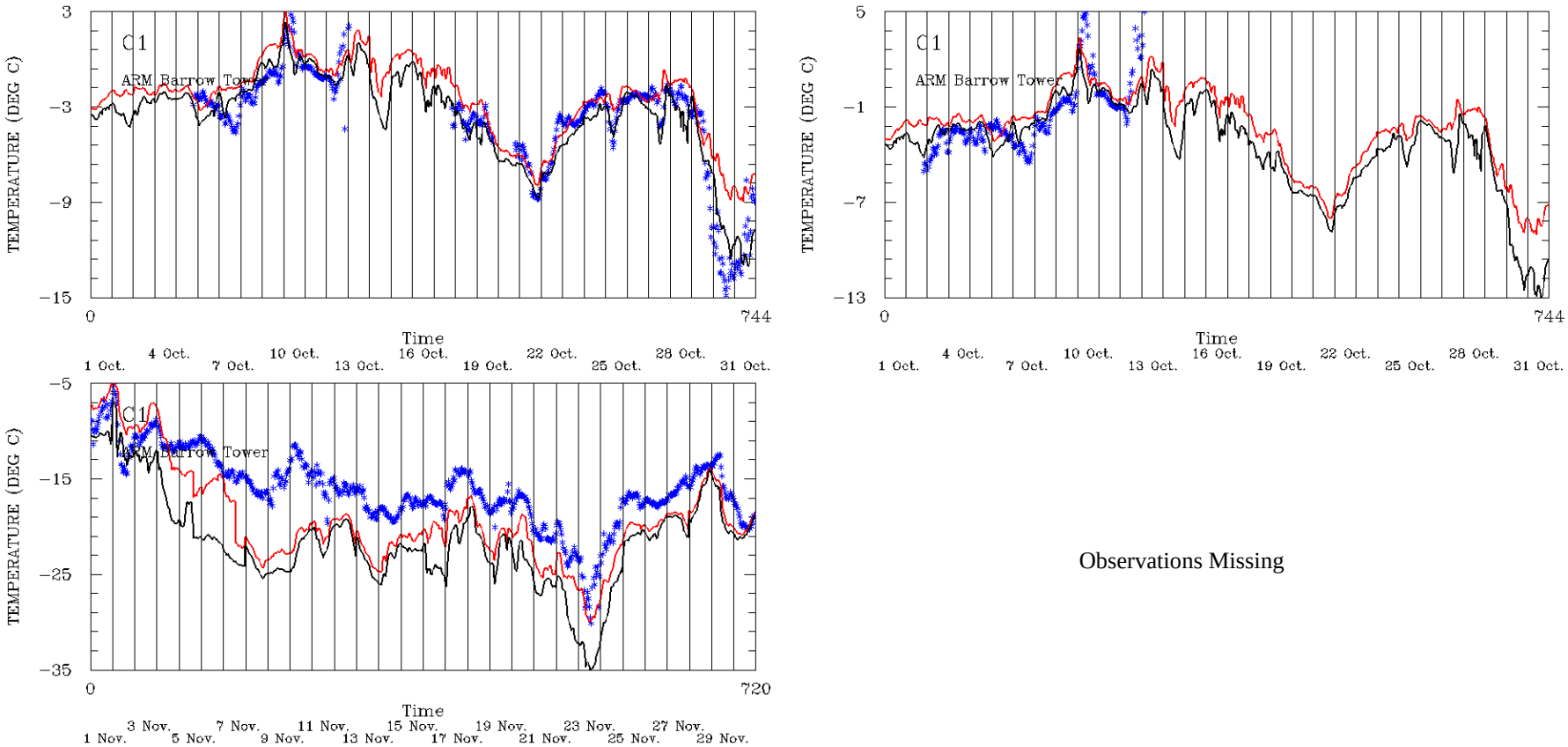

Figure 3-11. Hourly Temperature (C) Spatial Time Series for the ARM Barrow Tall Tower on the 4km Grid for October and November 2009. The Graphics on the Left are a Comparison of the 20m observation with the 18 m (Level 2) Model Estimate. The Graphics on the Right are a Comparison of the 40m observation with the 32m (Level 2) Model Estimate. The Spatial Envelope, which is Shown by the Black Line (minimum mixing ratio) and Red Line (maximum mixing ratio) and Generally Brackets the Blue Asterisks (observed mixing ratio), Represents a Nominal 14km (3.5, 4km grid cells) Search Radius about the Monitor.

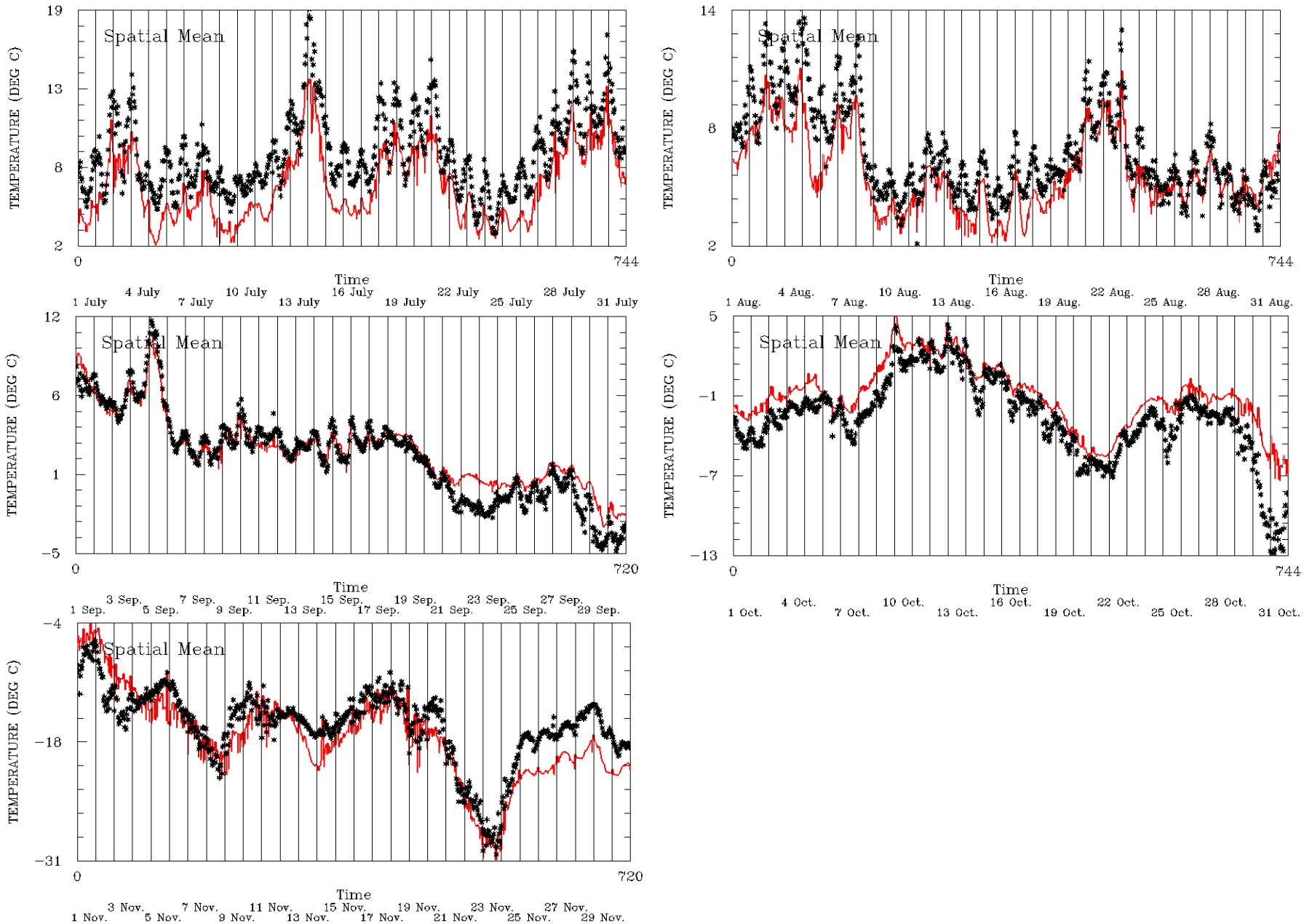

Figure 3-12. Hourly Spatial Mean Temperature (C) Time Series for North Coast Stations in the 4km Grid for July through November 2009. The Black Asterisks Represent the Hourly Mean of the Observed Temperatures from the North Coast Stations in the 4km Grid. The Red Line Represents the Hourly Mean of the Predicted Temperatures at the North Coast Stations in the 4km Grid.

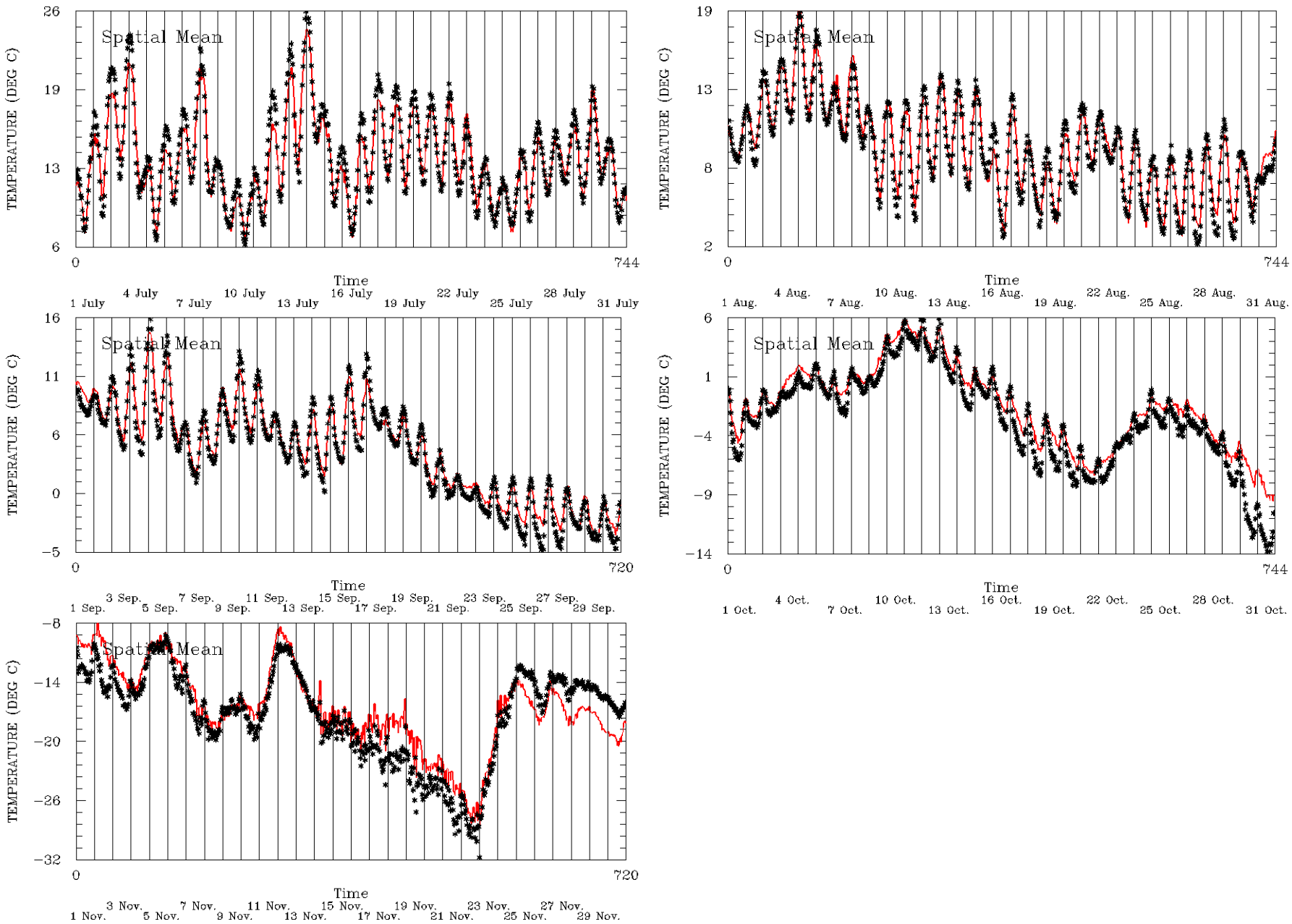

Figure 3-13. Hourly Spatial Mean Temperature (C) Time Series for All Stations in the 4km Grid for July through November 2009. The Black Asterisks Represent the Hourly Mean of the Observed Temperatures from All Stations in the 4km Grid. The Red Line Represents the Hourly Mean of the Predicted Temperatures at All Stations in the 4km Grid.

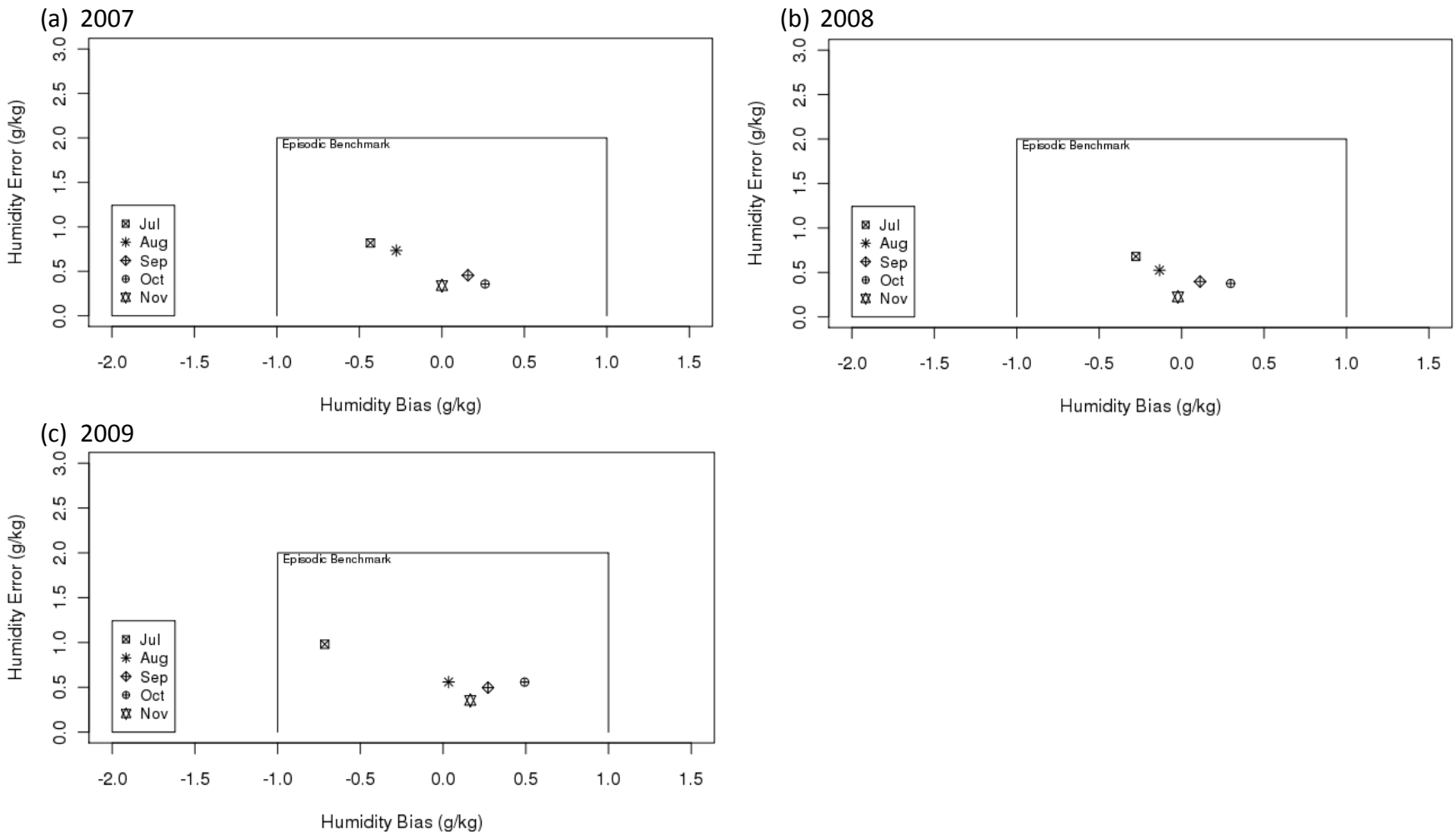

Figure 3-14. Mixing Ratio Bias and Error Soccer Plot by Month for All Stations in the 4km Domain for (a) 2007, (b) 2008, and (c) 2009.

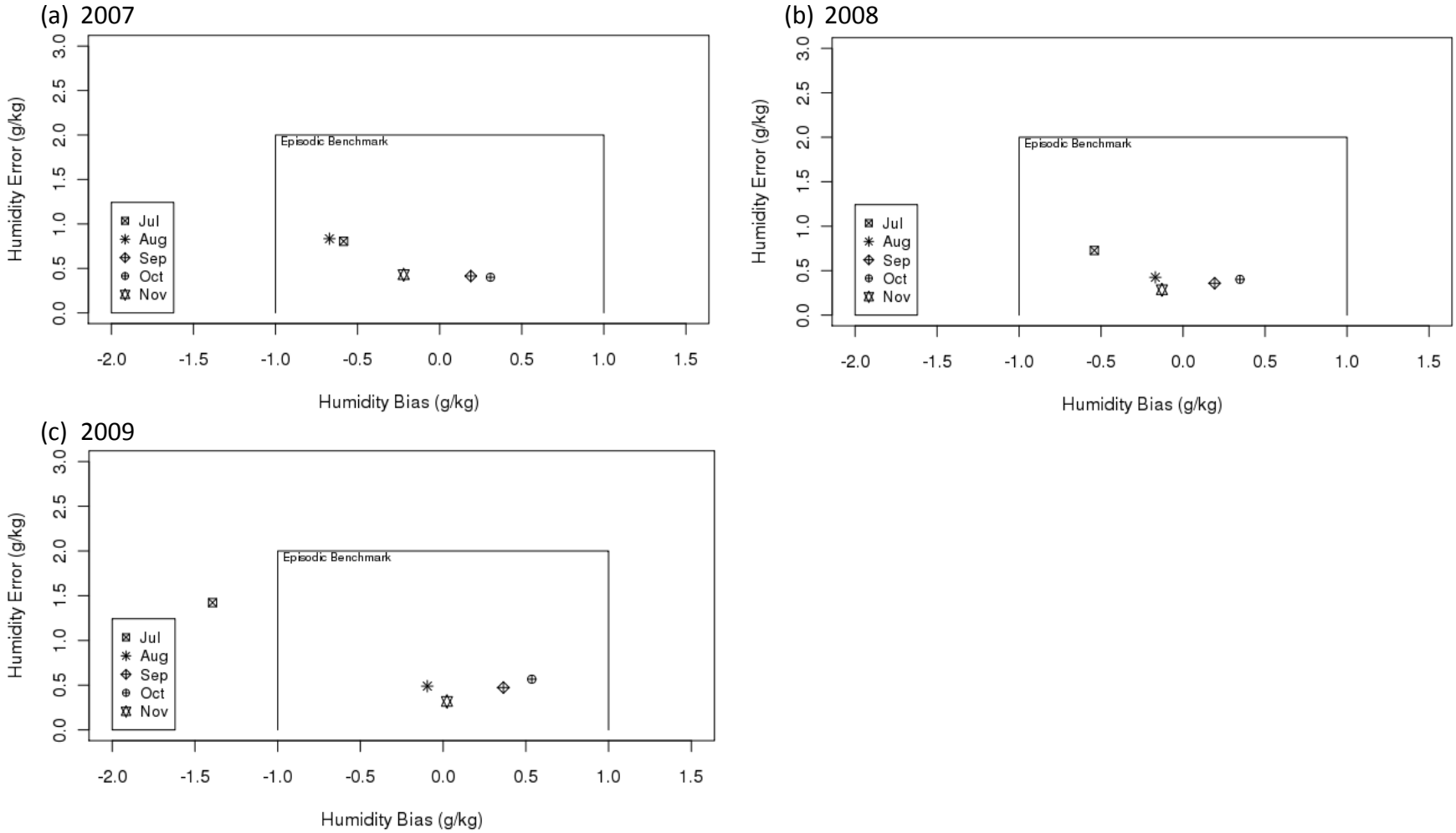

Figure 3-15. Mixing Ratio Bias and Error Soccer Plot by Month for North Coast Stations in the 4km Domain for (a) 2007, (b) 2008, and (c) 2009.

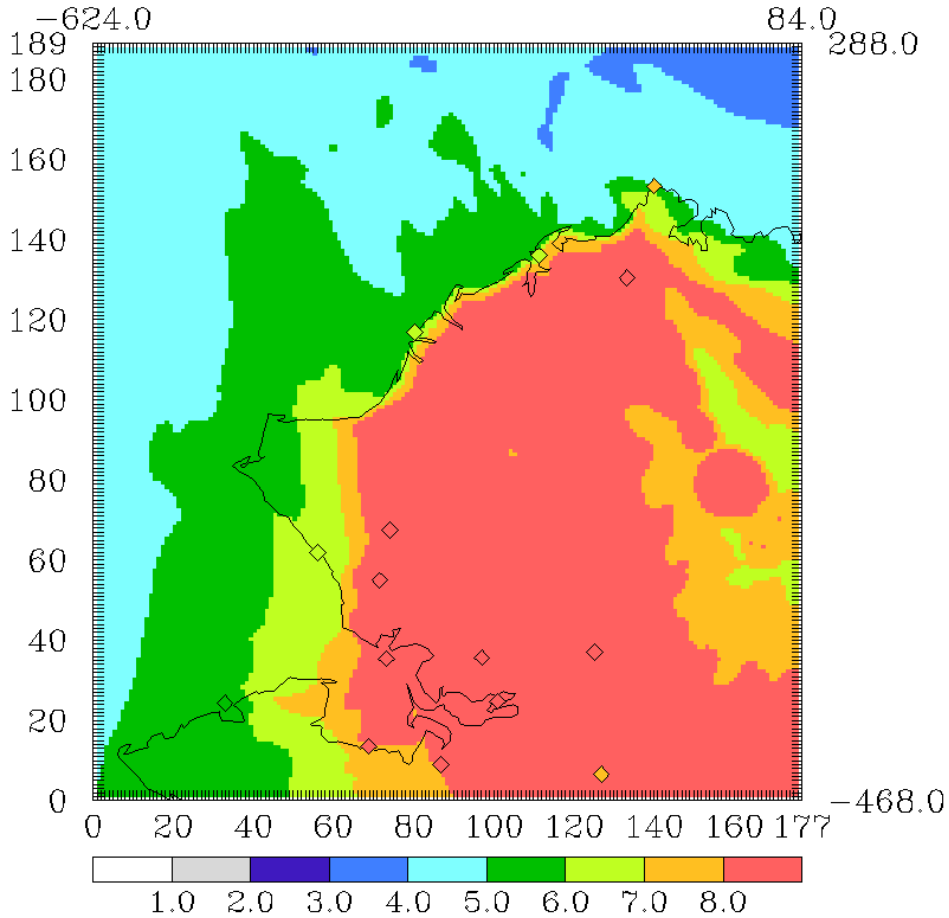

Figure 3-16. Mixing Ratio (g/kg) Spatial Plot for 4km Grid at 0Z (3:00 pm LST) 15 July 2009. Diamonds Represent Observations.

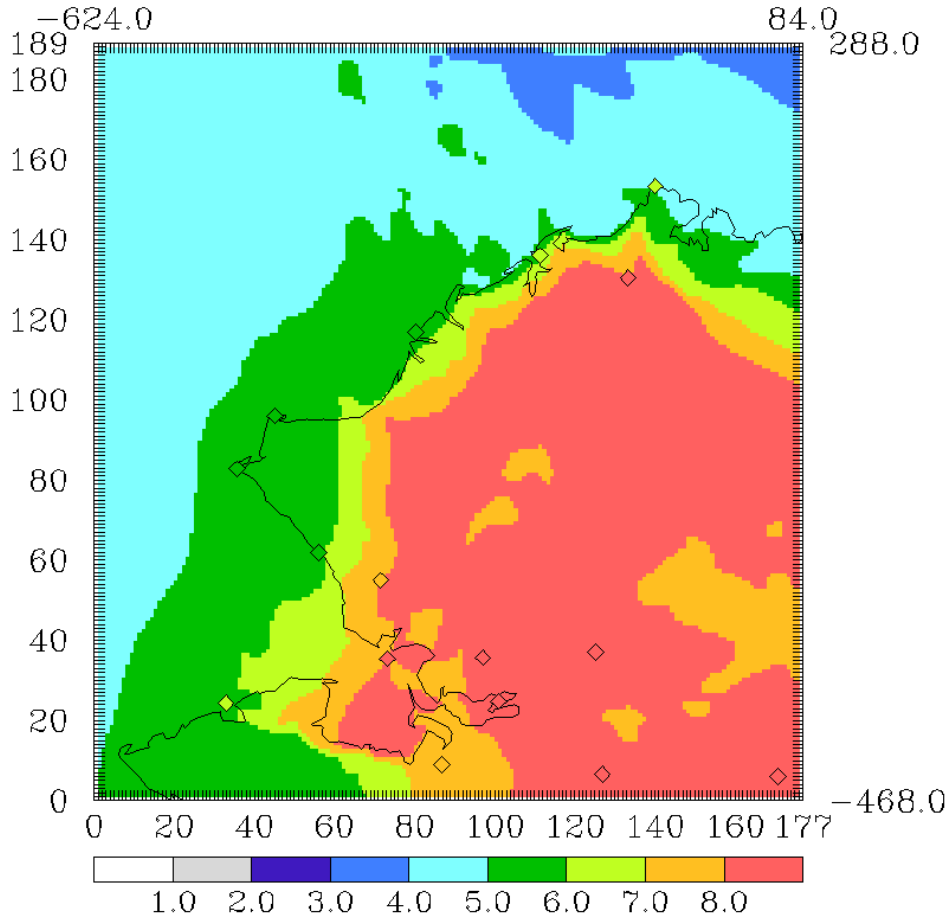

Figure 3-17. Mixing Ratio (g/kg) Spatial Plot for 4km Grid at 4Z (7:00 pm LST) 15 July 2009. Diamonds Represent Observations.

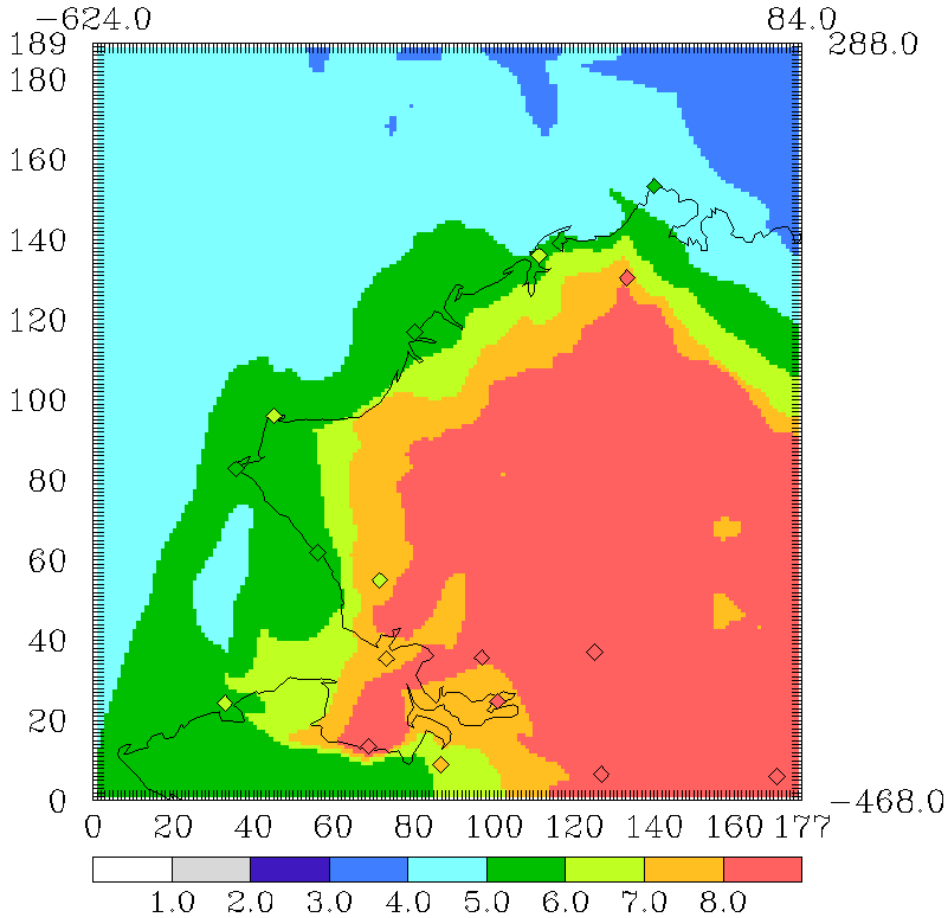

Figure 3-18. Mixing Ratio (g/kg) Spatial Plot for 4km Grid at 8Z (11:00 pm LST) 15 July 2009. Diamonds Represent Observations.

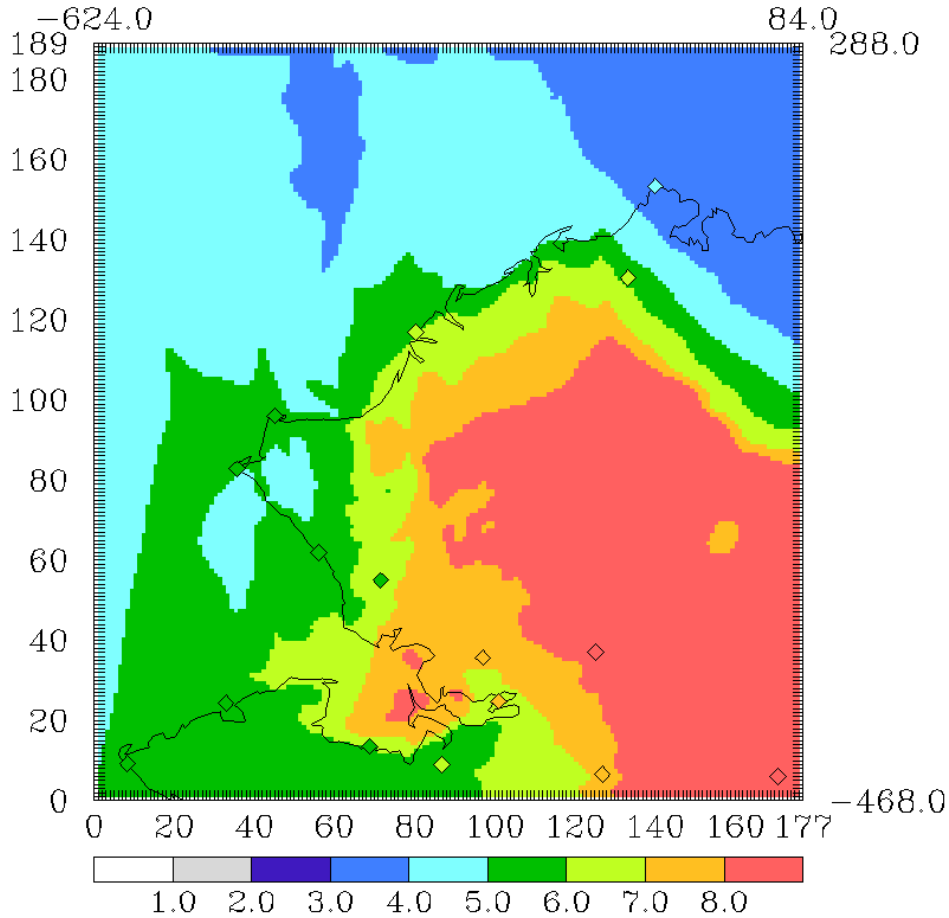

Figure 3-19. Mixing Ratio (g/kg) Spatial Plot for 4km Grid at 12Z (3:00 am LST) 15 July 2009. Diamonds Represent Observations.

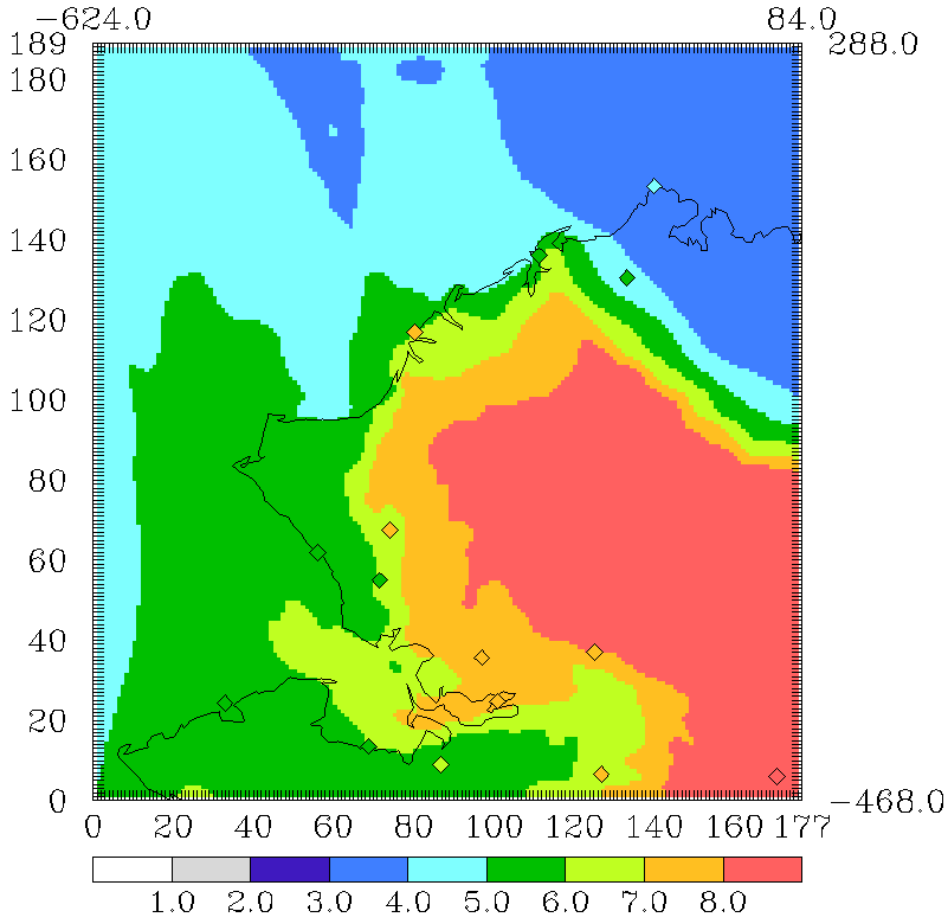

Figure 3-20. Mixing Ratio (g/kg) Spatial Plot for 4km Grid at 16Z (7:00 am LST) 15 July 2009. Diamonds Represent Observations.

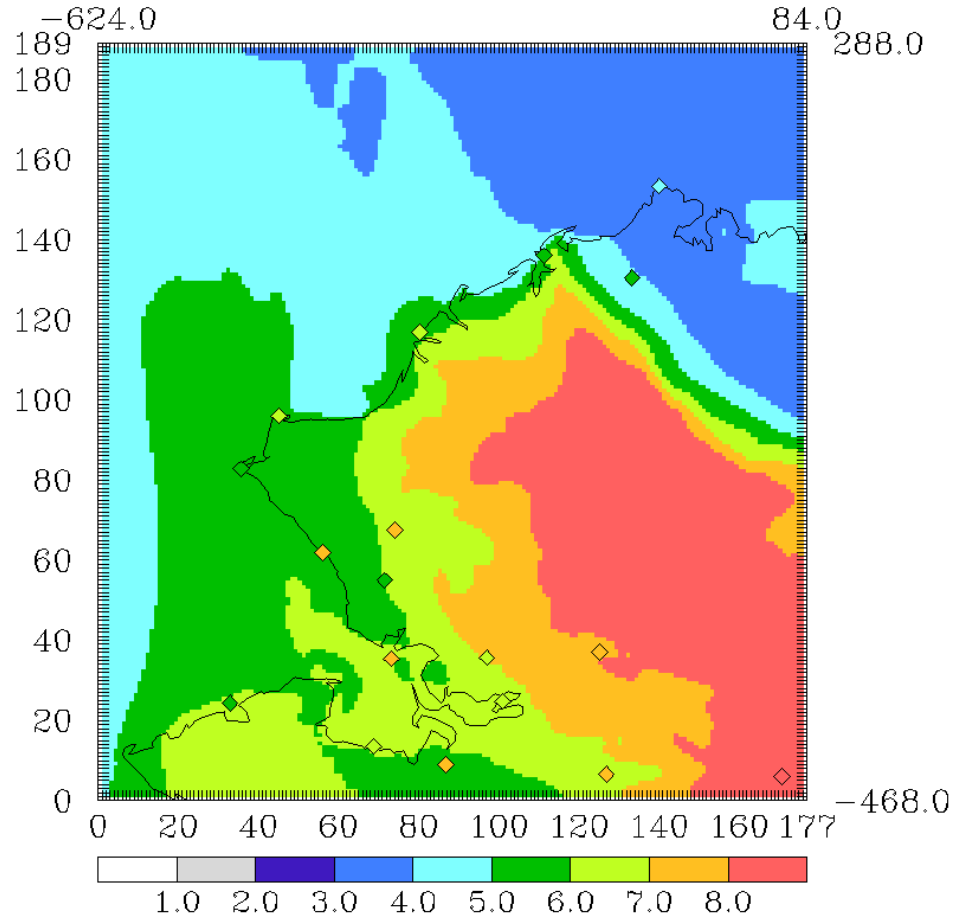

Figure 3-21. Mixing Ratio (g/kg) Spatial Plot for 4km Grid at 20Z (11:00 am LST) 15 July 2009. Diamonds Represent Observations.

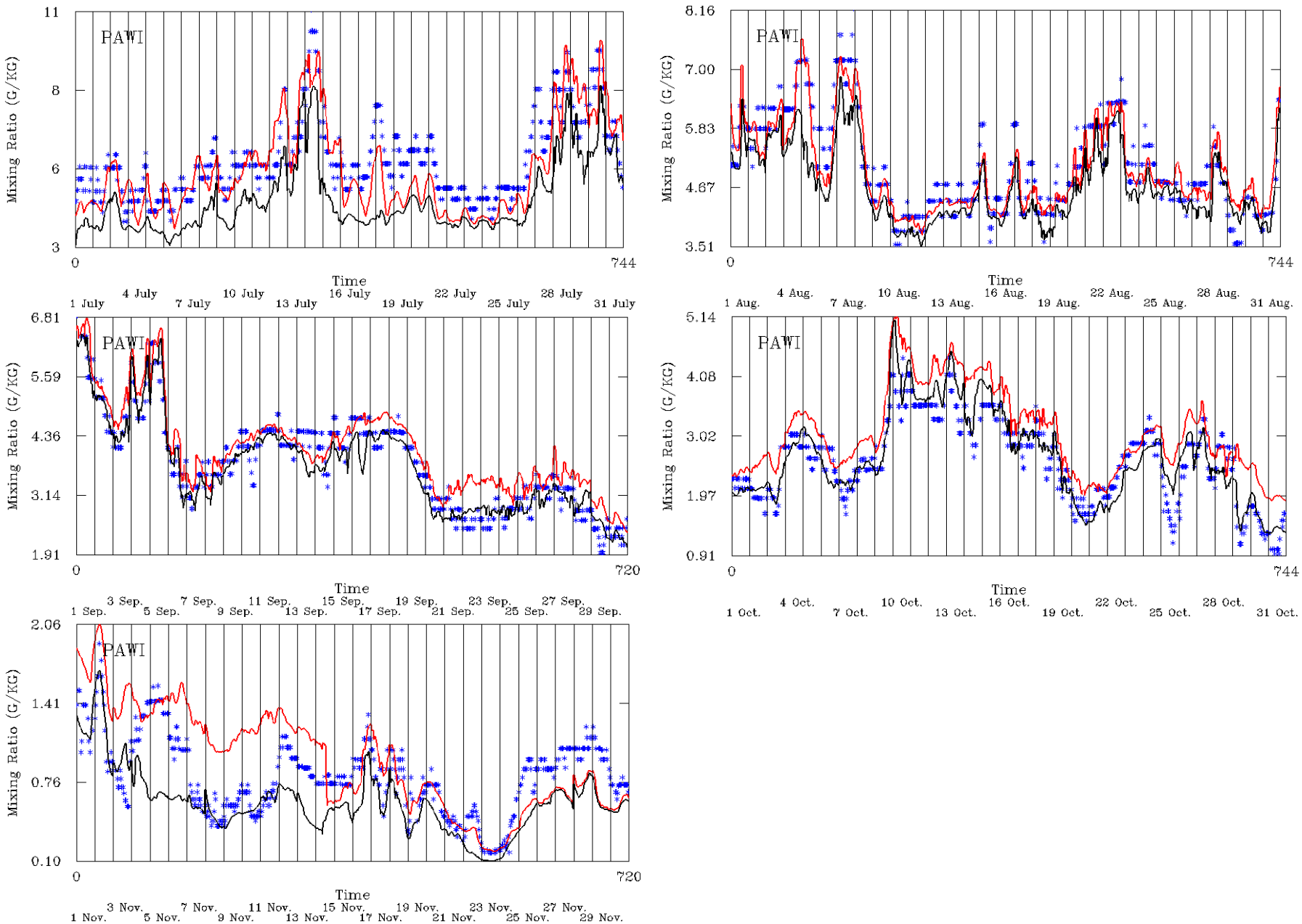

Figure 3-22. Hourly Mixing Ratio (g/kg) Spatial Time Series for Wainwright on the 4km Grid for July through November 2009. The Spatial Envelope, which is Shown by the Black Line (minimum mixing ratio) and Red Line (maximum mixing ratio) and Generally Brackets the Blue Asterisks (observed mixing ratio), Represents a Nominal 14km (3.5, 4km grid cells) Search Radius about the Wainwright Monitor.

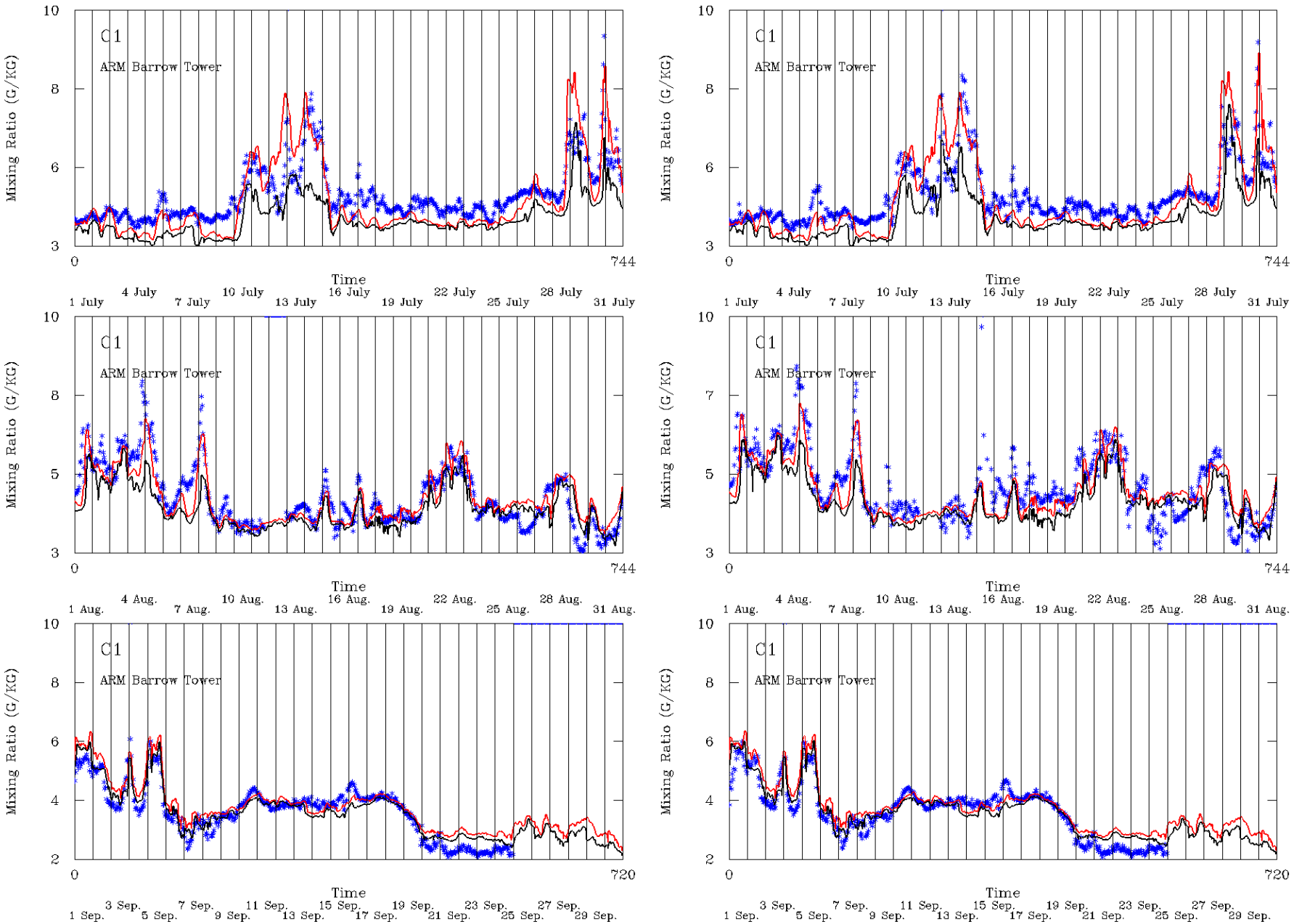

Figure 3-23. Hourly Mixing Ratio (g/kg) Spatial Time Series for the ARM Barrow Tall Tower on the 4km Grid for July through September through September 2009. The Graphics on the Left are a Comparison of the 20m observation with the 18 m (Level 2) Model Estimate. The Graphics on the Right are a Comparison of the 40m observation with the 32m (Level 2) Model Estimate. The Spatial Envelope, which is Shown by the Black Line (minimum mixing ratio) and Red Line (maximum mixing ratio) and Generally Brackets the Blue Asterisks (observed mixing ratio), Represents a Nominal 14km (3.5, 4km grid cells) Search Radius about the Monitor.

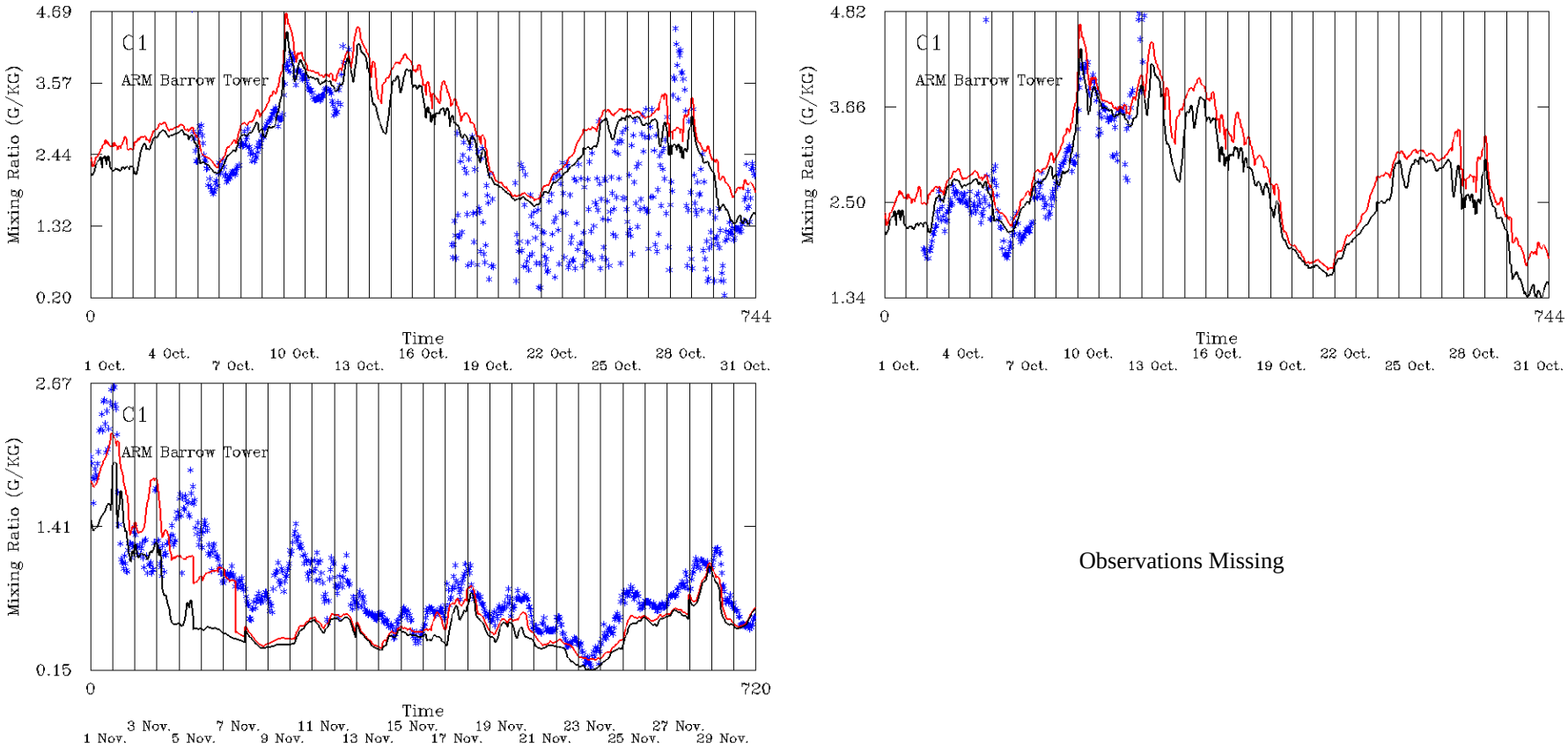

Figure 3-24. Hourly Mixing Ratio (g/kg) Spatial Time Series for the ARM Barrow Tall Tower on the 4km Grid for October and November 2009. The Graphics on the Left are a Comparison of the 20m observation with the 18 m (Level 2) Model Estimate. The Graphics on the Right are a Comparison of the 40m observation with the 32m (Level 2) Model Estimate. The Spatial Envelope, which is Shown by the Black Line (minimum mixing ratio) and Red Line (maximum mixing ratio) and Generally Brackets the Blue Asterisks (observed mixing ratio), Represents a Nominal 14km (3.5, 4km grid cells) Search Radius about the Monitor.

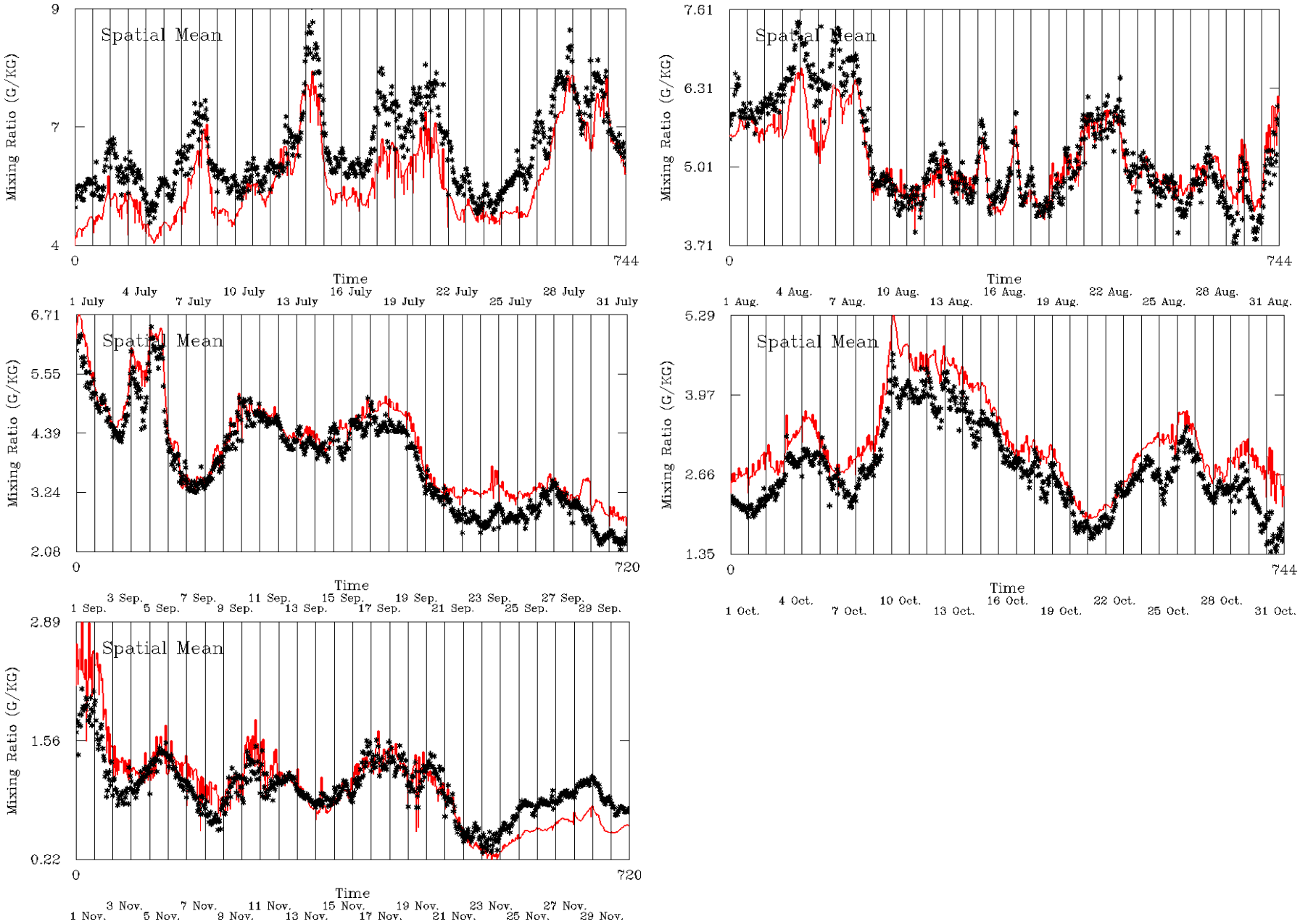

Figure 3-25. Hourly Spatial Mean Mixing Ratio (g/kg) Time Series for North Coast Stations in the 4km Grid for July through November 2009. The Black Asterisks Represent the Hourly Mean of the Observed Mixing Ratio from the North Coast Stations in the 4km Grid. The Red Line Represents the Hourly Mean of the Predicted Mixing Ratio at the North Coast Stations in the 4km Grid.

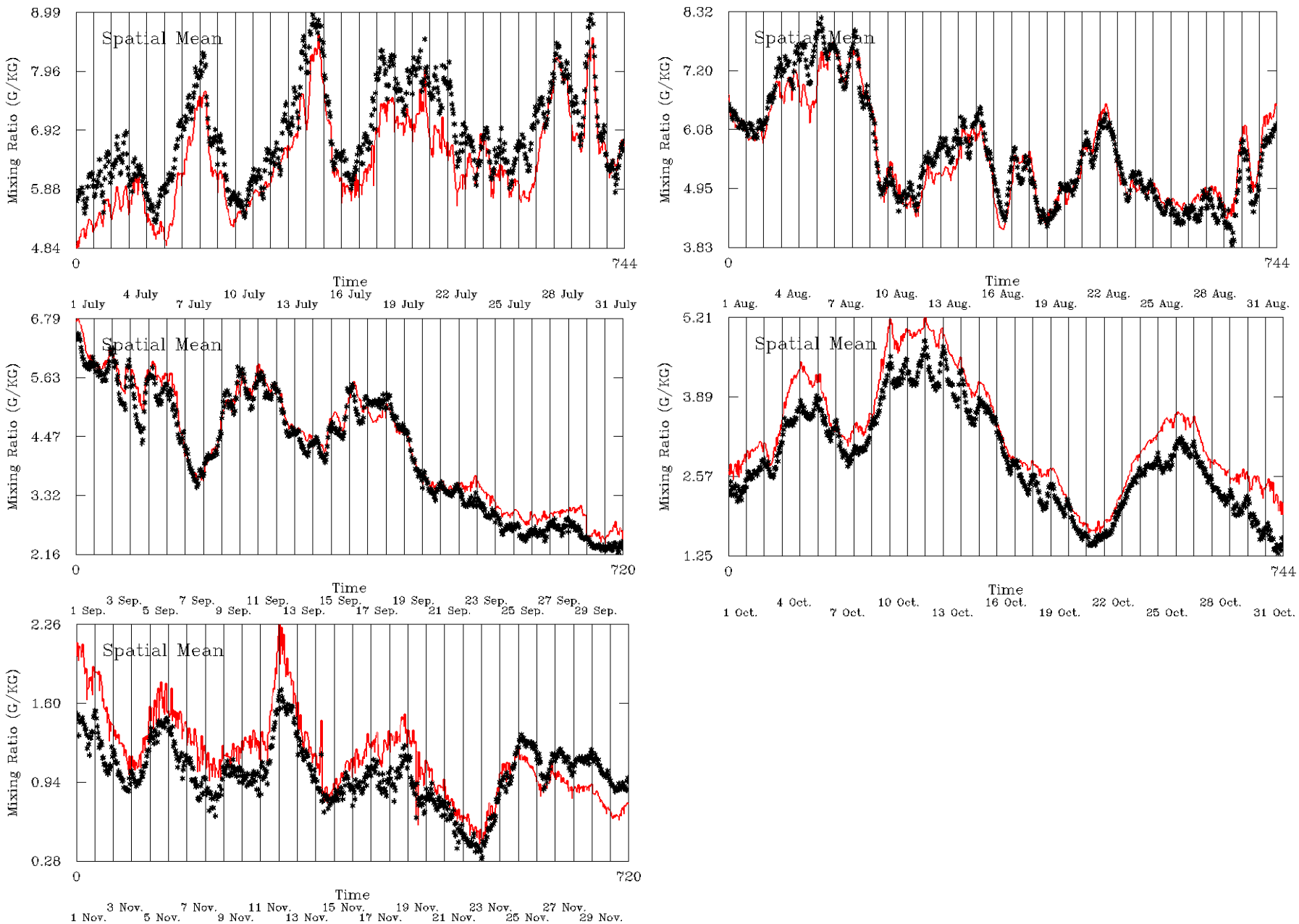

Figure 3-26. Hourly Spatial Mean Mixing Ratio (g/kg) Time Series for All Stations in the 4km Grid for July through November 2009. The Black Asterisks Represent the Hourly Mean of the Observed Mixing Ratio from All Stations in the 4km Grid. The Red Line Represents the Hourly Mean of the Predicted Mixing Ratio at All Stations in the 4km Grid.

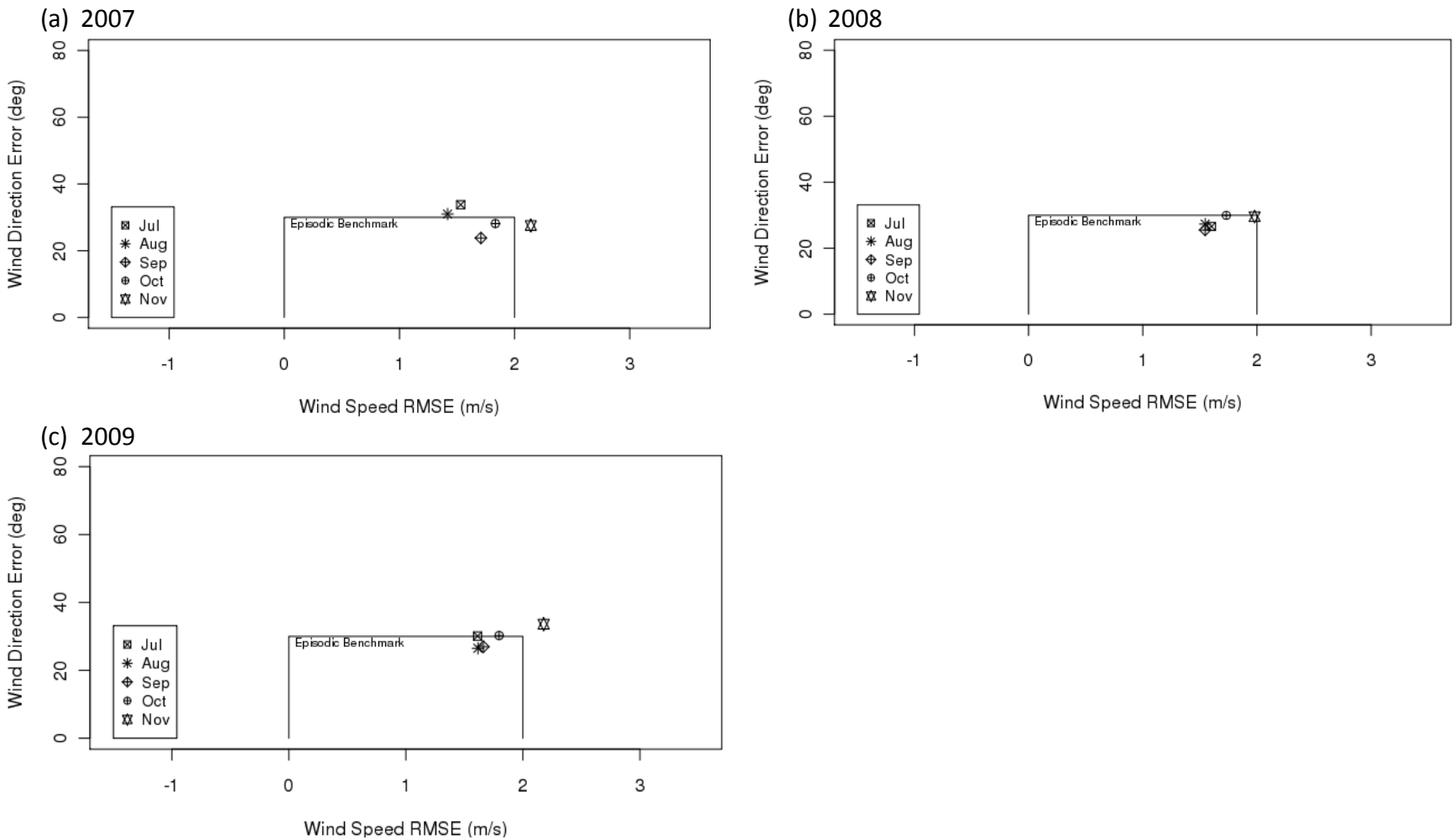

Figure 3-27. Wind Speed RMSE (m/s) Bias versus Wind Direction Error (deg) Soccer Plot by Month for All Stations in the 4km Domain for (a) 2007, (b) 2008, and (c) 2009.

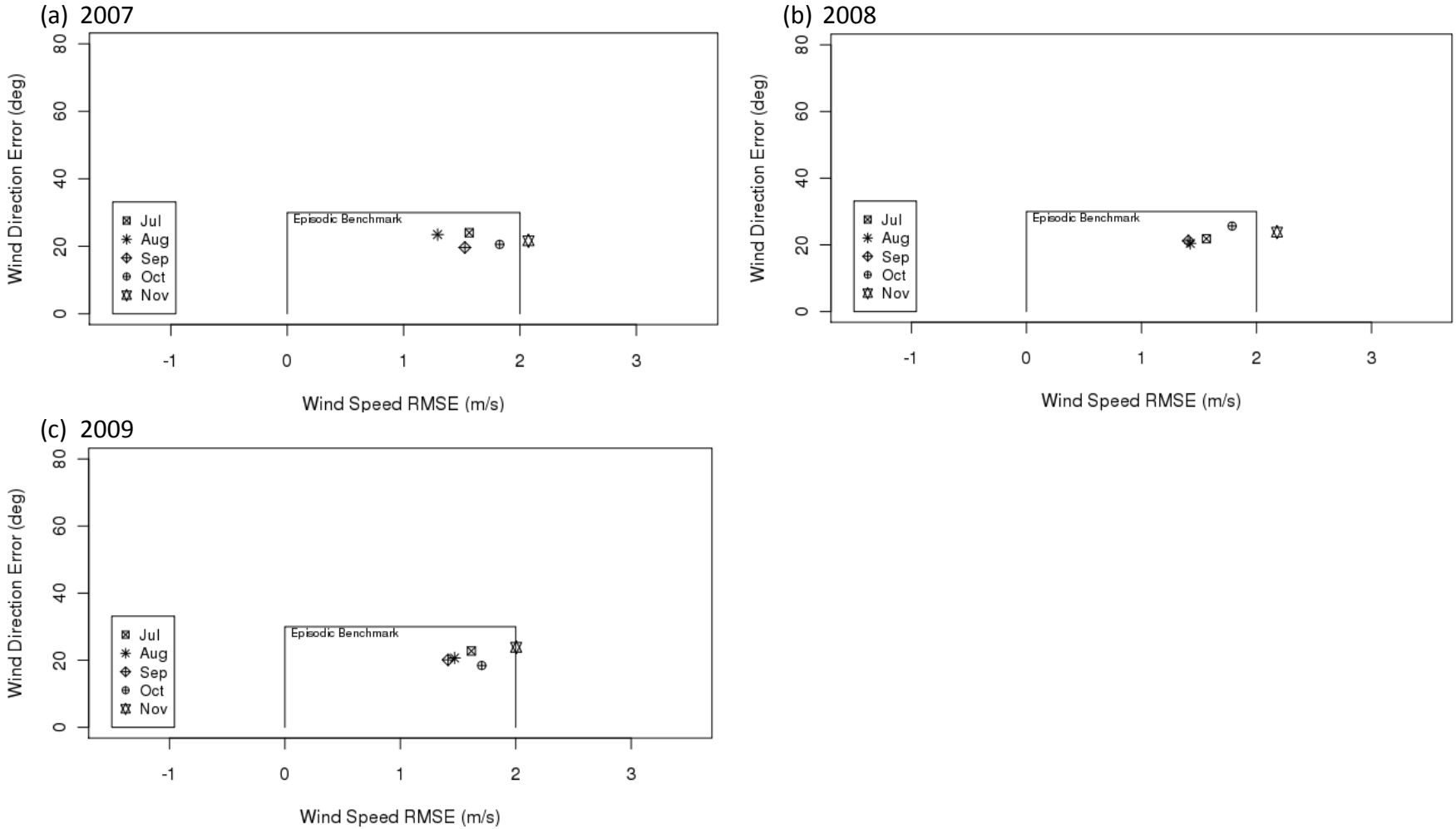

Figure 3-28. Wind Speed RMSE (m/s) Bias versus Wind Direction Error (deg) Soccer Plot by Month for North Coast Stations in the 4km Domain for (a) 2007, (b) 2008, and (c) 2009.

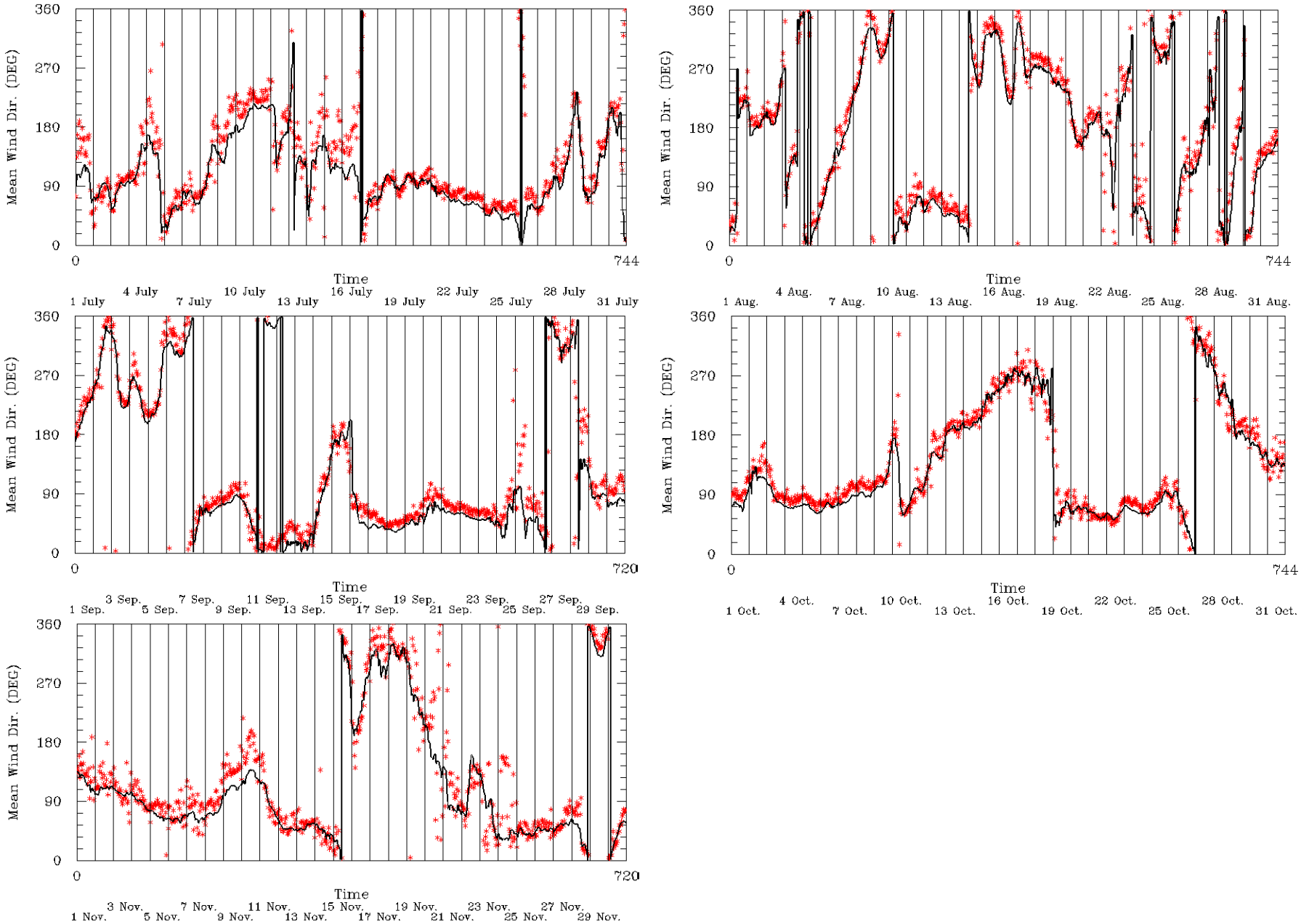

Figure 3-29. Hourly Spatial Mean Wind Direction (deg) Time Series for North Coast Stations in the 4km Grid for July through November 2009. The Black Asterisks Represent the Hourly Mean of the Observed Wind Direction from the North Coast Stations in the 4km Grid. The Red Line Represents the Hourly Mean of the Predicted Wind Direction at the North Coast Stations in the 4km Grid.

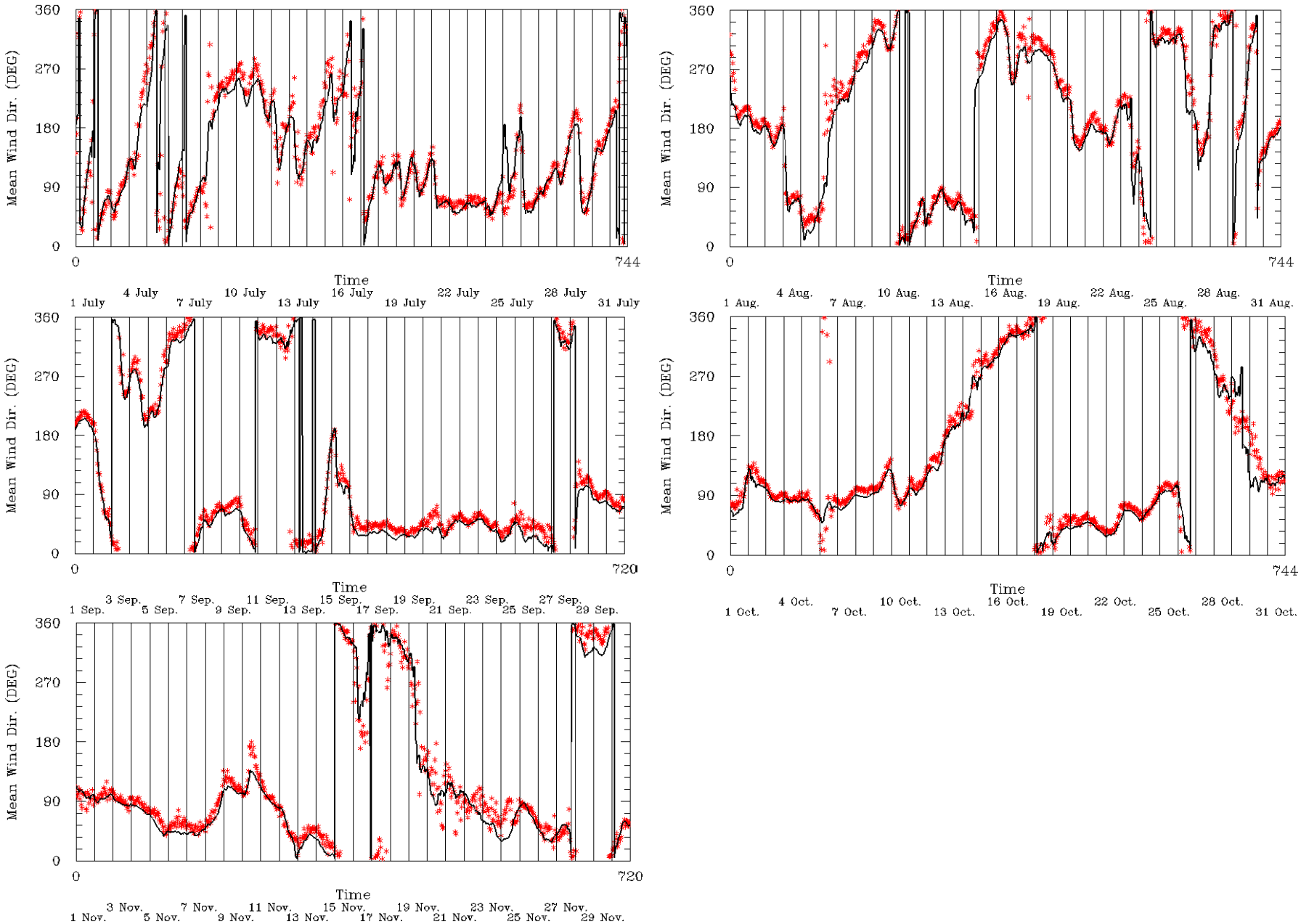

Figure 3-30. Hourly Spatial Mean Wind Direction (deg) Time Series for All Stations in the 4km Grid for July through November 2009. The Black Asterisks Represent the Hourly Mean of the Observed Wind Direction from All Stations in the 4km Grid. The Red Line Represents the Hourly Mean of the Predicted Wind Direction at All Stations in the 4km Grid.

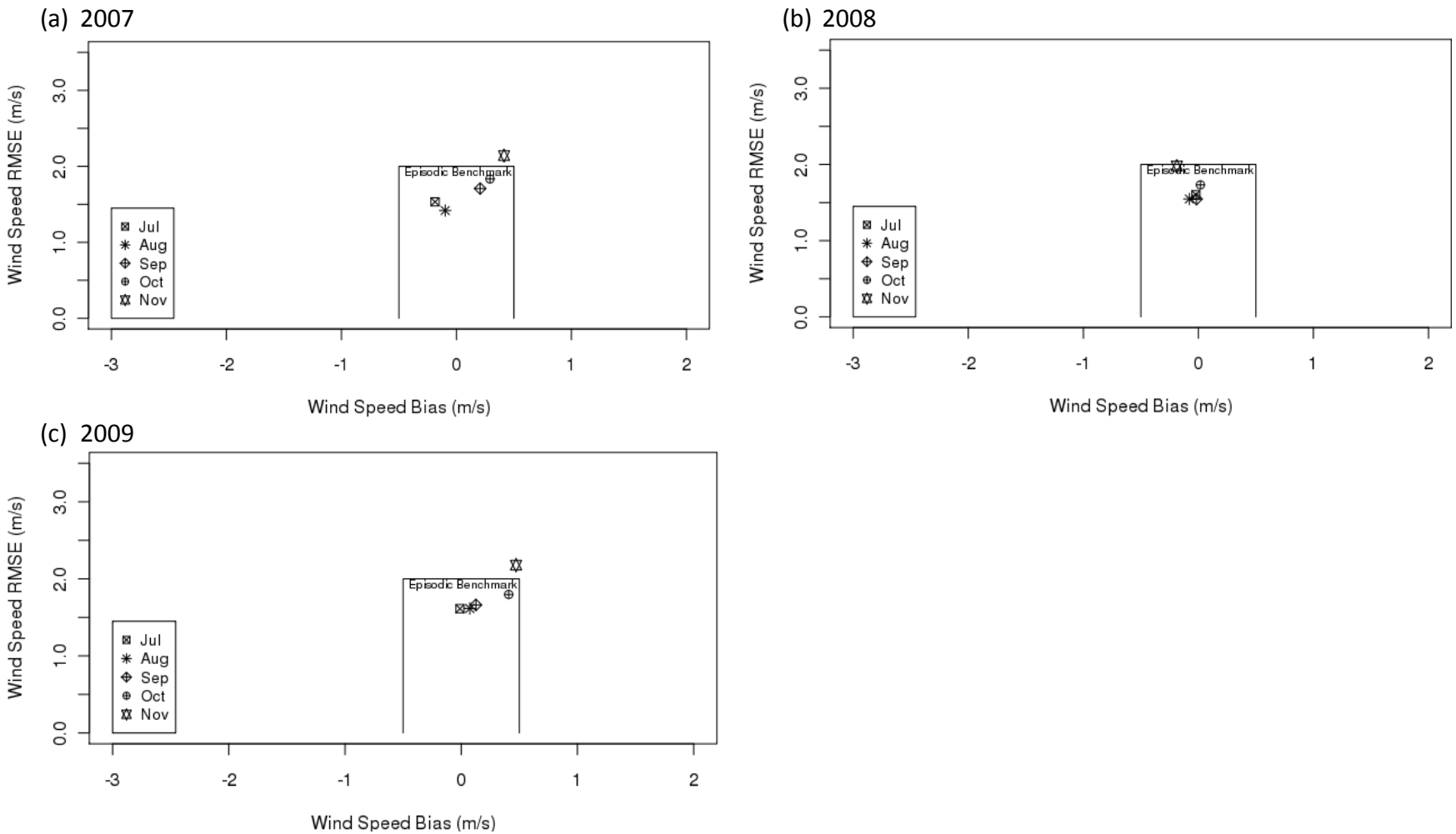

Figure 3-31. Wind Speed Bias (m/s) versus Wind Direction Error (deg) Soccer Plot by Month for All Stations in the 4km Domain for (a) 2007, (b) 2008, and (c) 2009.

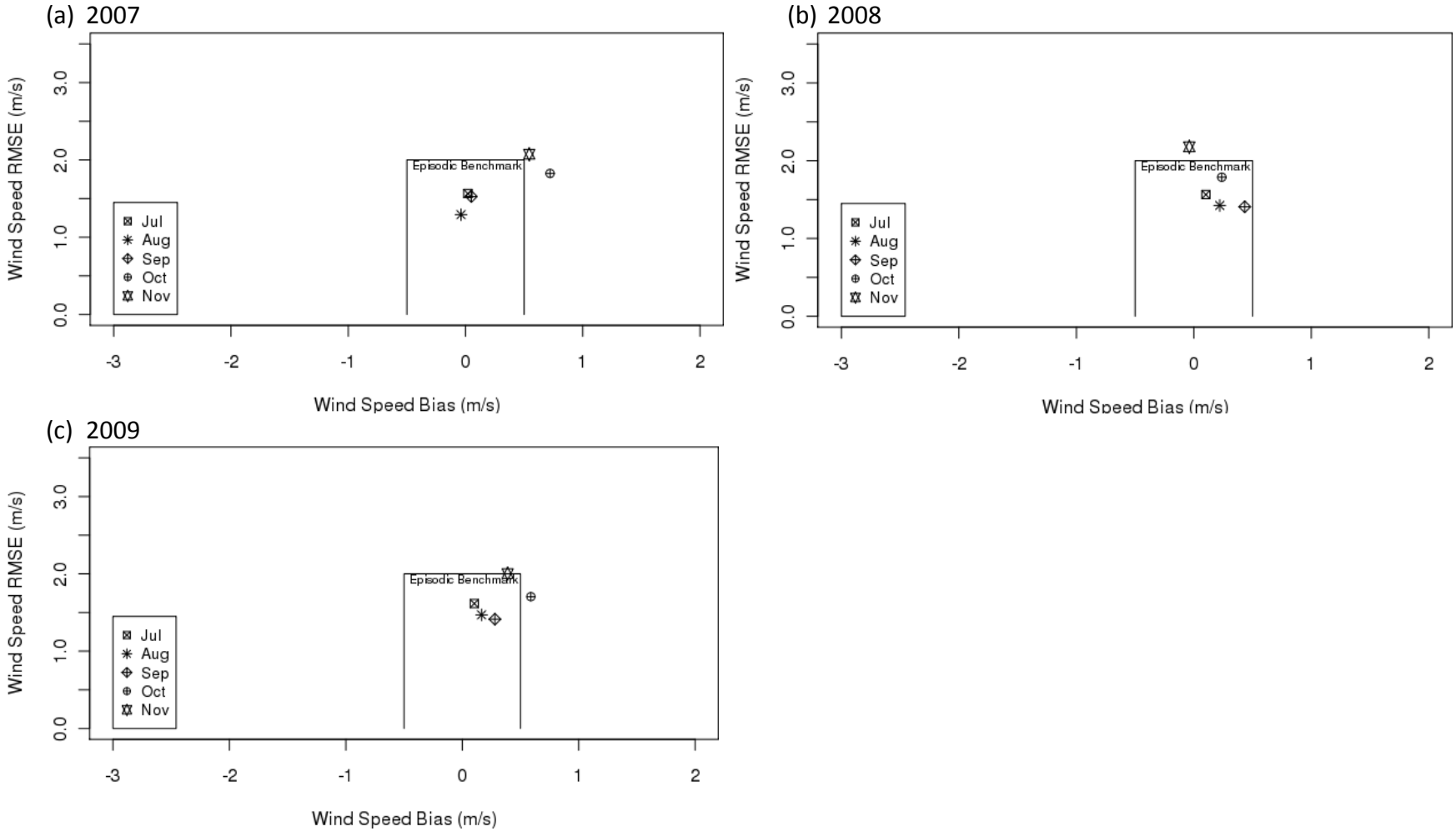

Figure 3-32. Wind Speed Bias (m/s) versus Wind Direction Error (deg) Soccer Plot by Month for North Coast Stations in the 4km Domain for (a) 2007, (b) 2008, and (c) 2009.

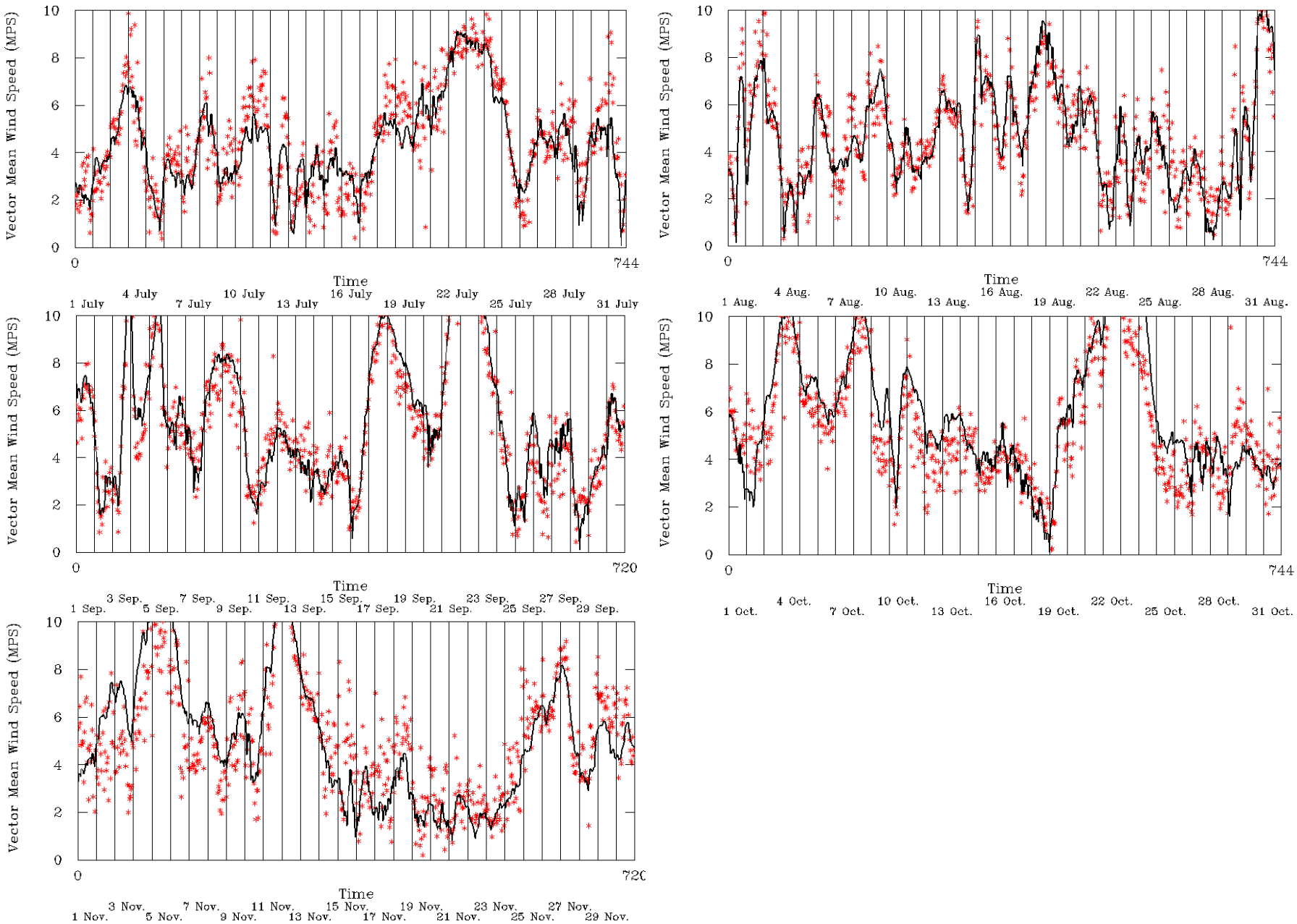

Figure 3-33. Hourly Spatial Vector Mean Wind Speed (m/s) Time Series for North Coast Stations in the 4km Grid for July through November 2009. The Black Asterisks Represent the Hourly Mean of the Observed Vector Wind Speed from North Coast Stations in the 4km Grid. The Red Line Represents the Hourly Mean of the Predicted Vector Wind Speed at North Coast Stations in the 4km Grid.

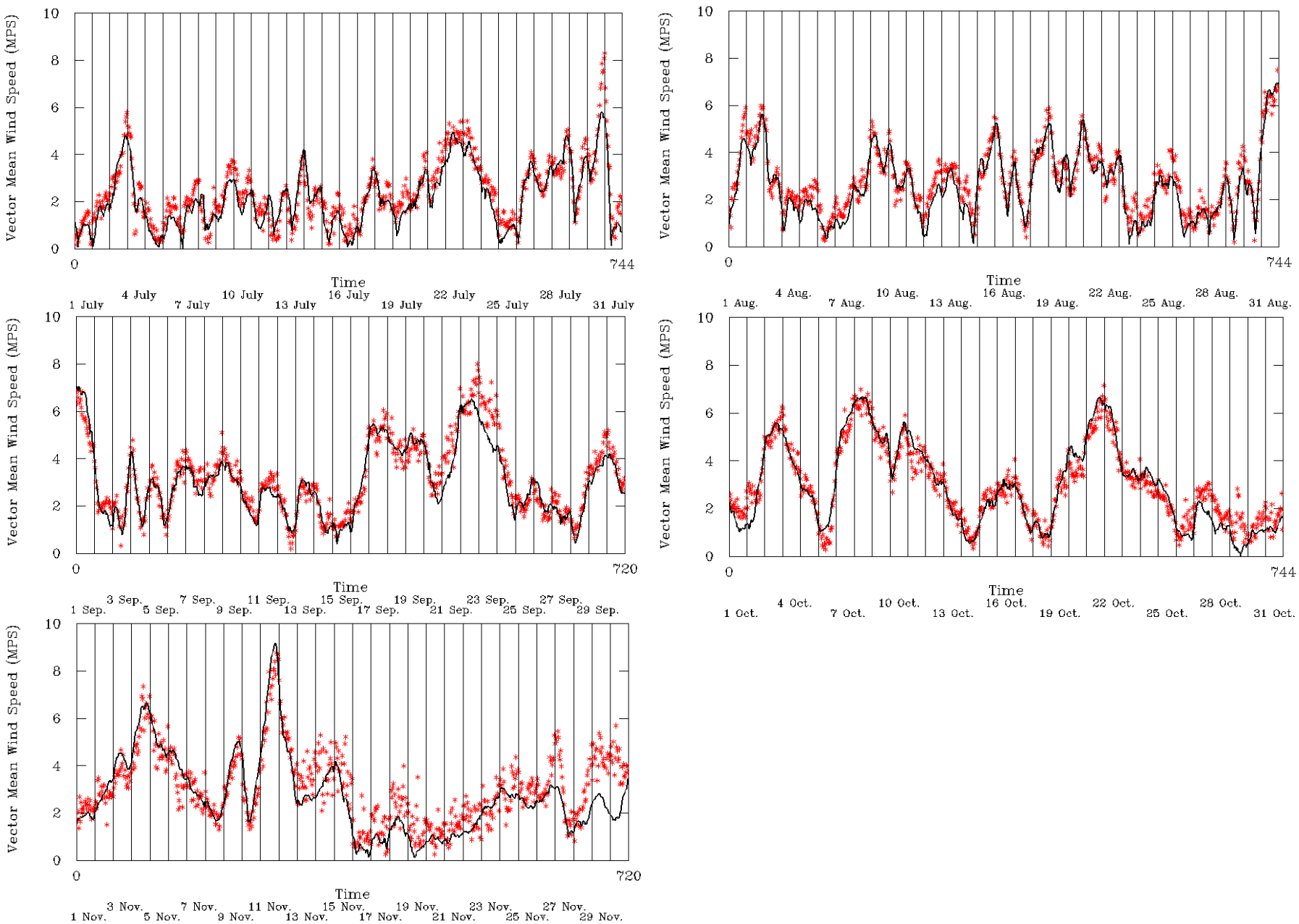

Figure 3-34. Hourly Spatial Vector Mean Wind Speed (m/s) Time Series for All Stations in the 4km Grid for July through November 2009. The Black Asterisks Represent the Hourly Mean of the Observed Vector Wind Speed from All Stations in the 4km Grid. The Red Line Represents the Hourly Mean of the Predicted Vector Wind Speed at All Stations in the 4km Grid.

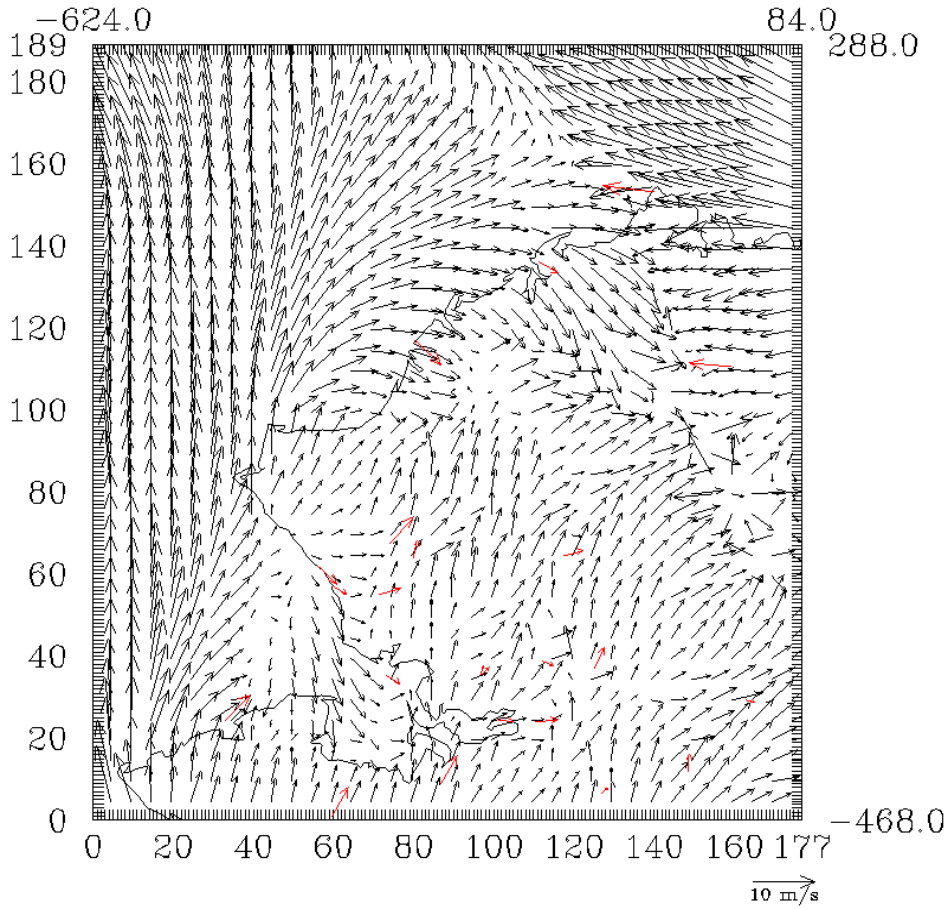

Figure 3-35. Vector Wind Speed (m/s) Spatial Plot for 4km Grid at 0Z (3:00 pm LST) 15 July 2009. Red arrows Represent Observations.

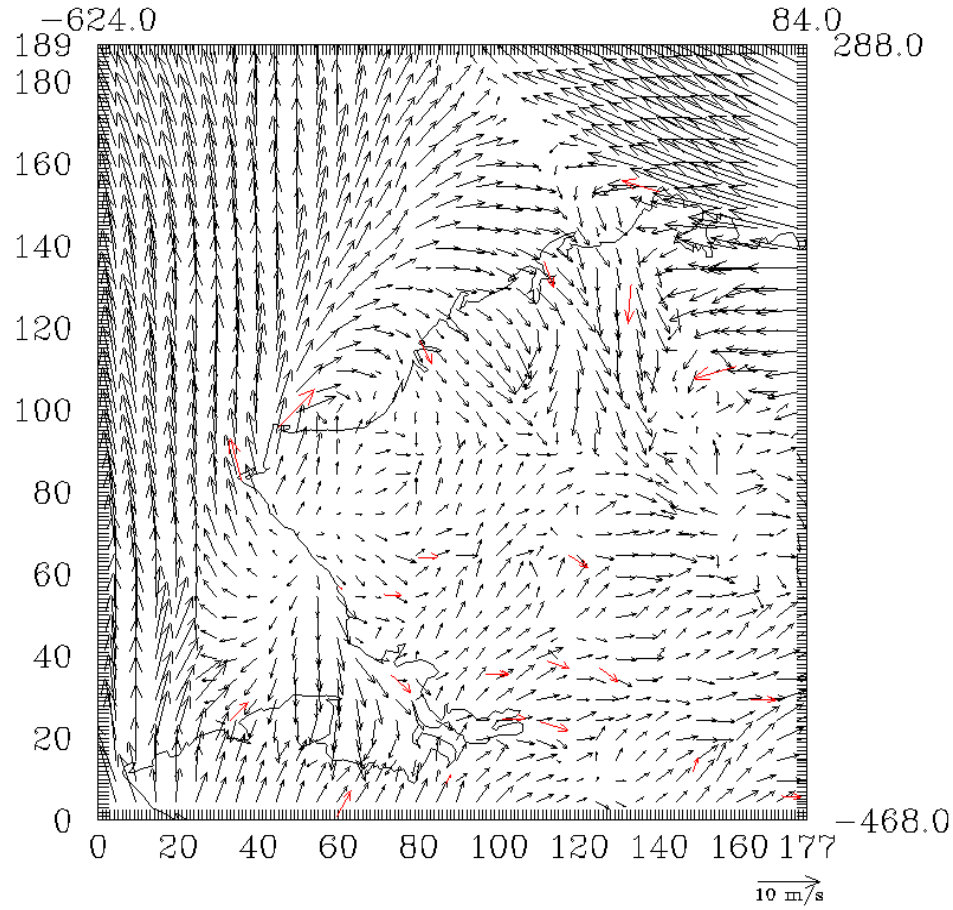

Figure 3-36. Vector Wind Speed (m/s) Spatial Plot for 4km Grid at 4Z (7:00 pm LST) 15 July 2009. Red arrows Represent Observations.

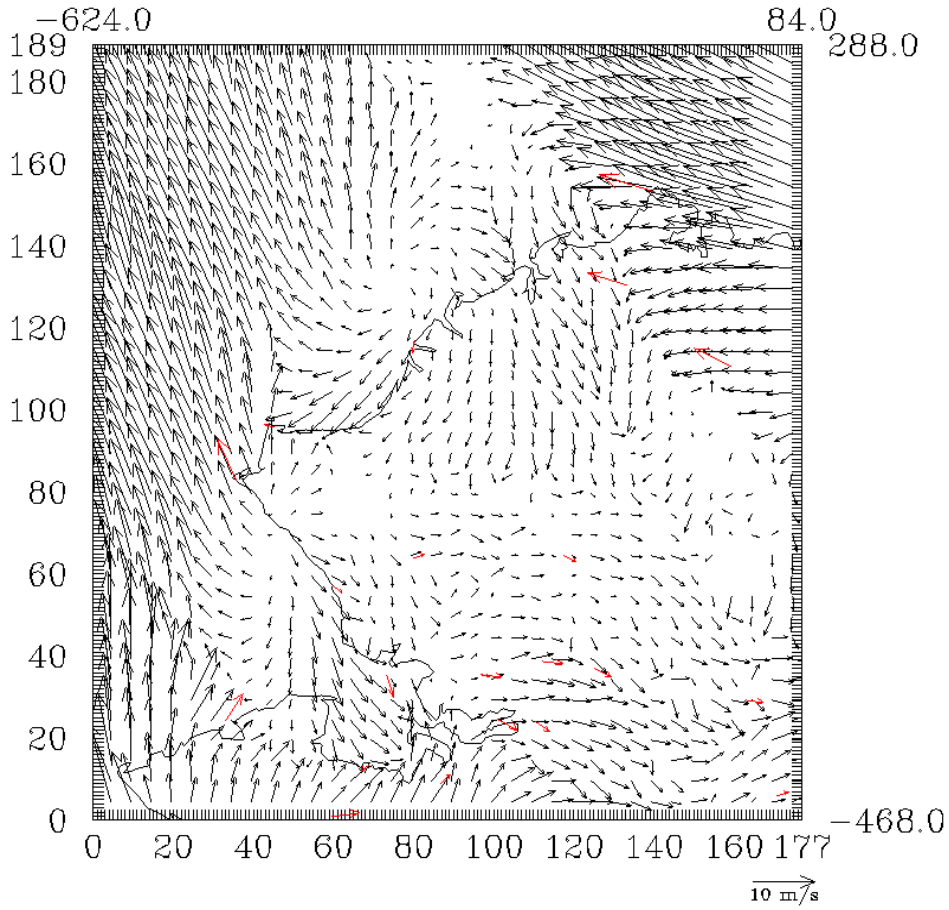

Figure 3-37. Vector Wind Speed (m/s) Spatial Plot for 4km Grid at 8Z (11:00 pm LST) 15 July 2009. Red Arrows Represent Observations.

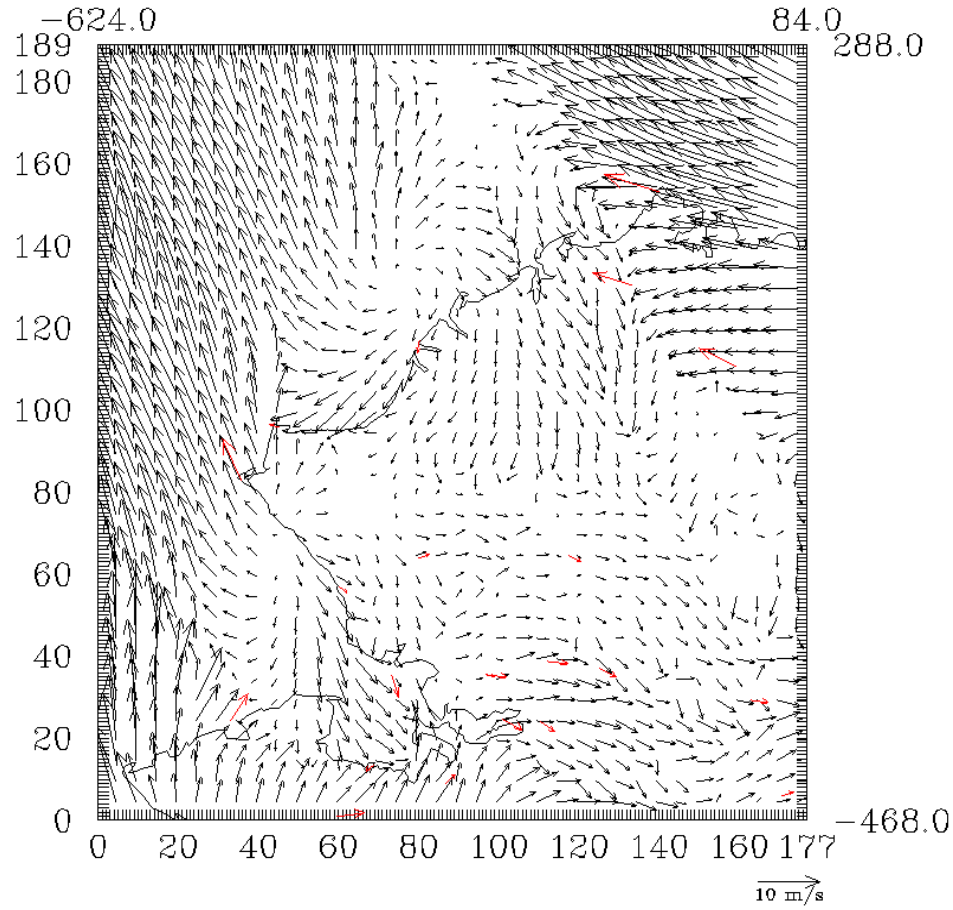

Figure 3-38. Vector Wind Speed (m/s) Spatial Plot for 4km Grid at 12Z (3:00 am LST) 15 July 2009. Red Arrows Represent Observations.

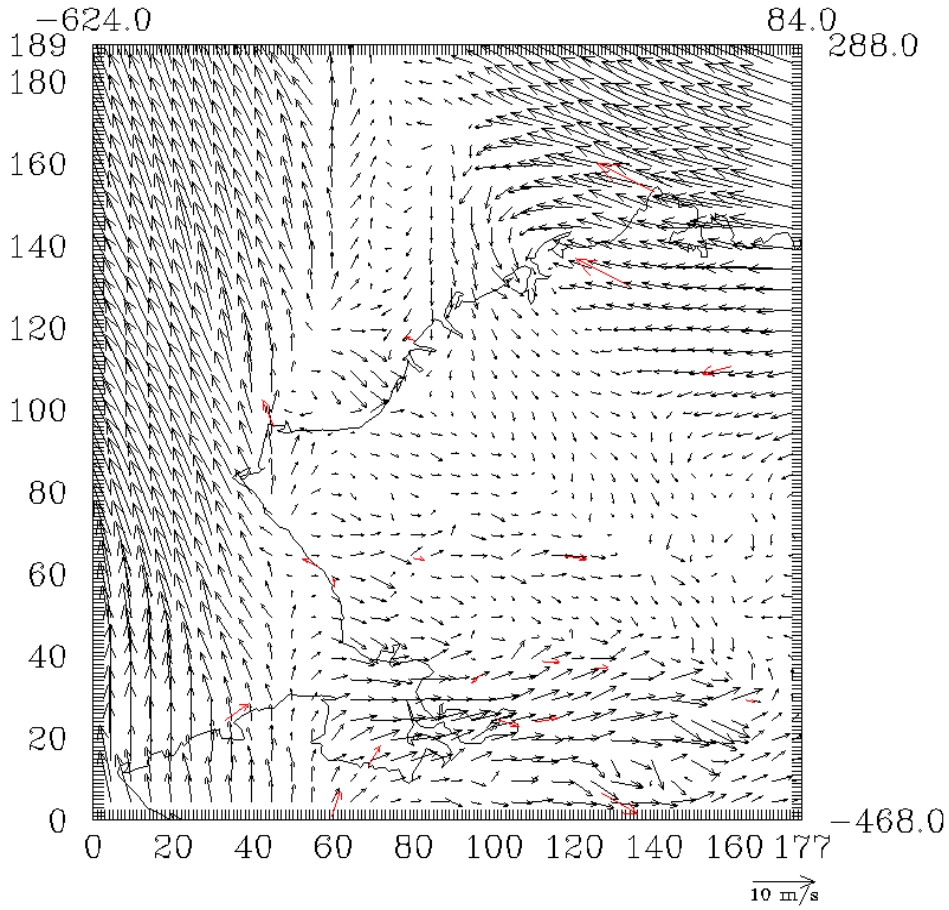

Figure 3-39. Vector Wind Speed (m/s) Spatial Plot for 4km Grid at 16Z (7:00 am LST) 15 July 2009. Red Arrows Represent Observations.

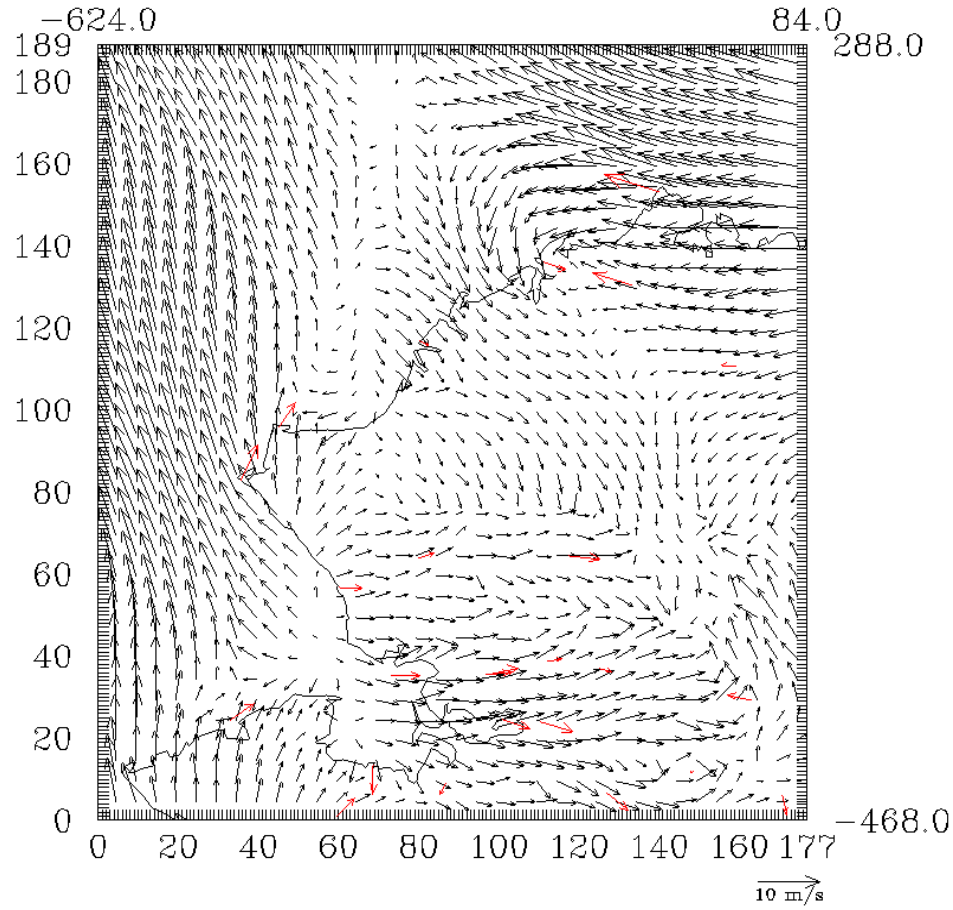

Figure 3-40. Vector Wind Speed (m/s) Spatial Plot for 4km Grid at 20Z (11:00 am LST) 15 July 2009. Red Arrows Represent Observations.

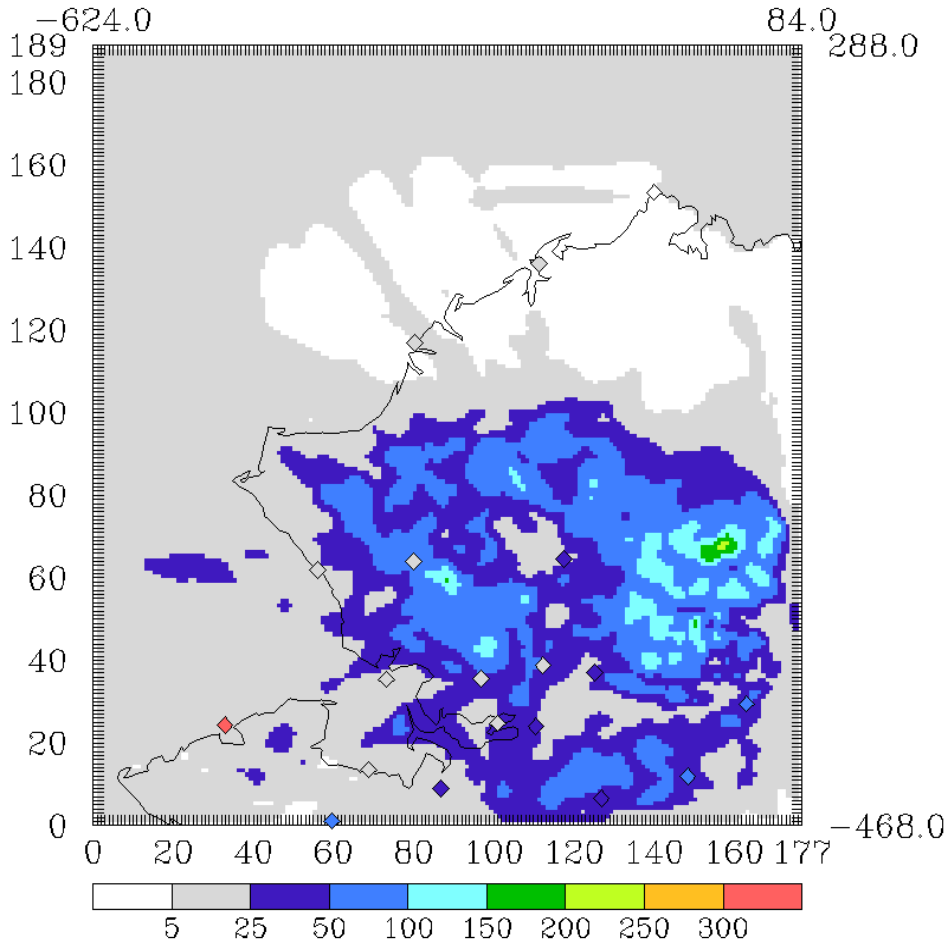

Figure 3-41. Monthly Total Precipitation (mm) Spatial Plot for 4km Grid for July 2007. Diamonds Represent Observations.

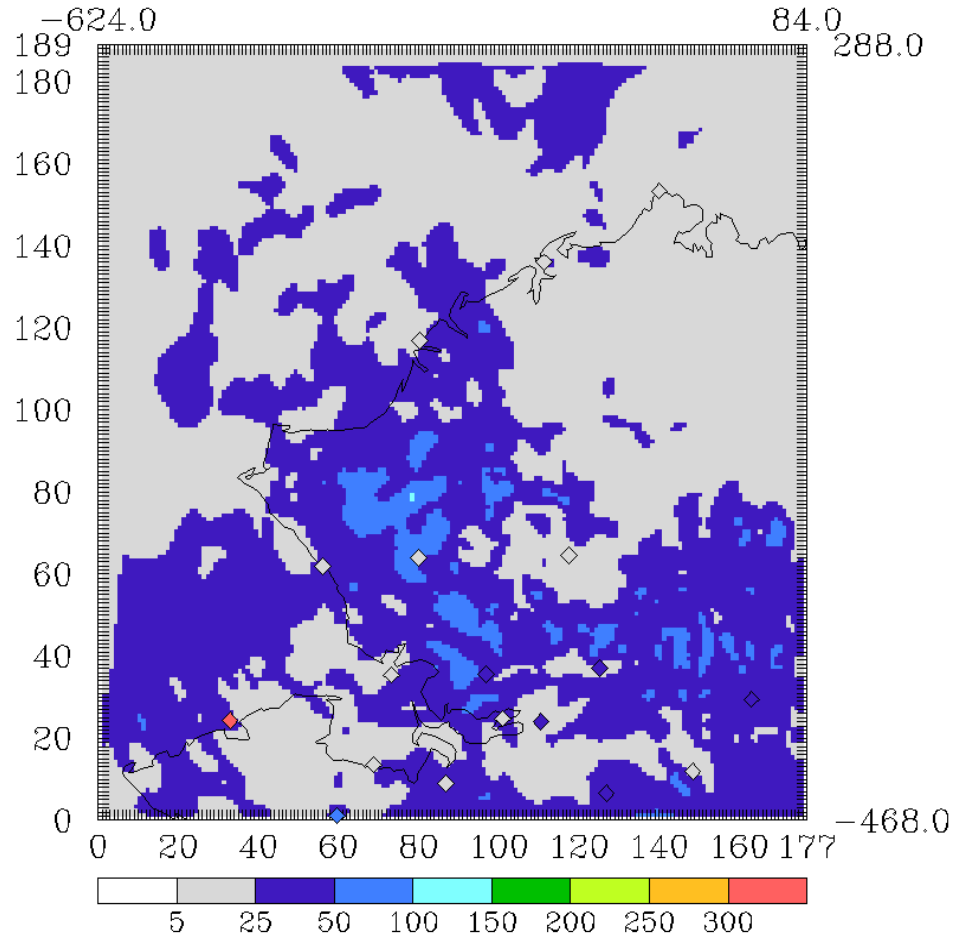

Figure 3-42. Monthly Total Precipitation (mm) Spatial Plot for 4km Grid for August 2007. Diamonds Represent Observations.

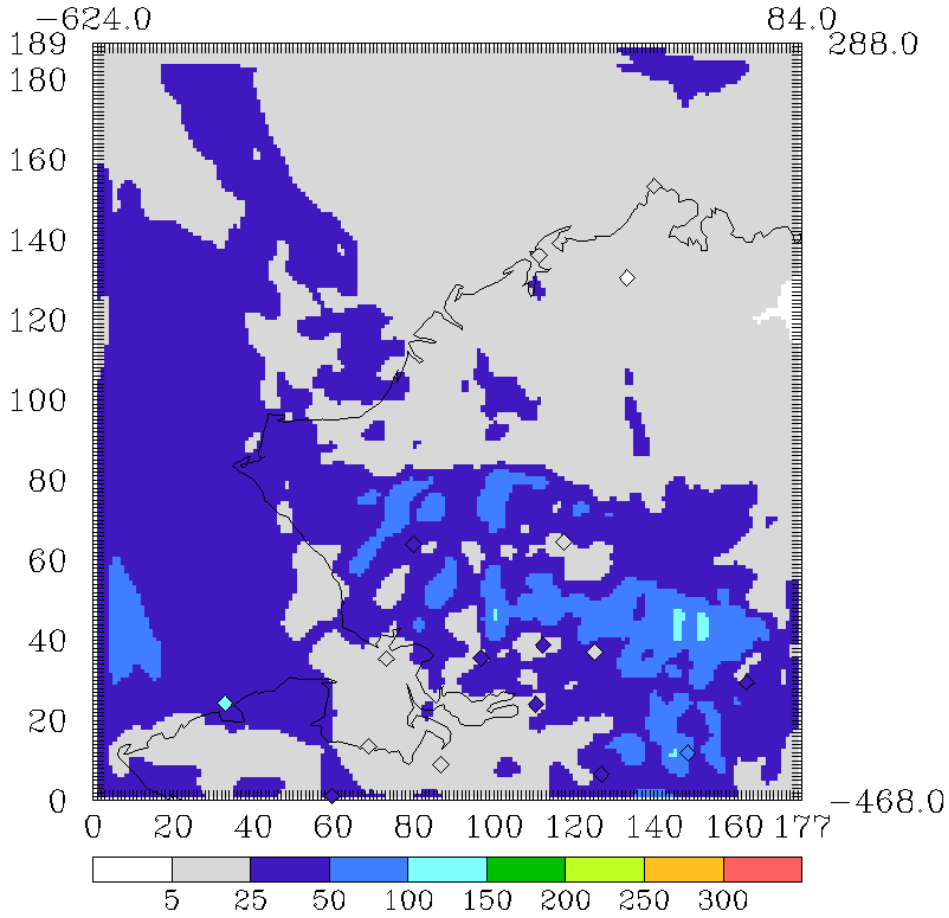

Figure 3-43. Monthly Total Precipitation (mm) Spatial Plot for 4km Grid for September 2007. Diamonds Represent Observations.

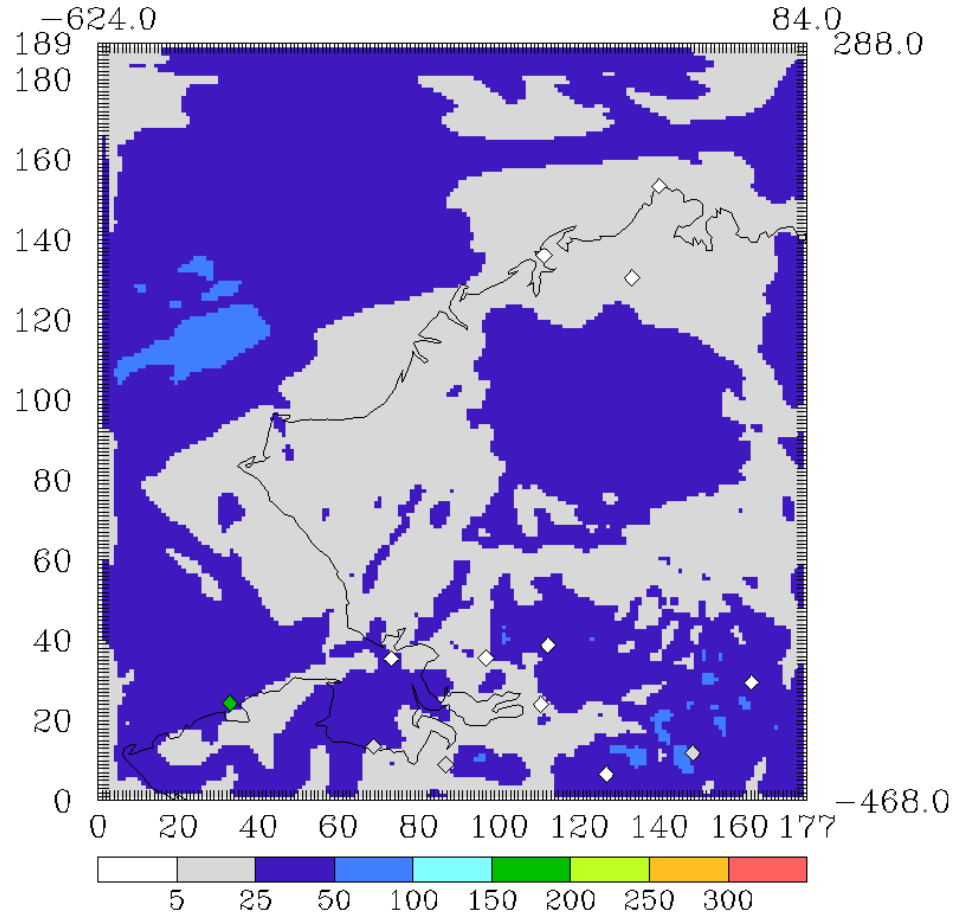

Figure 3-44. Monthly Total Precipitation (mm) Spatial Plot for 4km Grid for October 2007. Diamonds Represent Observations.

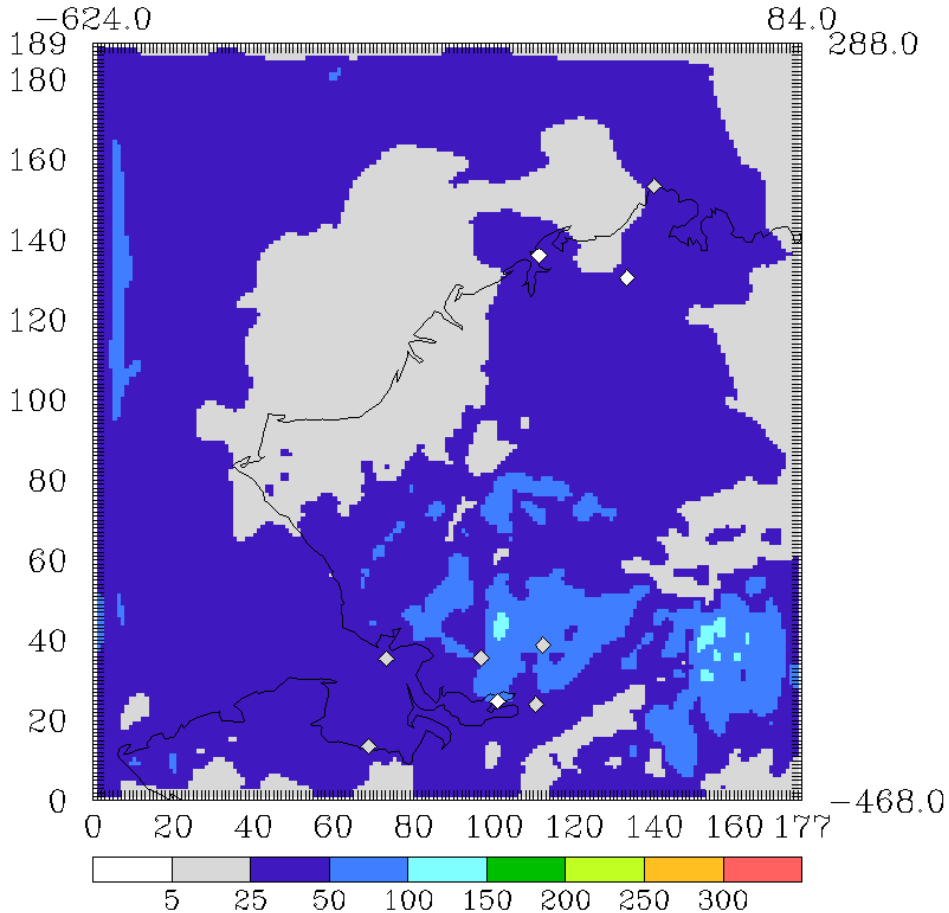

Figure 3-45. Monthly Total Precipitation (mm) Spatial Plot for 4km Grid for November 2007. Diamonds Represent Observations.

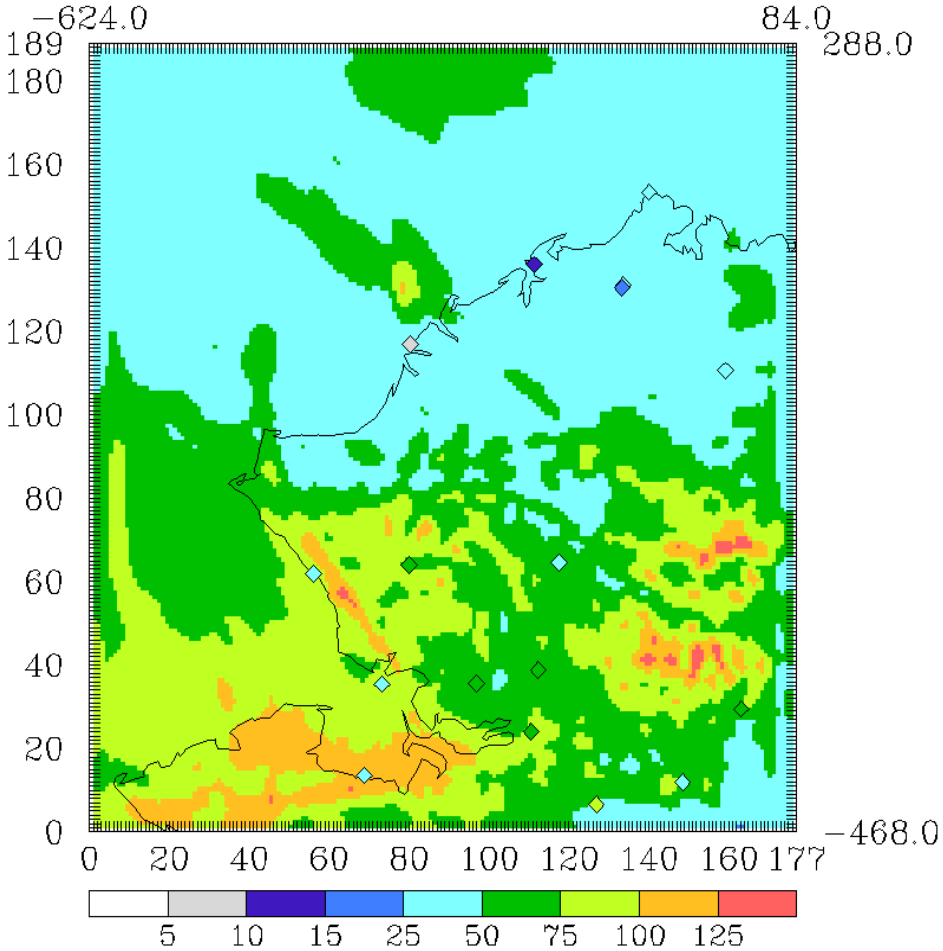

Figure 3-46. Monthly Total Precipitation (mm) Spatial Plot for 4km Grid for July 2008. Diamonds Represent Observations.

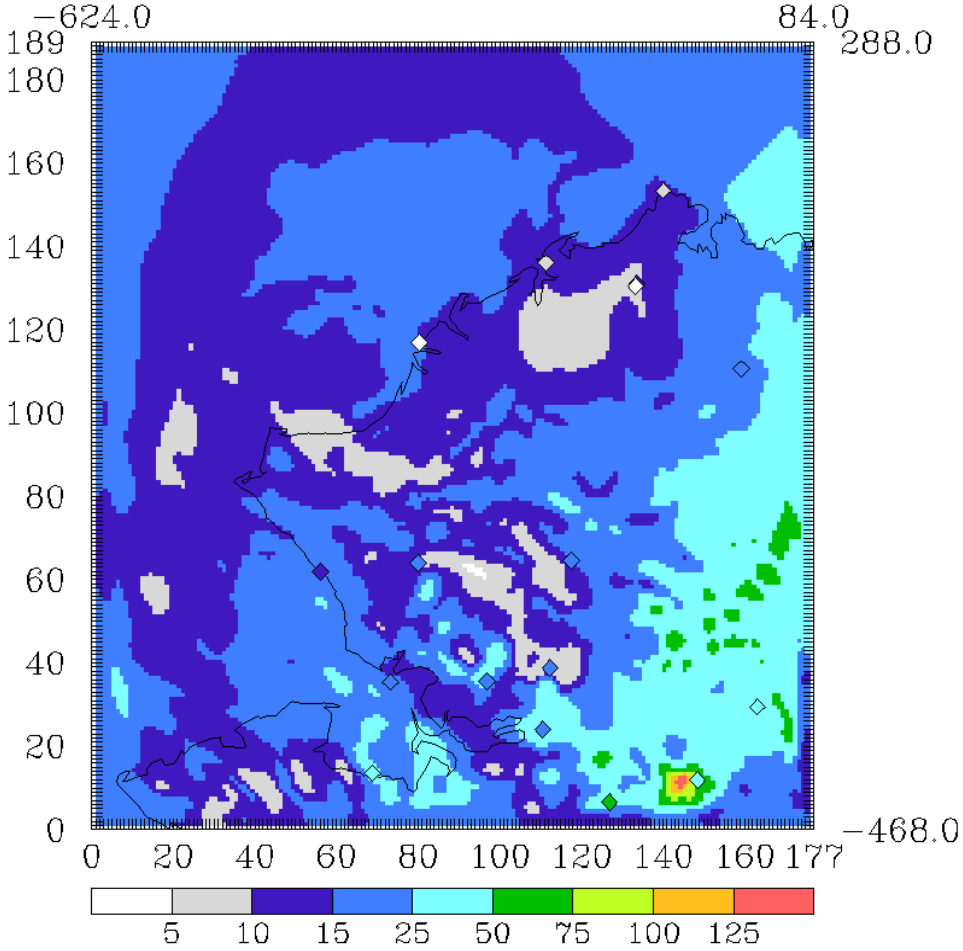

Figure 3-47. Monthly Total Precipitation (mm) Spatial Plot for 4km Grid for August 2008. Diamonds Represent Observations.

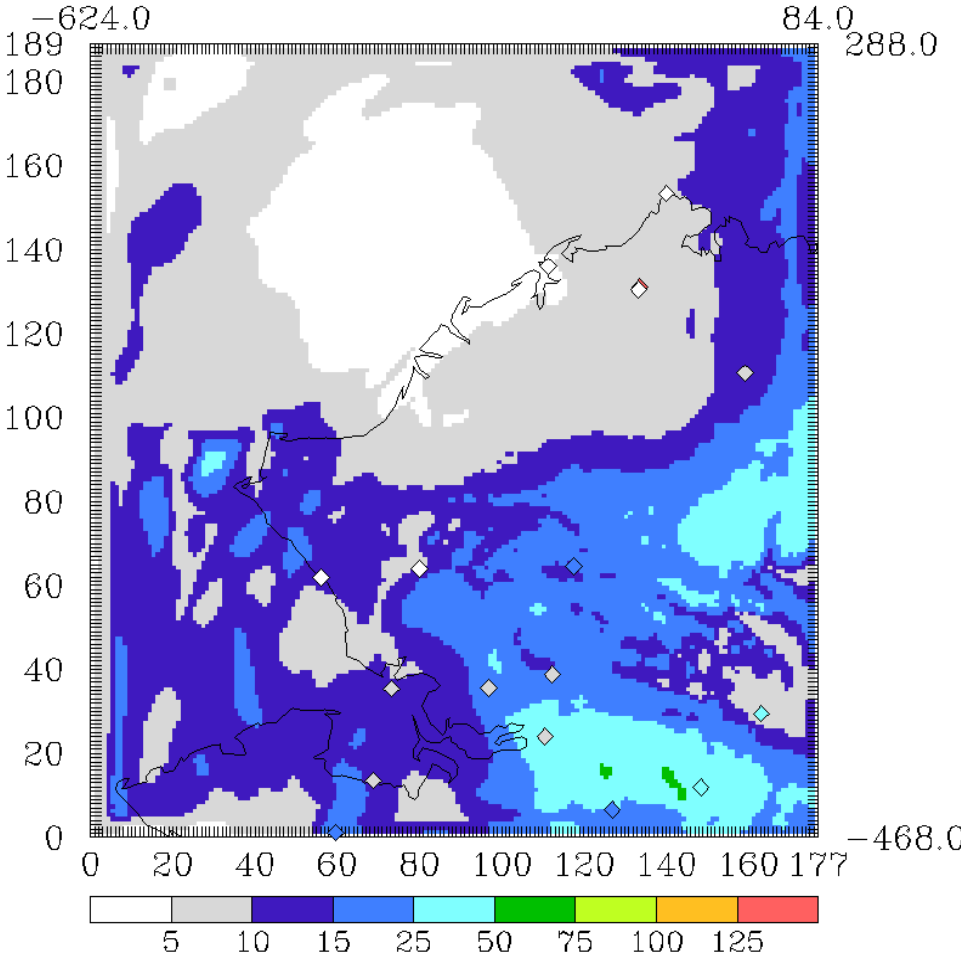

Figure 3-48. Monthly Total Precipitation (mm) Spatial Plot for 4km Grid for September 2008. Diamonds Represent Observations.

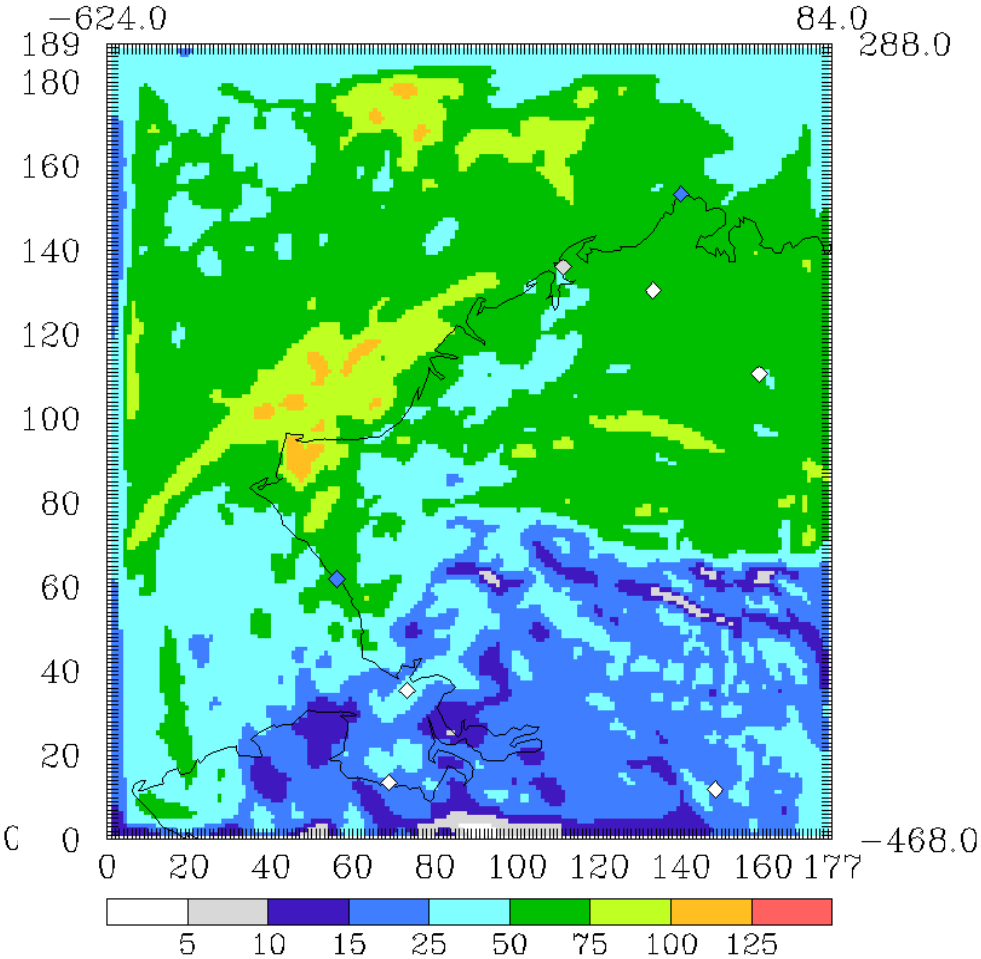

Figure 3-49. Monthly Total Precipitation (mm) Spatial Plot for 4km Grid for October 2008. Diamonds Represent Observations.

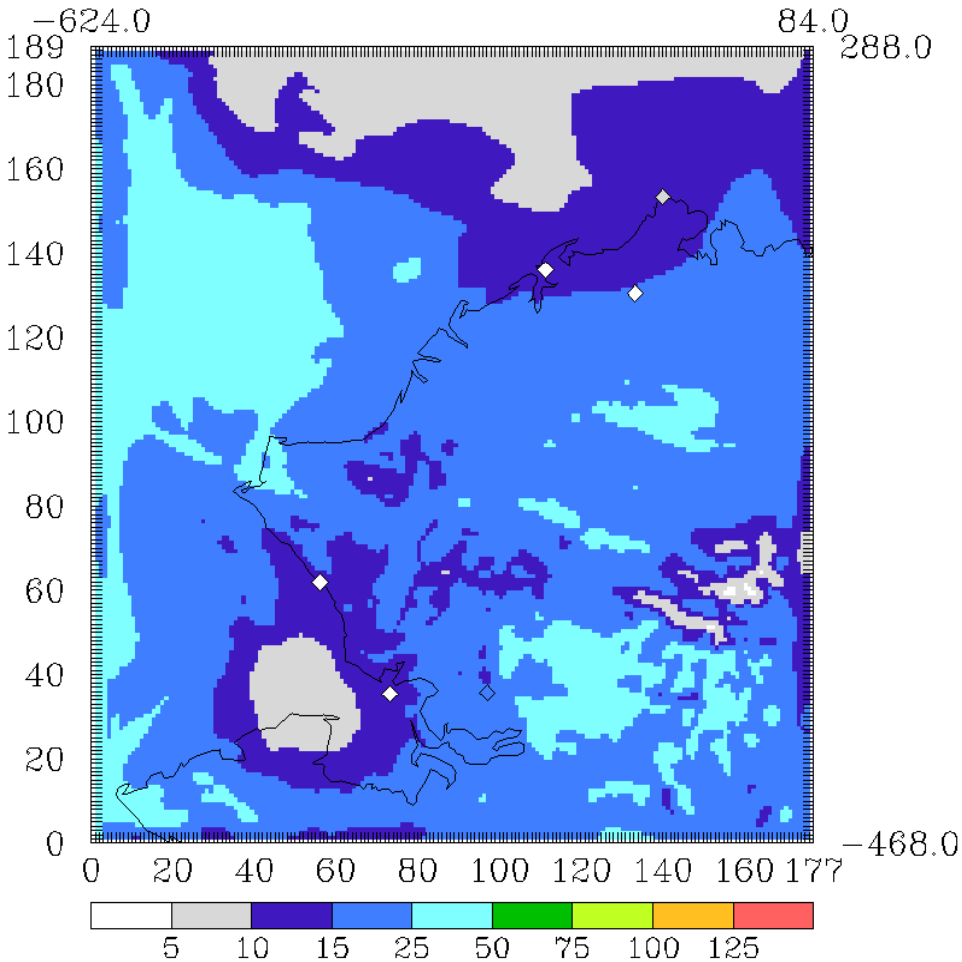

Figure 3-50. Monthly Total Precipitation (mm) Spatial Plot for 4km Grid for November 2008. Diamonds Represent Observations.

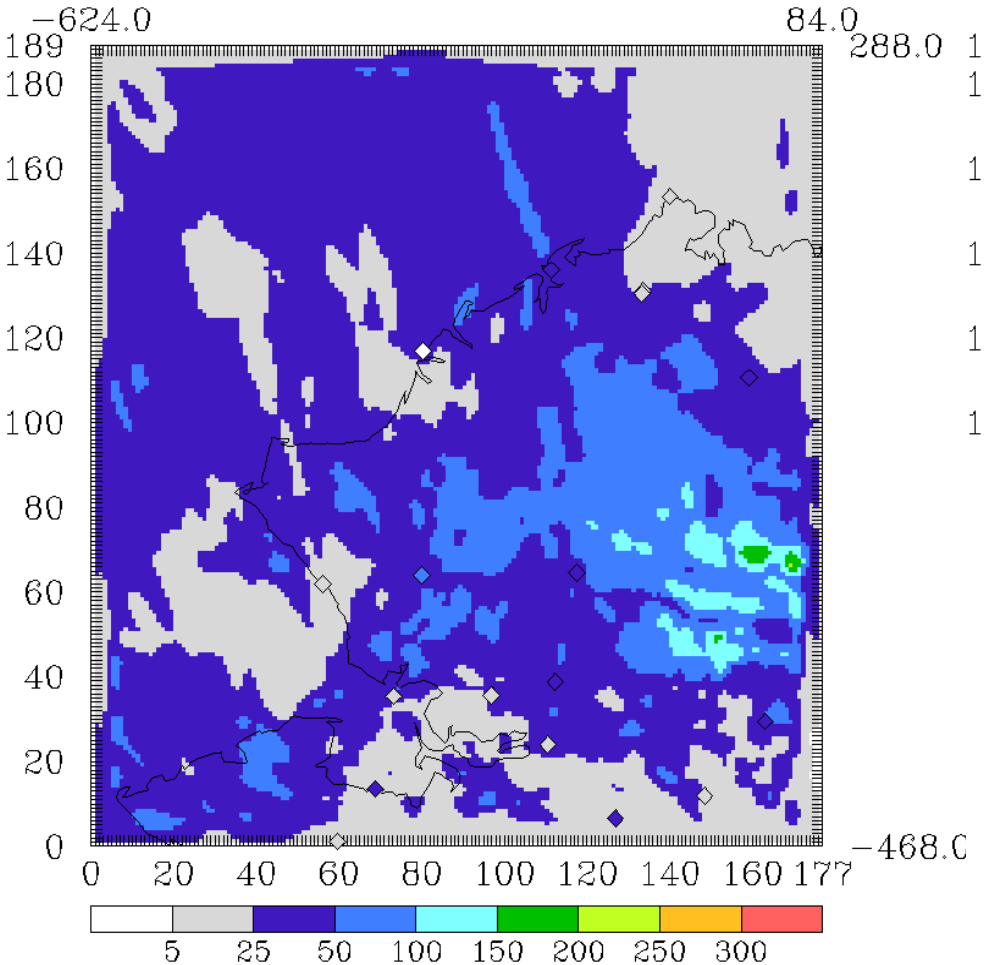

Figure 3-51. Monthly Total Precipitation (mm) Spatial Plot for 4km Grid for July 2009. Diamonds Represent Observations.

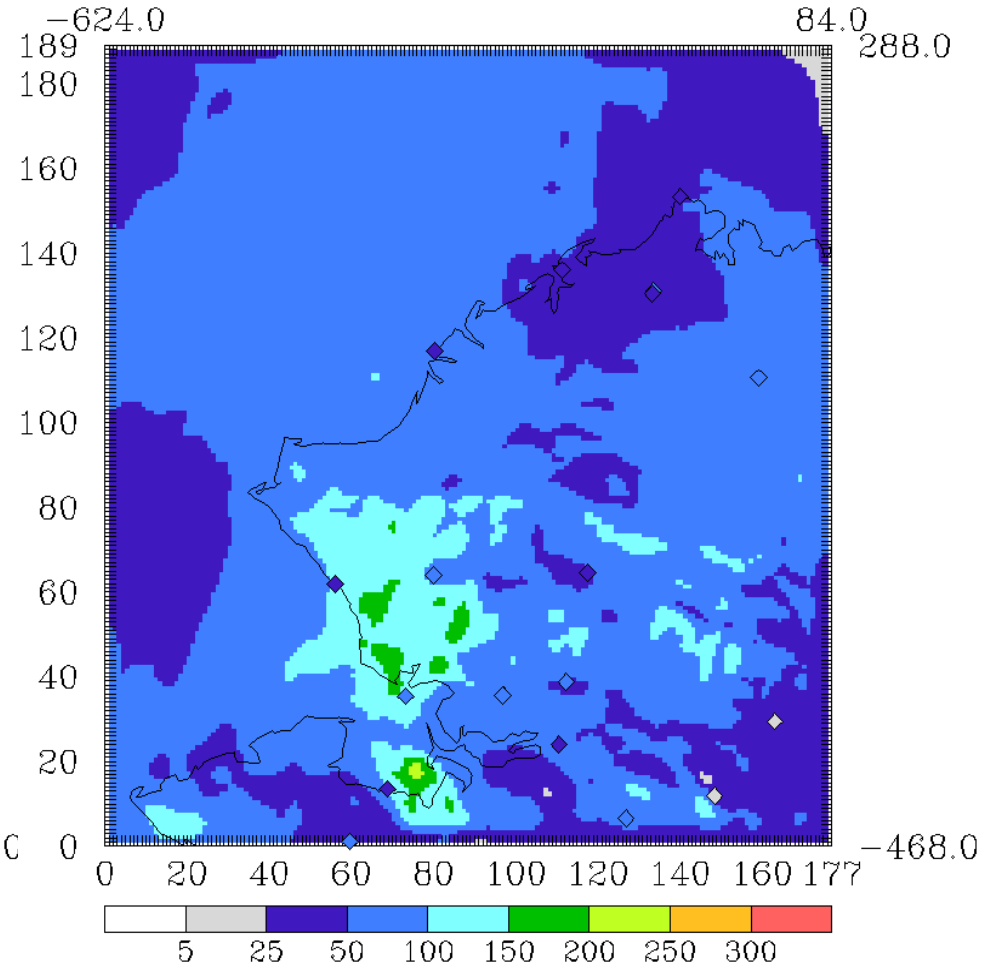

Figure 3-52. Monthly Total Precipitation (mm) Spatial Plot for 4km Grid for August 2009. Diamonds Represent Observations.

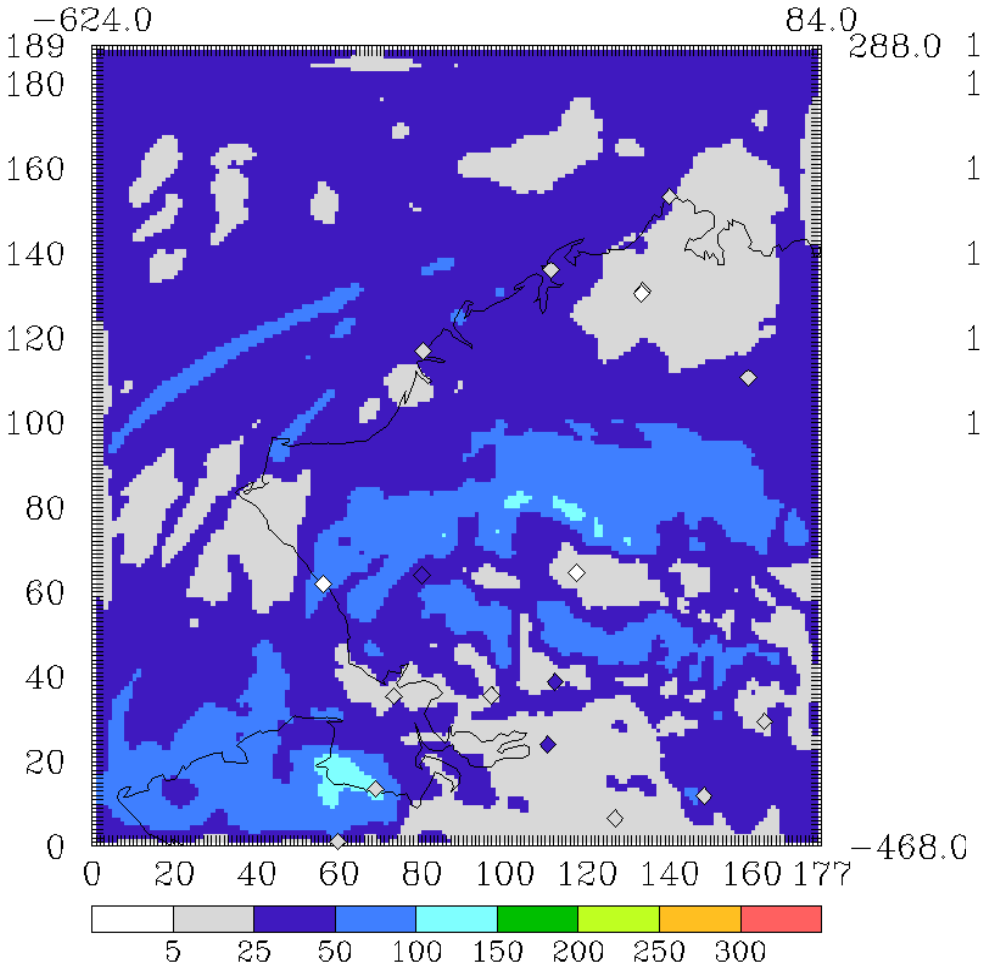

Figure 3-53. Monthly Total Precipitation (mm) Spatial Plot for 4km Grid for September 2009. Diamonds Represent Observations.

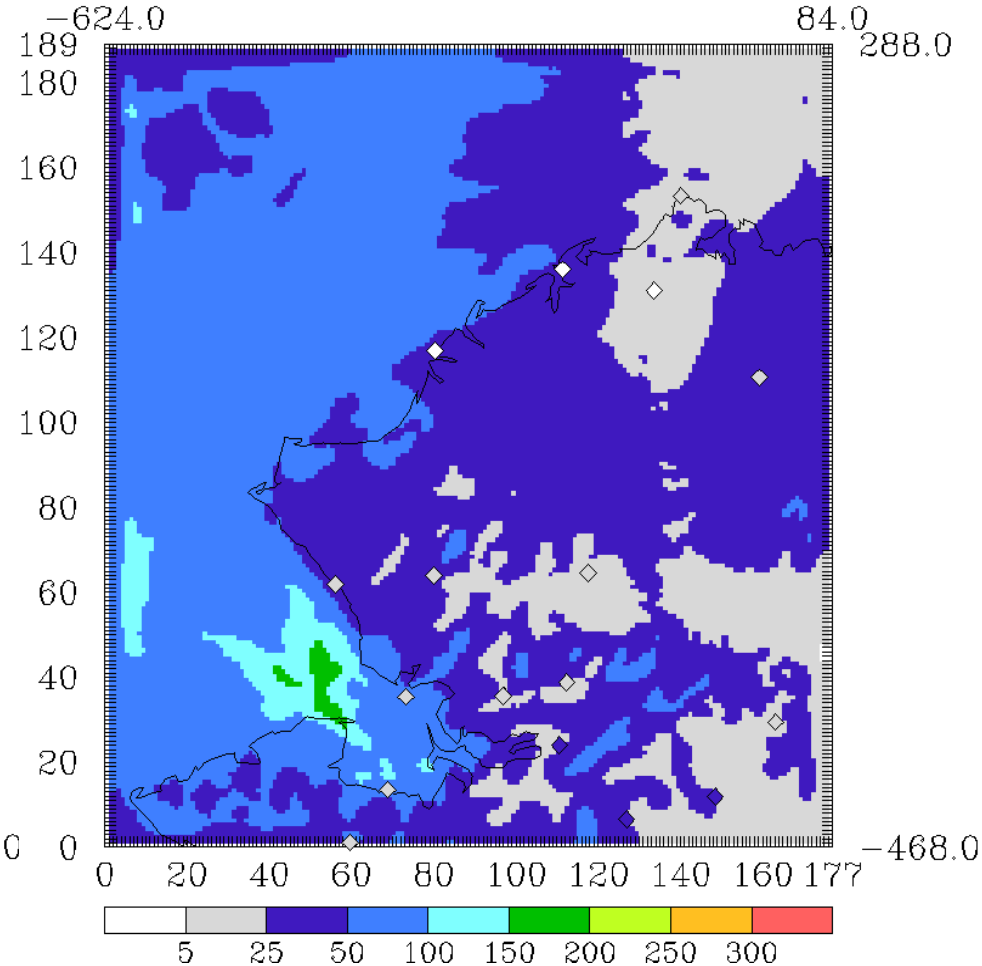

Figure 3-54. Monthly Total Precipitation (mm) Spatial Plot for 4km Grid for October 2009. Diamonds Represent Observations.

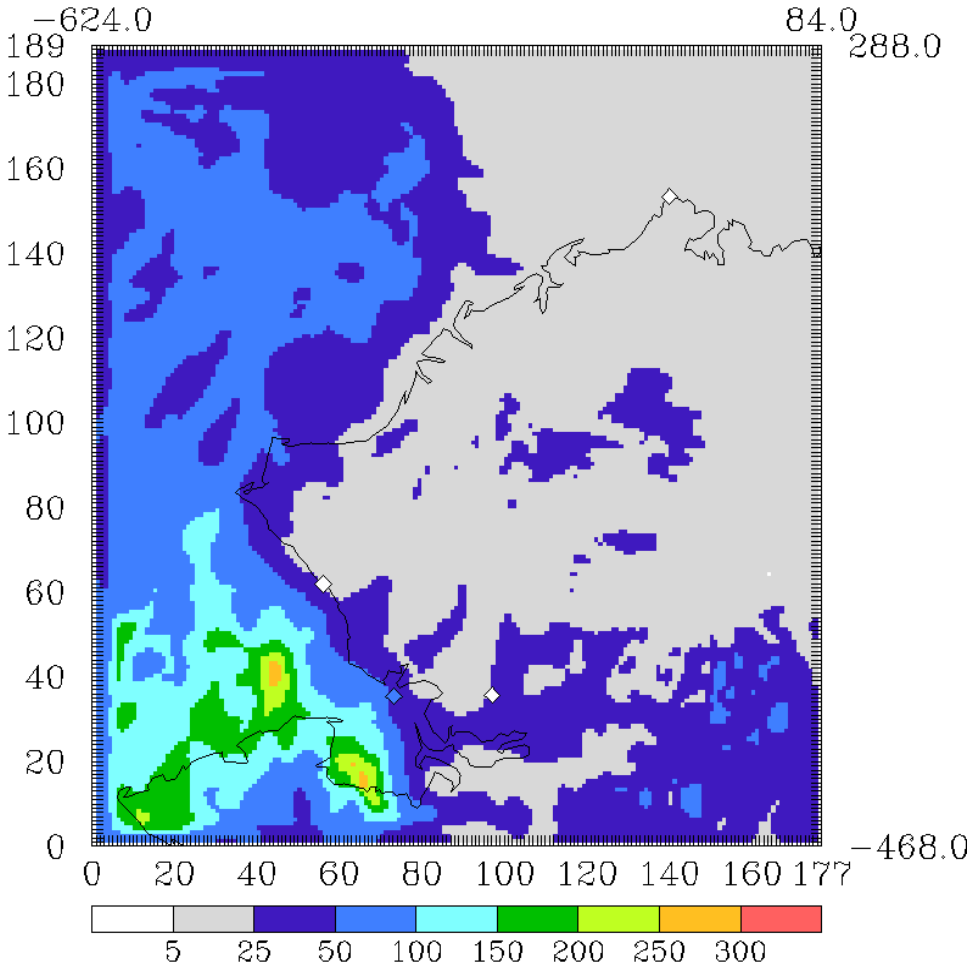

Figure 3-55. Monthly Total Precipitation (mm) Spatial Plot for 4km Grid for November 2009. Diamonds Represent Observations.

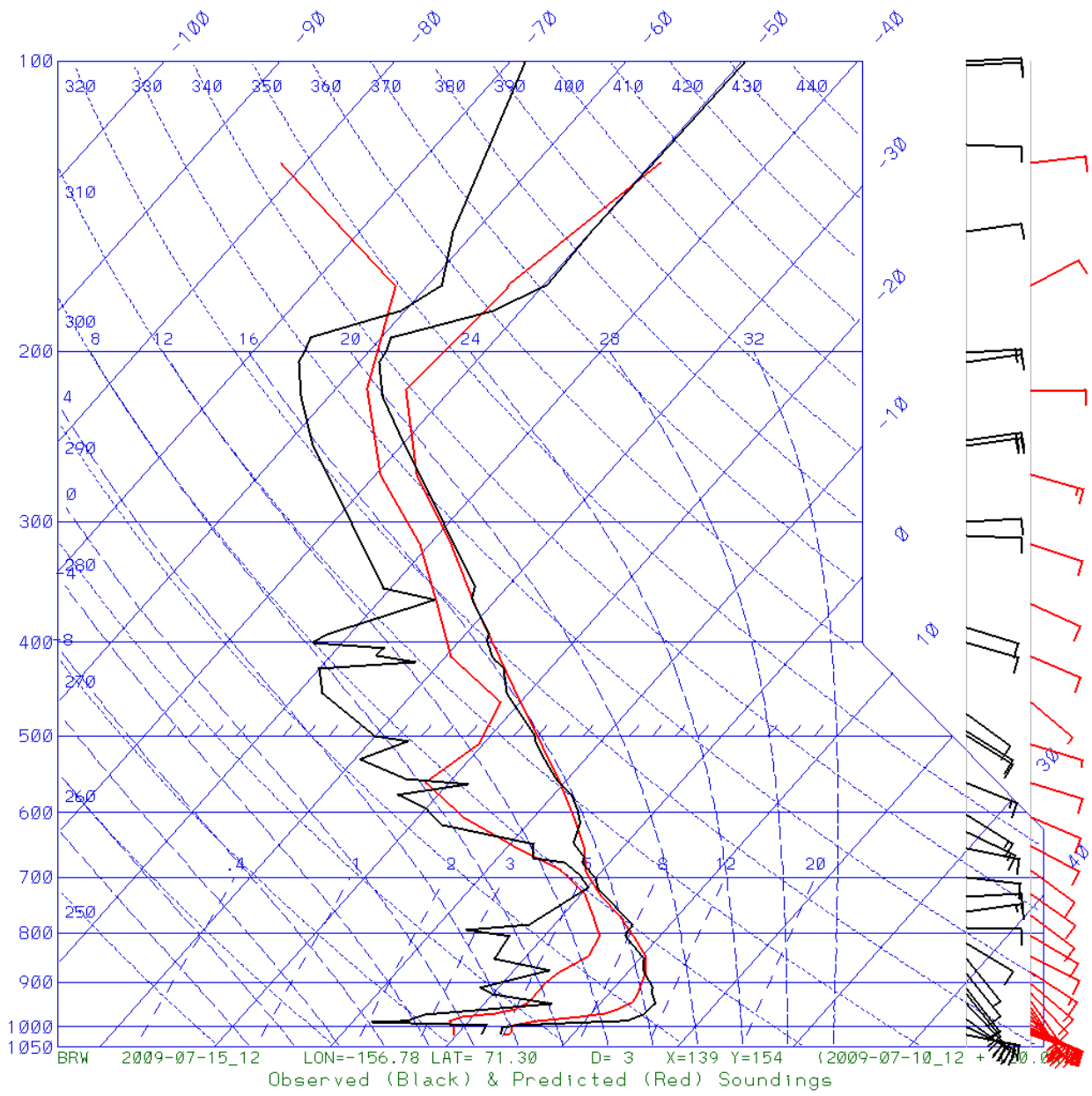

Figure 3-56. Skew-T-log-P Diagram for Barrow at 12Z (3:00 am LST) on 15 July 2009. Red Lines Denote WRF Estimates. Black Lines Denote Observations.

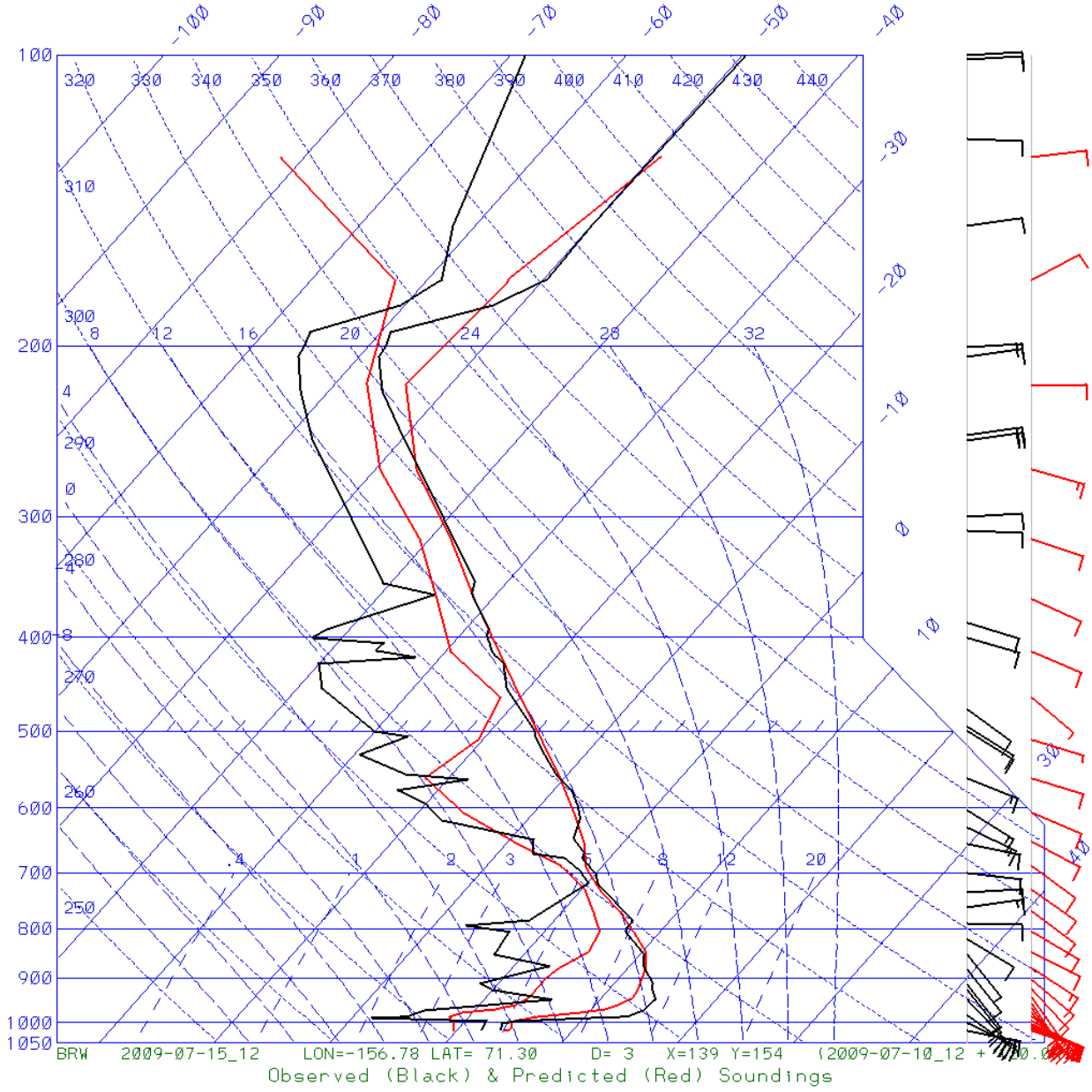

Figure 3-57. Skew-T-log-P Diagram for Barrow at 12Z (3:00 am LST) on 15 July 2009. Red Lines Denote WRF Estimates. Black Lines Denote Observations.

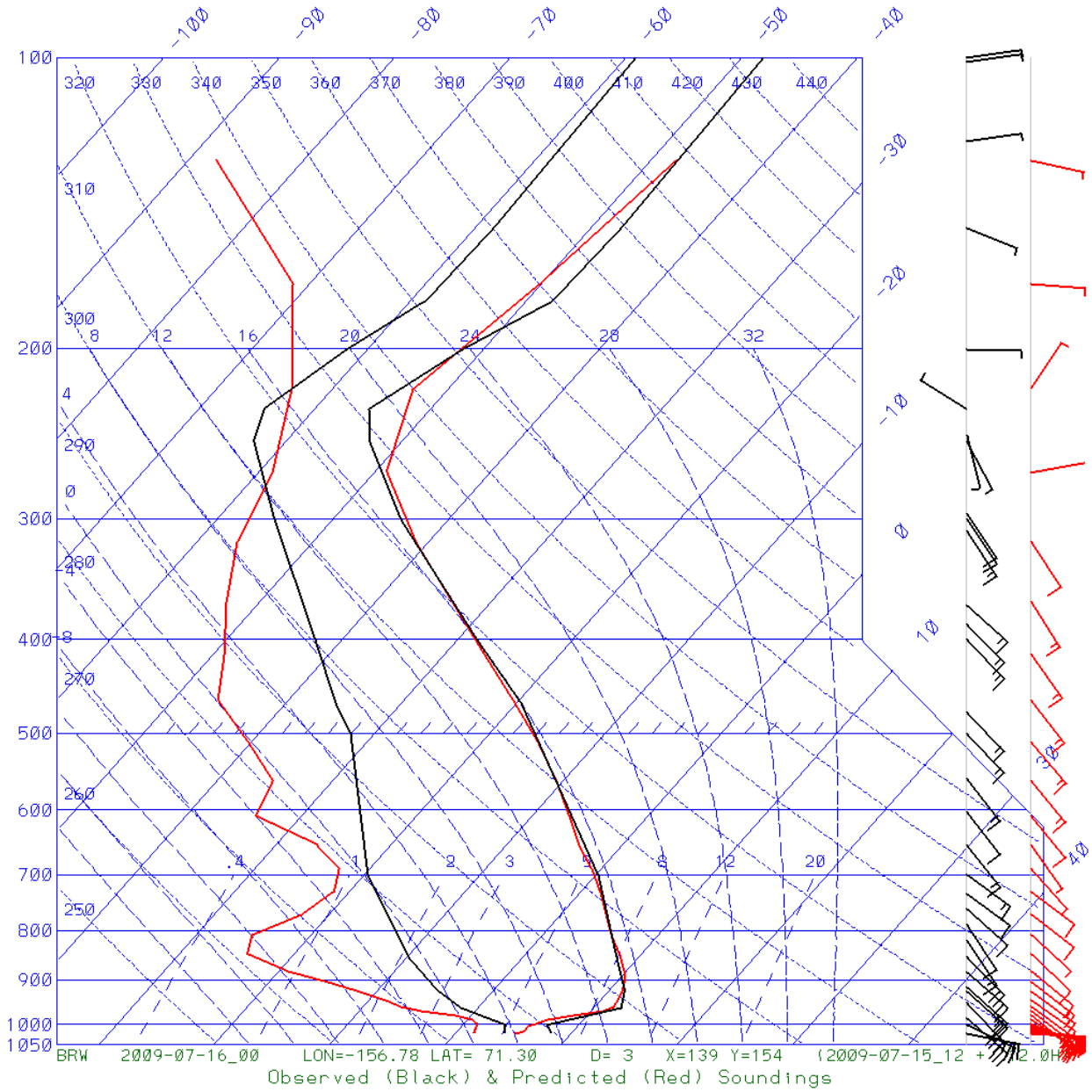

Figure 3-58. Skew-T-log-P Diagram for Barrow at 0Z (3:00 pm LST) on 16 July 2009. Red Lines Denote WRF Estimates. Black Lines Denote Observations.

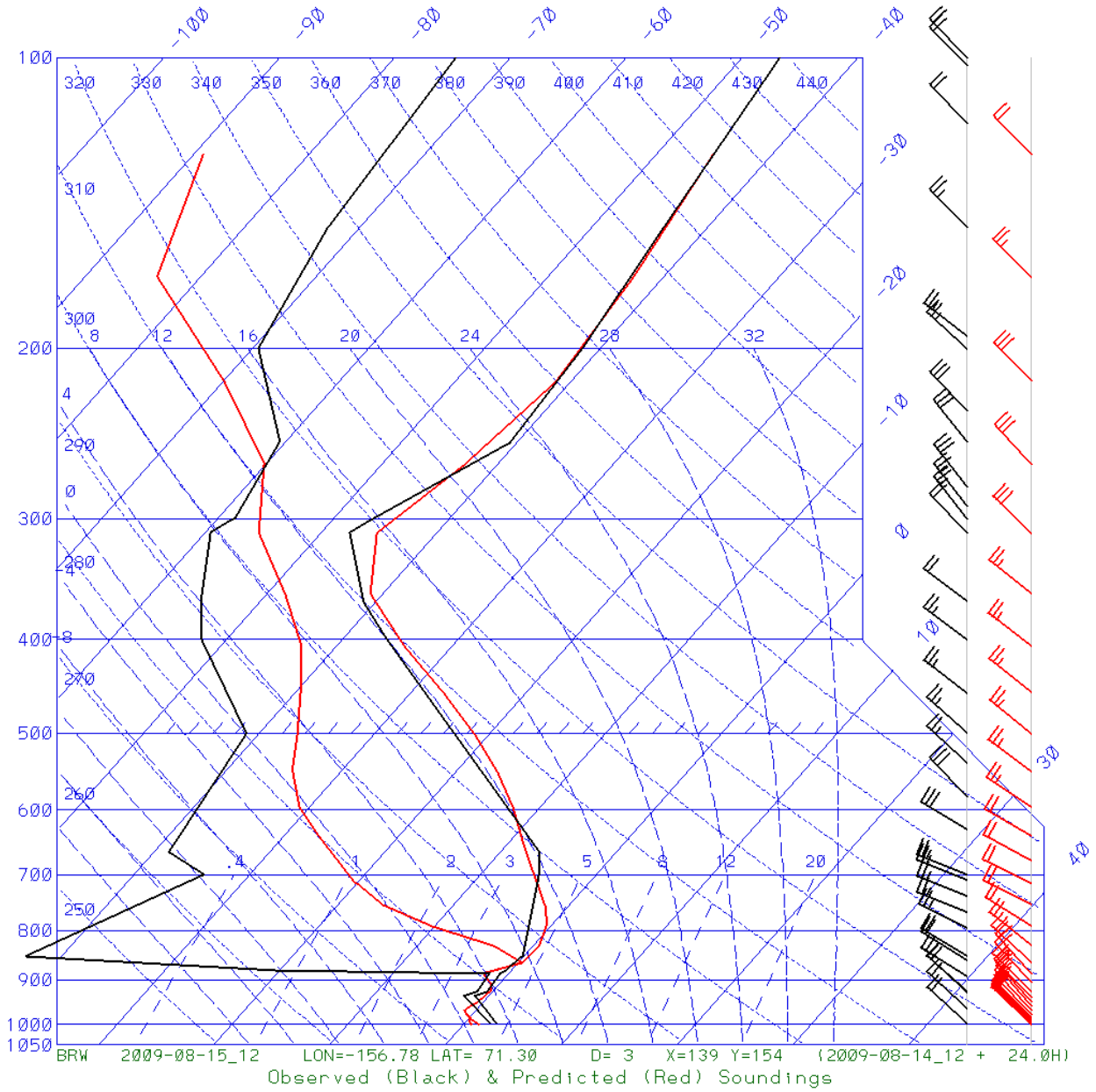

Figure 3-59. Skew-T-log-P Diagram for Barrow at 12Z (3:00 am LST) on 15 August 2009. Red Lines Denote WRF Estimates. Black Lines Denote Observations.

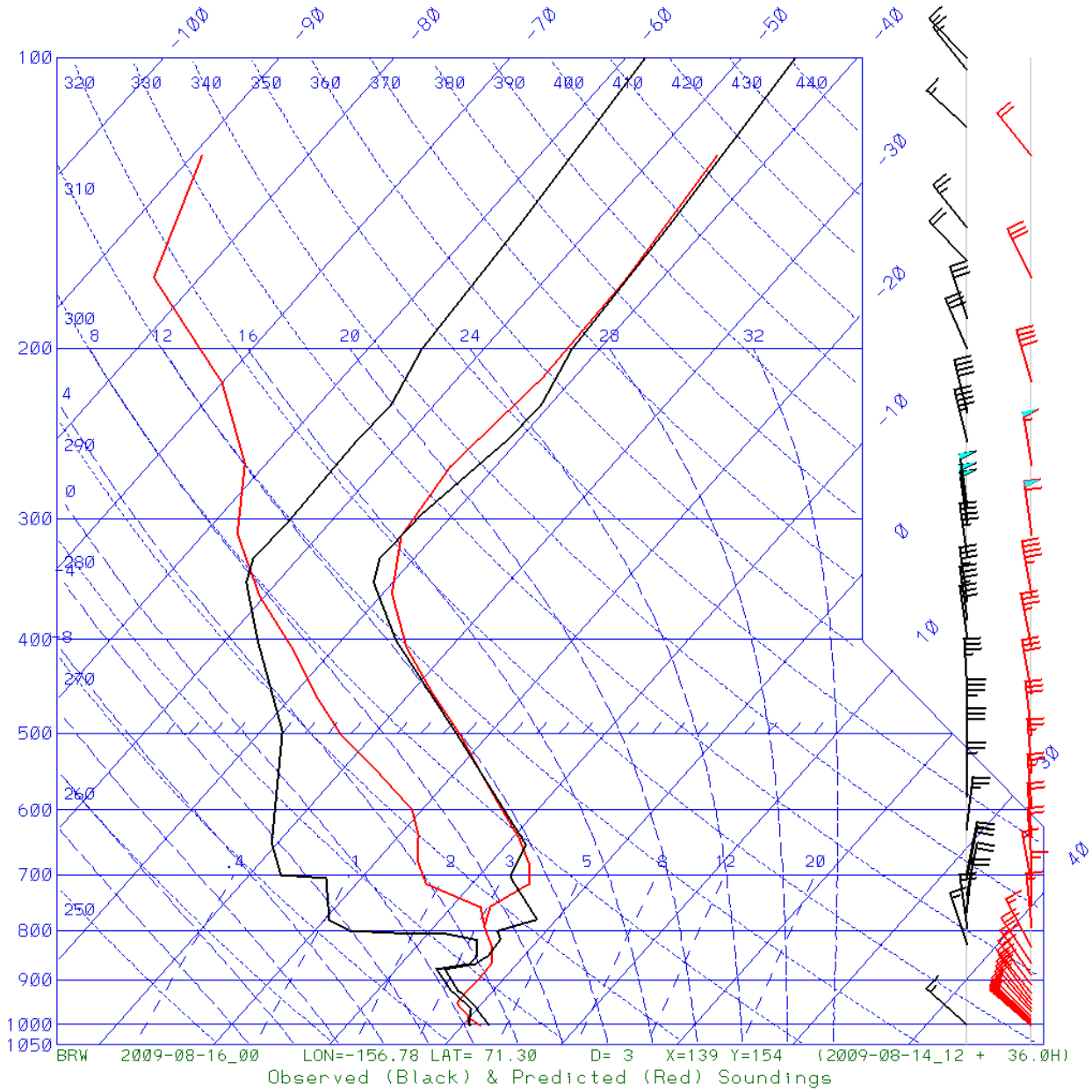

Figure 3-60. Skew-T-log-P Diagram for Barrow at 0Z (3:00 pm LST) on 16 August 2009. Red Lines Denote WRF Estimates. Black Lines Denote Observations.

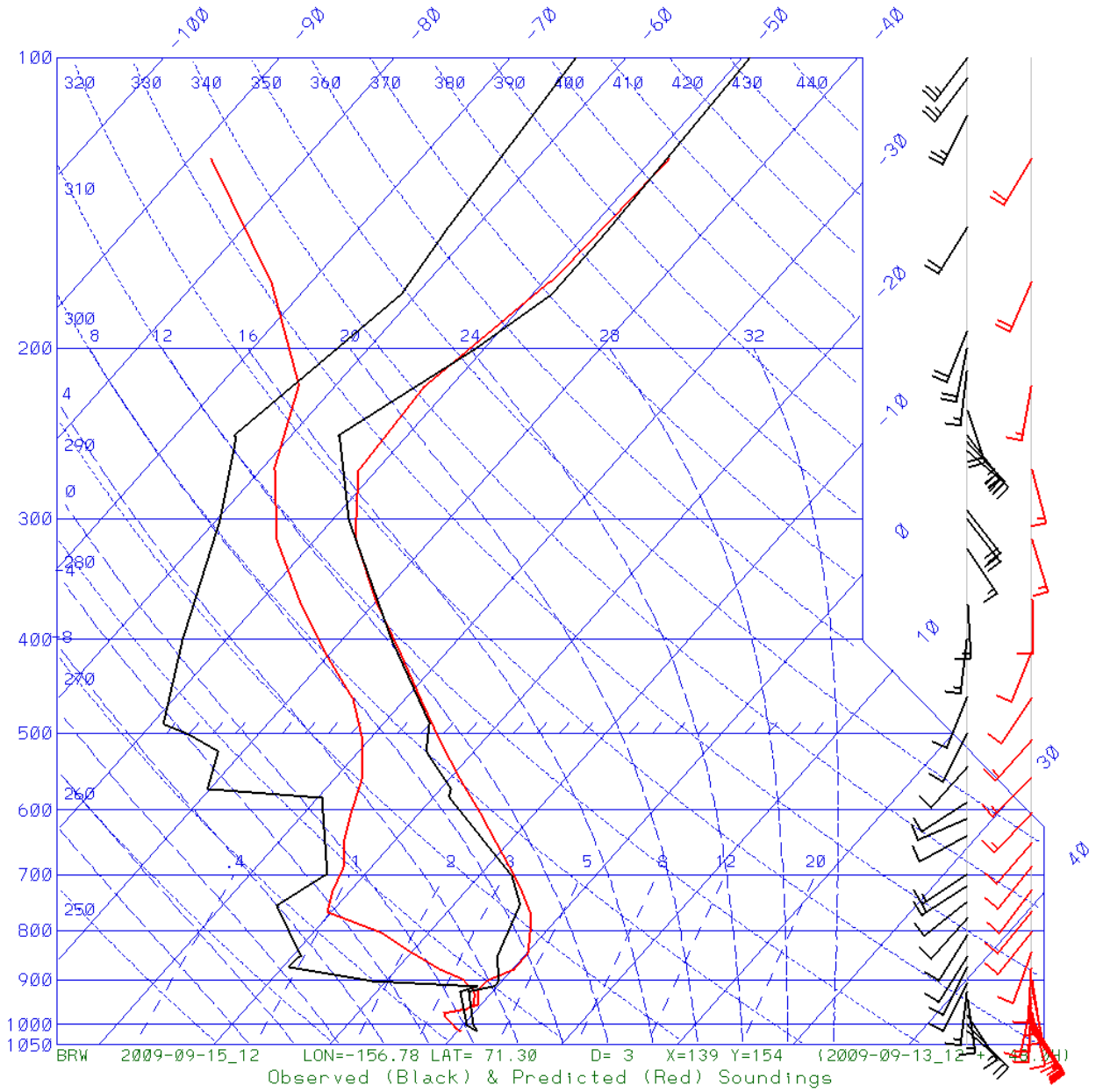

Figure 3-61. Skew-T-log-P Diagram for Barrow at 12Z (3:00 am LST) on 15 September 2009. Red Lines Denote WRF Estimates. Black Lines Denote Observations.

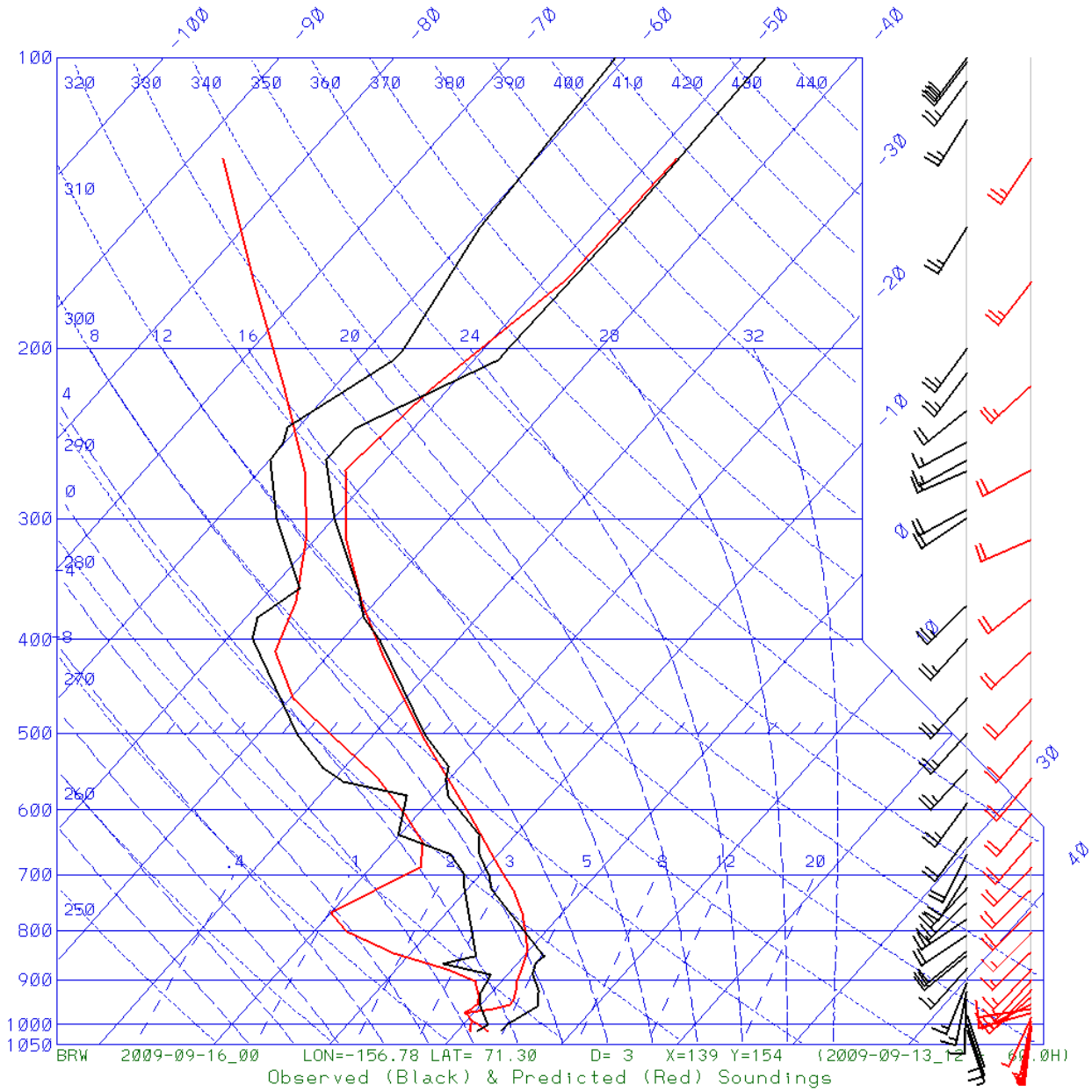

Figure 3-62. Skew-T-log-P Diagram for Barrow at 0Z (3:00 pm LST) on 16 September 2009. Red Lines Denote WRF Estimates. Black Lines Denote Observations.

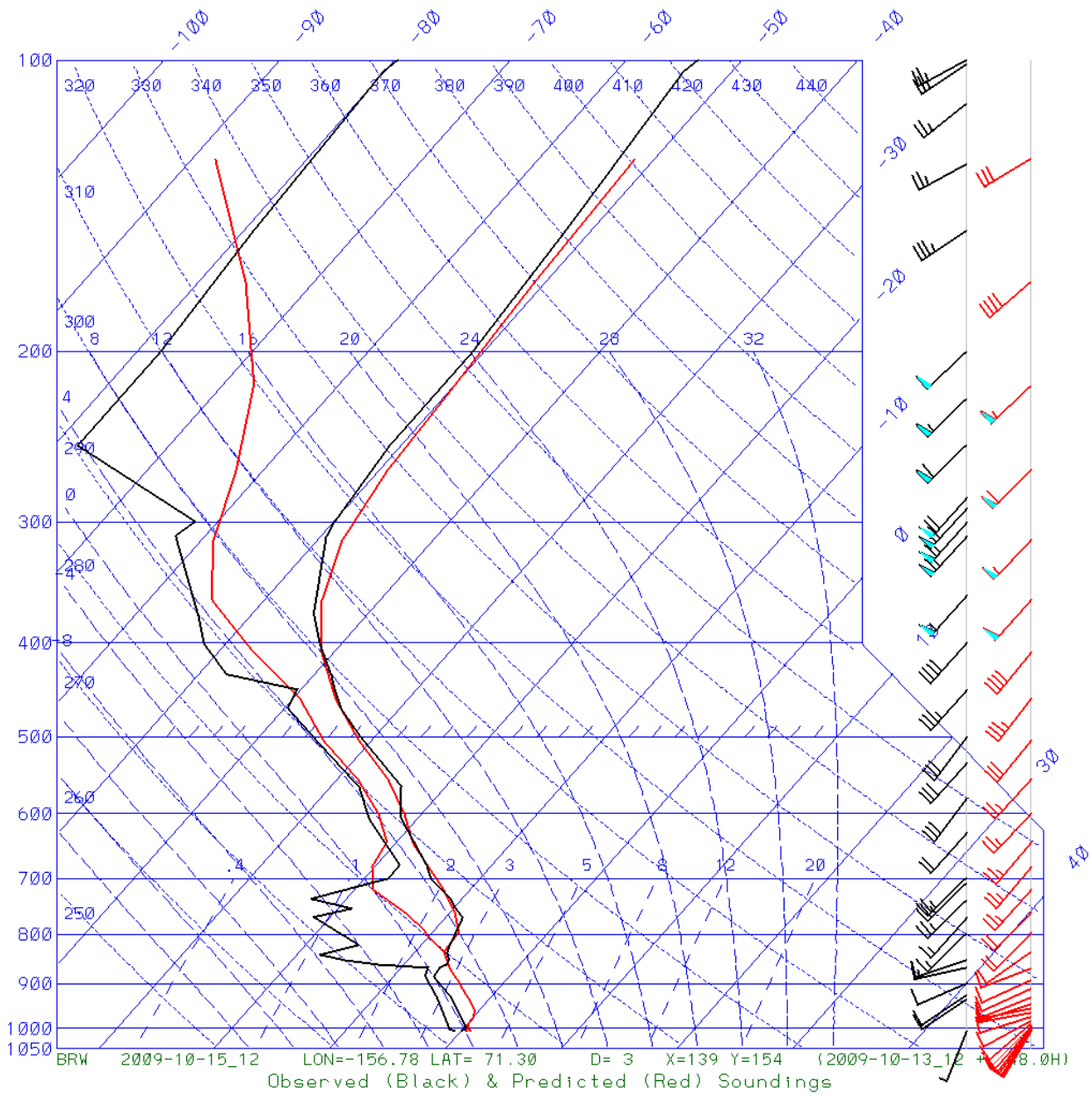

Figure 3-63. Skew-T-log-P Diagram for Barrow at 12Z (3:00 am LST) on 15 October 2009. Red Lines Denote WRF Estimates. Black Lines Denote Observations.

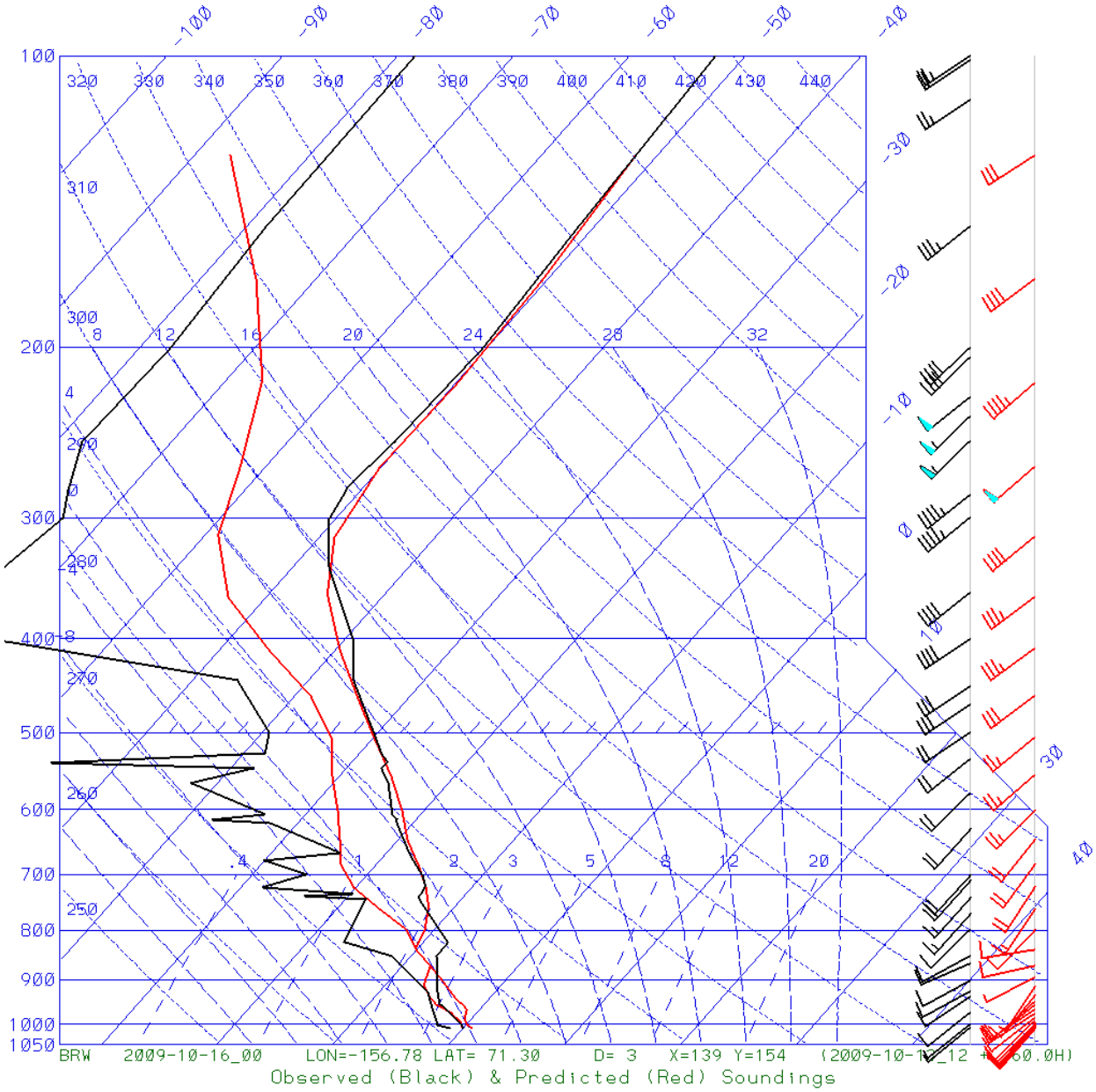

Figure 3-64. Skew-T-log-P Diagram for Barrow at 0Z (3:00 pm LST) on 16 October 2009. Red Lines Denote WRF Estimates. Black Lines Denote Observations.

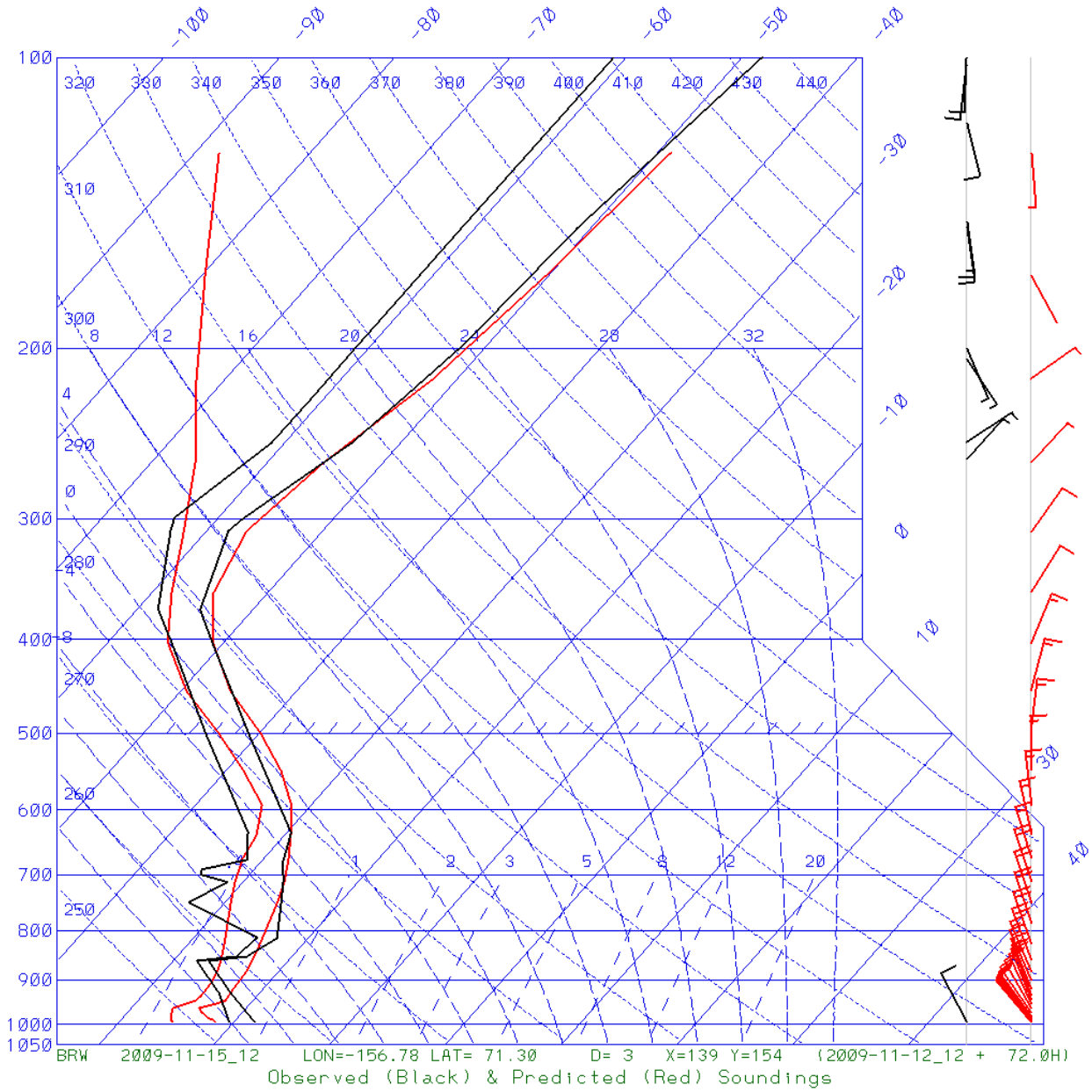

Figure 3-65. Skew-T-log-P Diagram for Barrow at 12Z (3:00 am LST) on 15 November 2009. Red Lines Denote WRF Estimates. Black Lines Denote Observations.

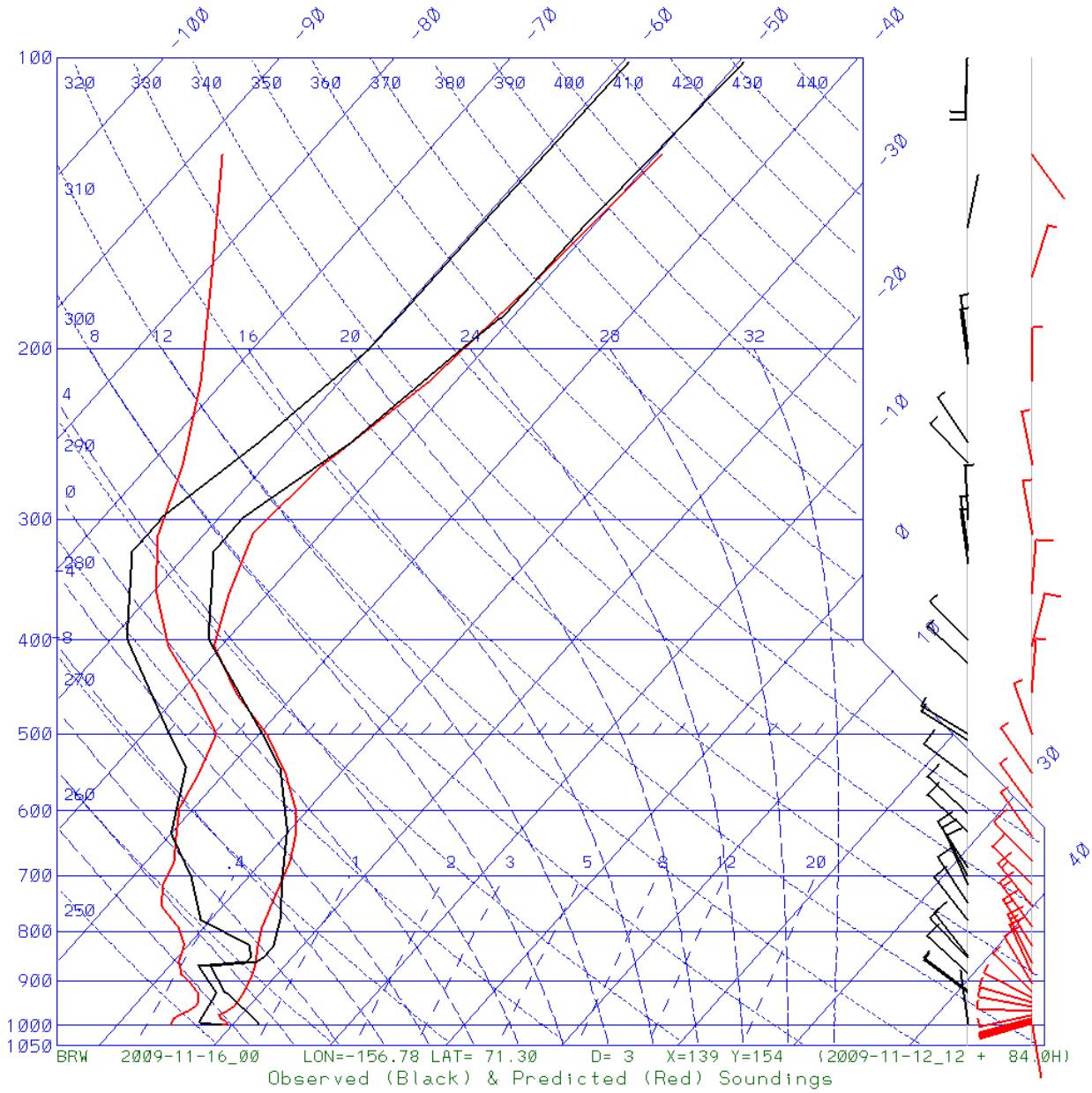

Figure 3-66. Skew-T-log-P Diagram for Barrow at 0Z (3:00 pm LST) on 16 November 2009. Red Lines Denote WRF Estimates. Black Lines Denote Observations.

Appendix A: SAMPLE WPS NAMELIST

```
&share
 wrf_core = 'ARW',
 max_dom = 3,
 start_date = '2009-07-05_12:00:00','2009-07-05_12:00:00','2009-07-
05_12:00:00','2009-07-05_12:00:00',
 end_date   = '2009-07-11_12:00:00','2009-07-11_12:00:00','2009-07-
11_12:00:00','2009-07-11_12:00:00',
 interval_seconds = 21600
 io_form_geogrid = 2,
/

&geogrid
 parent_id         =   1,   1,  2,  3,
 parent_grid_ratio =   1,   3,  3,  2,
 i_parent_start    =   1,  40, 33, 42,
 j_parent_start    =   1,  28, 28,128,
 e_we              = 135, 130,178,131,
 e_sn              =  99, 121,190,131,
 geog_data_res     = '10m','2m','30s','30s','30s'
 dx =36000,
 dy =36000,
 map_proj = 'polar',
 truelat1  =  70.0,
 stand_lon = -155.0,
 ref_lat   =  70.0,
 ref_lon   = -155.0,
 truelat2  =  70.0,
 geog_data_path = '../../geog',
 opt_geogrid_tbl_path = '../geogrid',
/

&ungrib
 out_format = 'WPS',
 prefix = 'XXXX',
/

&metgrid
 fg_name = 'FILE','SST',
 io_form_metgrid = 2,
 opt_metgrid_tbl_path  = '../metgrid',
/

&mod_levs
 press_pa = 201300 , 200100 , 100000 ,
            95000 ,  90000 ,
            85000 ,  80000 ,
            75000 ,  70000 ,
            65000 ,  60000 ,
            55000 ,  50000 ,
            45000 ,  40000 ,
            35000 ,  30000 ,
            25000 ,  20000 ,
            15000 ,  10000 ,
             5000 ,   1000
/
```

Appendix B: SAMPLE WRF NAMELIST

```
 &time_control
 run_days                            = 6,
 run_hours                           = 00,
 run_minutes                         = 0,
 run_seconds                         = 0,
 start_year                          = 2009, 2009, 2009, 2009,
 start_month                         = 07, 07, 07, 07,
 start_day                           = 05, 05, 05, 05,
 start_hour                          = 12,   12,  12,  12,
 start_minute                        = 00,   00,  00,  00,
 start_second                        = 00,   00,  00,  00,
 end_year                            = 2009, 2009, 2009, 2009,
 end_month                           = 07, 07, 07, 07,
 end_day                             = 11, 11, 11, 11,
 end_hour                            = 12,   12,  12,  12,
 end_minute                          = 00,   00,  00,  00,
 end_second                          = 00,   00,  00.  00,
 interval_seconds                    = 21600
 input_from_file                     = .true.,.true.,.true.,.true.
 history_interval                    = 60,   60, 60, 60,
 frames_per_outfile                  = 24,   24, 24, 24,
 restart                             = .false.,
 restart_interval                    = 5000,
 io_form_history                     = 2
 io_form_restart                     = 2
 io_form_input                       = 2
 io_form_boundary                    = 2
 debug_level                         = 0
 io_form_auxinput4                   = 2
 auxinput4_inname                    = "wrflowinp_d<domain>"
 auxinput4_interval                  = 360, 360, 360,
 /

 &domains
 time_step                           = 90,
 time_step_fract_num                 = 0,
 time_step_fract_den                 = 1,
 max_dom                             = 3,
 s_we                                = 1,     1,   1,   1,
 e_we                                = 135, 130, 178, 131,
 s_sn                                = 1,     1,   1,   1,
 e_sn                                =  99, 121, 190, 131,
 s_vert                              = 1,     1,   1,   1,
 e_vert                              = 37,   37,  37,  44,
 p_top_requested                     = 5000,
 eta_levels                          =
1.0000,0.9985,0.9970,0.9950,0.9930,
0.9910,0.9880,0.9850,0.9800,0.9700,
0.9600,0.9500,0.9400,0.9300,0.9100,
0.8900,0.8700,0.8400,0.8000,0.7600,
0.7200,0.6800,0.6400,0.6000,0.5500,
0.5000,0.4500,0.4000,0.3500,0.3000,
0.2500,0.2000,0.1500,0.1000,0.0600,
0.027,0.000
 num_metgrid_levels                  = 27
```

```
num_metgrid_soil_levels             = 4,
dx                                  = 36000, 12000, 4000, 2000,
dy                                  = 36000, 12000, 4000, 2000,
grid_id                             = 1,     2,     3,    4,
parent_id                           = 0,     1,      2,   3,
i_parent_start                      = 1,     40,    33, 103,
j_parent_start                      = 1,     28,    28,  58,
parent_grid_ratio                   = 1,     3,      3,   2,
parent_time_step_ratio              = 1,     3,      3,   2,
feedback                            = 0,
smooth_option                       = 0,
numtiles                            = 1,
nproc_x                             = 2,
nproc_y                             = 4
use_adaptive_time_step              = .false.,
step_to_output_time                 = .true.,
target_cfl                          = 1.2, 1.2, 1.2,
max_step_increase_pct               = 5,   51,  51,
starting_time_step                  = -1,  -1, -1,
max_time_step                       = -1,  -1, -1,
min_time_step                       = -1,  -1, -1,
adaptation_domain                   =  1,

/

&physics
mp_physics                          = 10,    10,   10,   6,
ra_lw_physics                       = 4,     4,    4,   1,
ra_sw_physics                       = 4,     4,    4,   1,
radt                                = 10,   10,   10,  10,
sf_sfclay_physics                   = 1,     1,    1,   1,
sf_surface_physics                  = 2,     2,    2,   2,
bl_pbl_physics                      = 1,     1,    1,   1,
num_soil_layers                     = 4,
bldt                                = 0,     0,    0,   0,
cu_physics                          = 1,     1,    0,   0,
cudt                                = 5,     5,    5,   5,
maxiens                             = 1,
maxens                              = 3,
maxens2                             = 3,
maxens3                             = 16,
ensdim                              = 144,
isfflx                              = 1,
ifsnow                              = 1,
icloud                              = 1,
surface_input_source                = 1,
sf_urban_physics                    = 0,
maxiens                             = 1,
maxens                              = 3,
maxens2                             = 3,
maxens3                             = 16,
ensdim                              = 144,
topo_shading                        = 0,0,1,1,
shadlen                             = 25000.,
slope_rad                           = 0,0,1,1,
sst_update                          = 1,
/
```

```
 &fdda
 grid_fdda                          = 1,  1,  1,
 gfdda_inname                       = "wrffdda_d<domain>",
 GFDDA_END_H                        = 1310, 1310, 1310,
 gfdda_interval_m                   = 360, 360, 360,
 fgdt                               = 0,
 if_no_pbl_nudging_uv               = 0,
 if_no_pbl_nudging_t                = 1, 1, 0,
 if_no_pbl_nudging_q                = 1, 1, 0,
 if_zfac_uv                         = 0,
  k_zfac_uv                         = 0,
 if_zfac_t                          = 0,
  k_zfac_t                          = 0,
 if_zfac_q                          = 0,
  k_zfac_q                          = 0,
 guv                                = 5.0E-4,3.0E-4,0.0,
 gt                                 = 5.0E-4,3.0E-4,0.0,
 gq                                 = 1.E-5,1.E-5,0.0,
 if_ramping                         = 0,
 dtramp_min                         = 60.0,
 io_form_gfdda                      = 2,
 grid_sfdda                        = 0, 0, 1,
 sgfdda_inname                     = "wrfsfdda_d<domain>",
 sgfdda_end_h                      = 1310, 1310, 1310,
 sgfdda_interval_m                 = 60, 60, 60,
 io_form_sgfdda                    = 2,
 guv_sfc                           = 5.0E-4,3.0E-4,1.0E-04
 gt_sfc                            = 0.0,0.0,0.0,
 gq_sfc                            = 0.0,0.0,0.0,
 rinblw                            = 40.0,
obs_nudge_opt                       = 0,0,1,0,0,
max_obs                             = 950000,
fdda_start                          =     0.,     0.,     0.,     0.,
0.
fdda_end                            = 99999., 99999., 99999., 99999.,
99999.
obs_nudge_wind                      = 0,0,1,0,0
obs_coef_wind                       = 3.E-4,3.E-4,1.E-4,6.E-4,6.E-4
obs_nudge_temp                      = 0,0,1,0,0
obs_coef_temp                       = 3.E-4,3.E-4,1.E-4,6.E-4,6.E-4
obs_nudge_mois                      = 0,0,1,0,0
obs_coef_mois                       = 6.E-4,6.E-4,1.E-5,6.E-4,6.E-4
obs_rinxy                           = 240.,240.,50.,180,180
obs_rinsig                          = 0.1,
obs_twindo                          =
0.6666667,0.6666667,0.6666667,0.6666667,0.6666667,
obs_npfi                            = 10,
obs_ionf                            = 2, 2, 2, 2, 2,
obs_idynin                          = 0,
obs_dtramp                          = 40.,
obs_prt_freq                        = 10, 10, 10, 10, 10,
obs_prt_max                         = 10
obs_ipf_errob                       = .true.
obs_ipf_nudob                       = .true.
obs_ipf_in4dob                      = .true.
obs_ipf_init                        = .true.
```

```
 /

 &dynamics
 w_damping                           = 1,
 diff_opt                            = 1,
 km_opt                              = 4,
 diff_6th_opt                        = 2,      2,     2,  2,
 diff_6th_factor                     = 0.25,   0.25, 0.25, 0.12,
 base_temp                           = 290.
 damp_opt                            = 3,
 zdamp                               = 5000.,  5000.,  5000., 5000.,
 dampcoef                            = 0.20,    0.20, 0.20, 0.20,
 khdif                               = 0,      0,     0,   0,
 kvdif                               = 0,      0,     0,   0,
 non_hydrostatic                     = .true., .true., .true., .true.,
 moist_adv_opt                       = 2,      2,   2,  2,
 scalar_adv_opt                      = 2,      2,   2,  2,
 /

 &bdy_control
 spec_bdy_width                      = 5,
 spec_zone                           = 1,
 relax_zone                          = 4,
 specified                           = .true., .false., .false.,
.false.
 nested                              = .false., .true., .true.,  .true.
 /

 &grib2
 /

 &namelist_quilt
 nio_tasks_per_group = 0,
 nio_groups = 1,
 /
```